BERKELEY LAB
Lawrence Berkeley National Laboratory

U.S. DEPARTMENT OF ENERGY

Charged-particle detection

Andrew M. Rogers
Nuclear Science Division
Lawerence Berkeley National Laboratory

Exotic Beam Summer School (EBSS) 2013
Friday August 2nd, 2013

Lecture outline

- General comments
  - Radiation interactions
  - Detector principles of operation
  - Ionization chambers
- Silicon detectors
  - Band structure in crystals
  - The p-n junction
  - Impurities and doping
  - Silicon detectors
- Science with exotic beams
  - Decay spectroscopy with silicon
  - Transfer-reaction studies

Introduction

What do we mean by particle detection?

- Counting
- Spectroscopy
  - Gamma-ray spectroscopy
  - Charged-particle spectroscopy
  - Decay spectroscopy
- Particle Identification
  - Nuclei: *Z, A*
  - Neutron, gamma??

Introduction

What do we mean by particle detection?

- Counting
- Spectroscopy
  - Gamma-ray spectroscopy
  - Charged-particle spectroscopy
  - Decay spectroscopy
- Particle Identification
  - Nuclei: *Z, A*
  - Neutron, gamma??

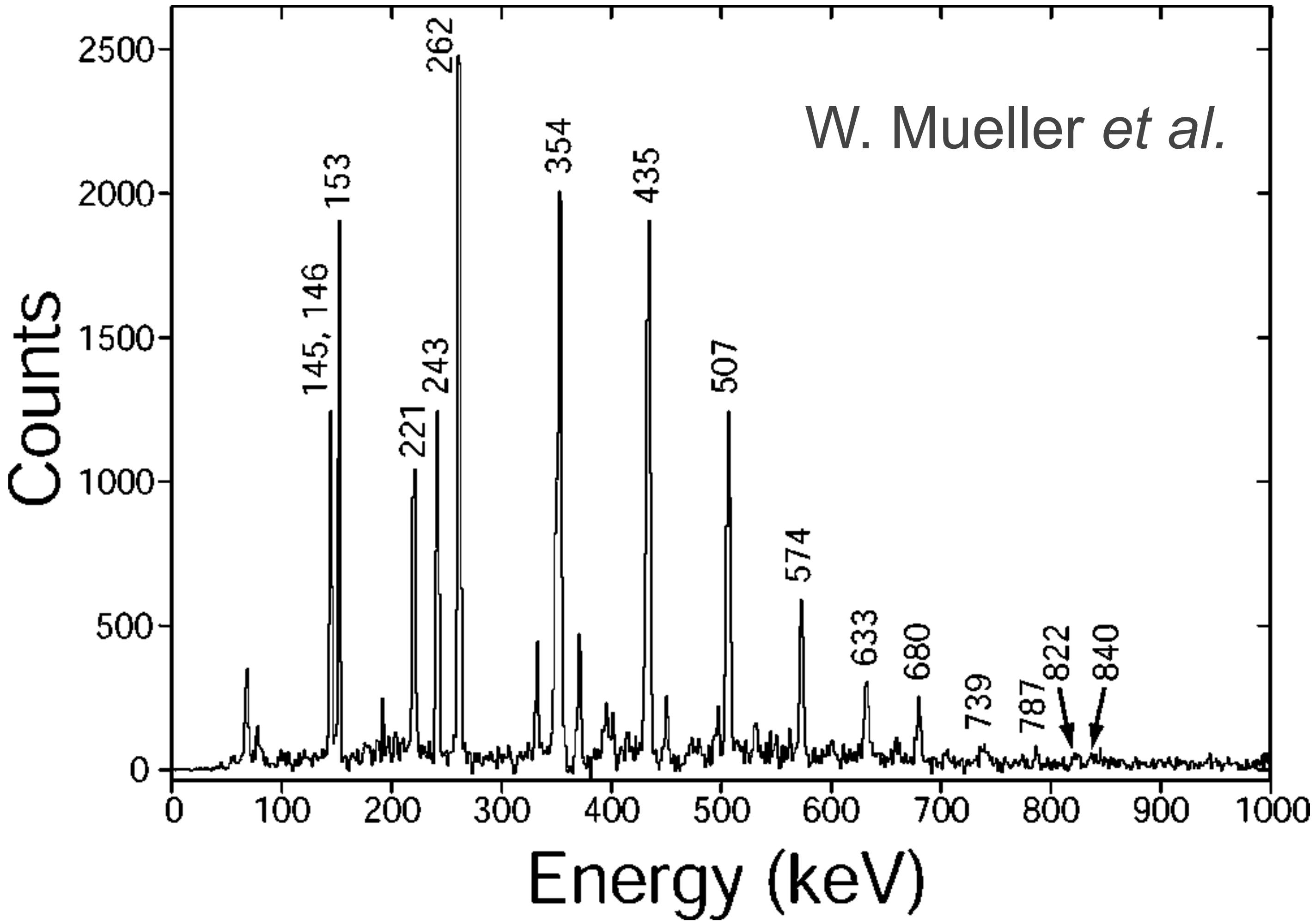

Introduction

What do we mean by particle detection?

- Counting
- Spectroscopy
    - Gamma-ray spectroscopy
    - Charged-particle spectroscopy
    - Decay spectroscopy
- Particle Identification
    - Nuclei: *Z, A*
    - Neutron, gamma??

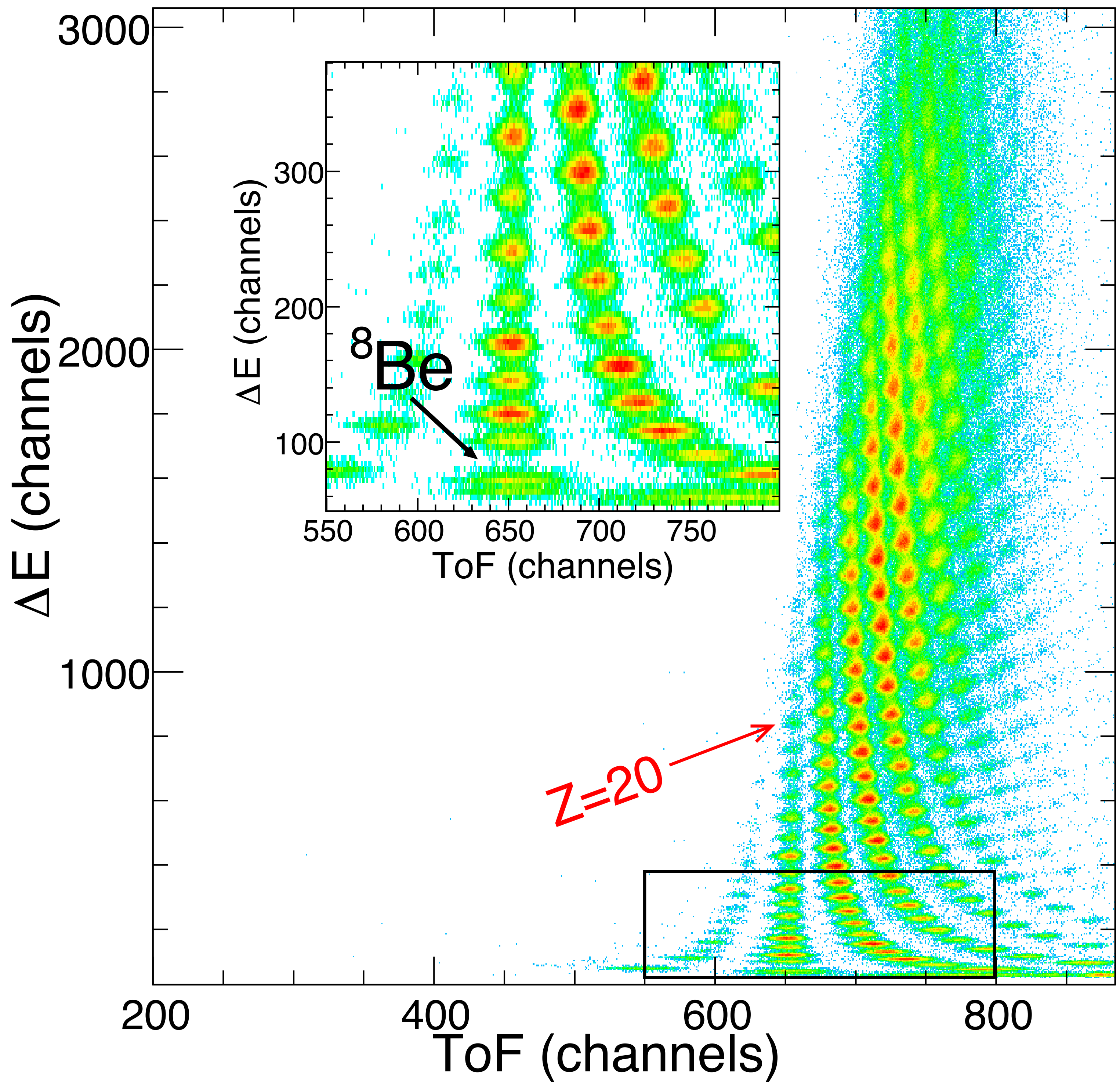

General role and uses of particle detectors

- Nuclear and particle physics.
- Astronomy
- Medicine
- Industry

Discover of the neutron by Chadwick (1932)

$^{9}\mathrm{Be}(\alpha,n)$

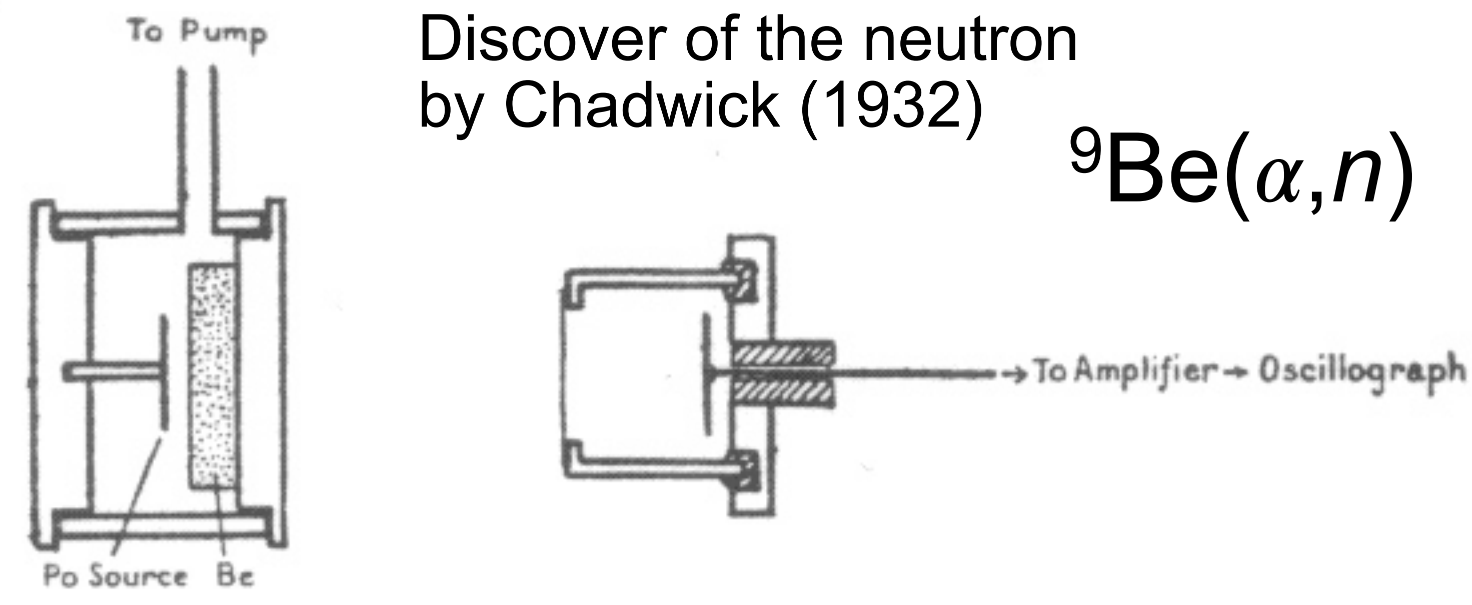

FIG. 1.

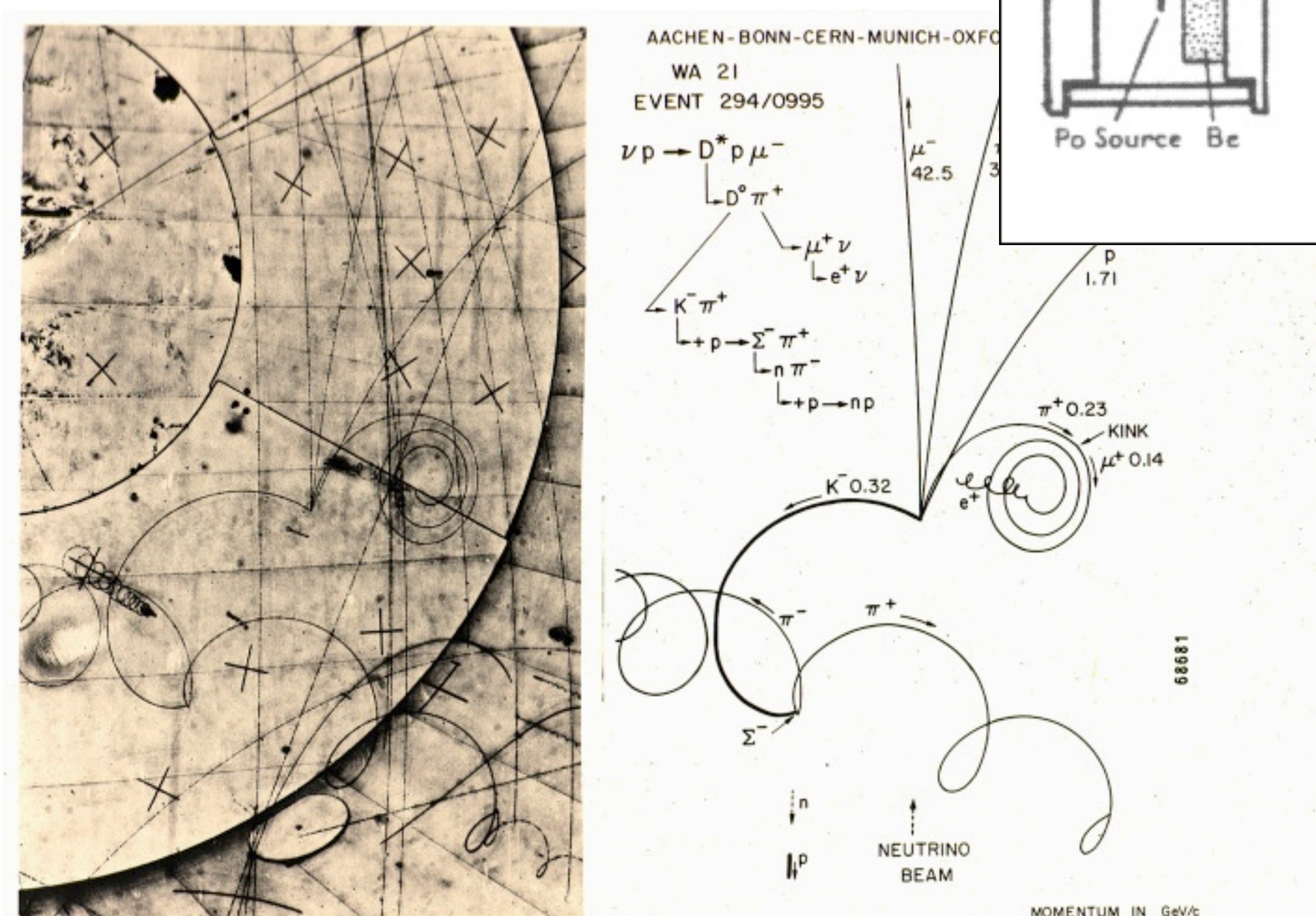

General role and uses of particle detectors

- Nuclear and particle physics.
- Astronomy
- Medicine
- Industry
- . . .

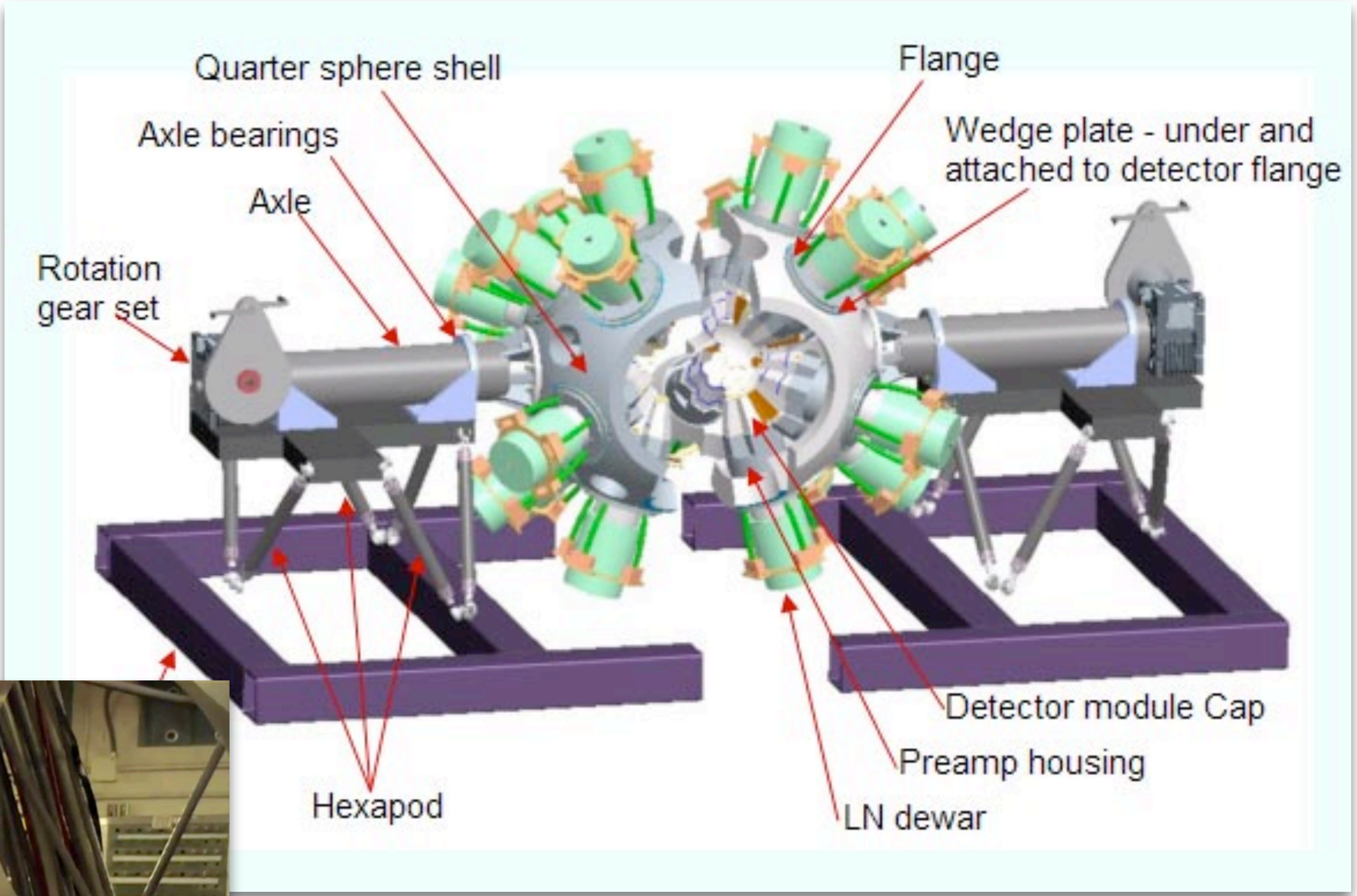

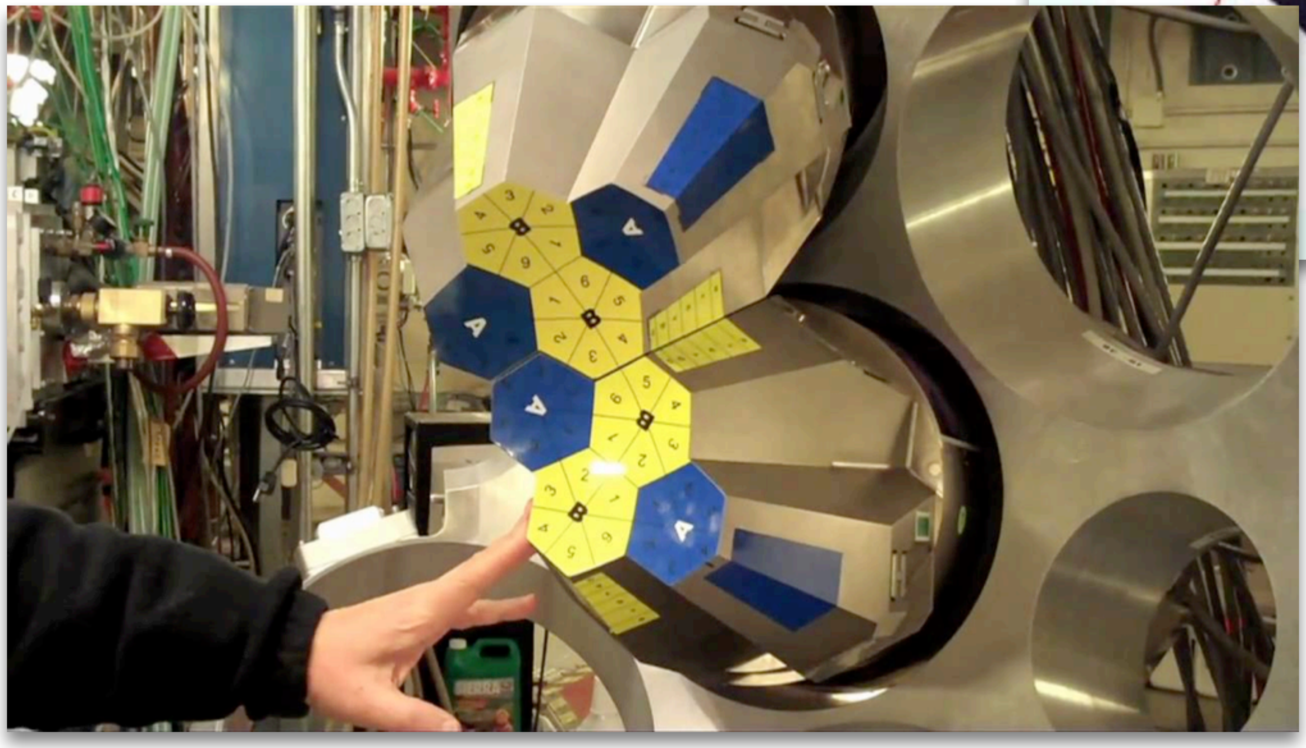

General role and uses of particle detectors

- Nuclear and particle physics.
- Astronomy
- Medicine
- Industry
- . . .

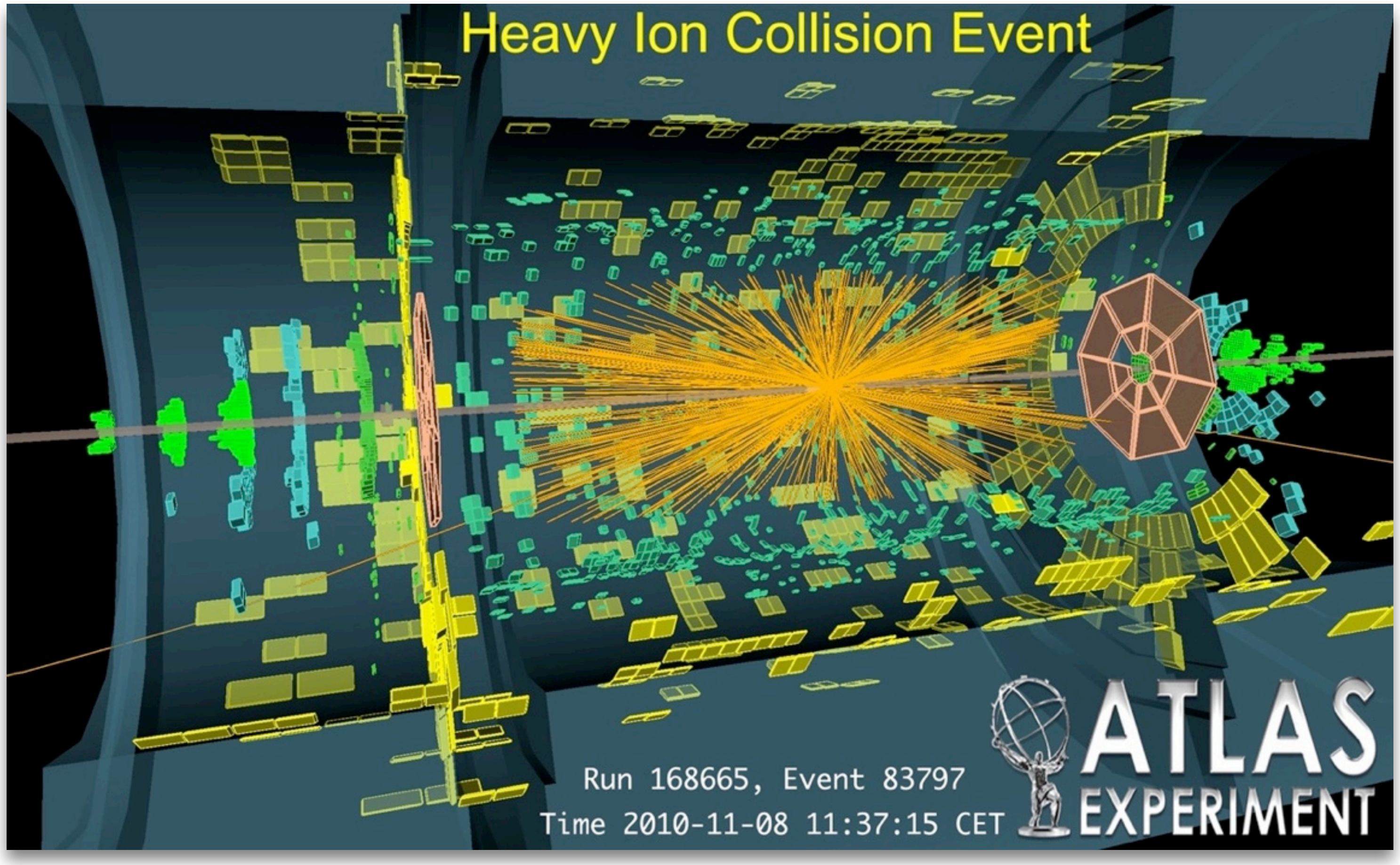

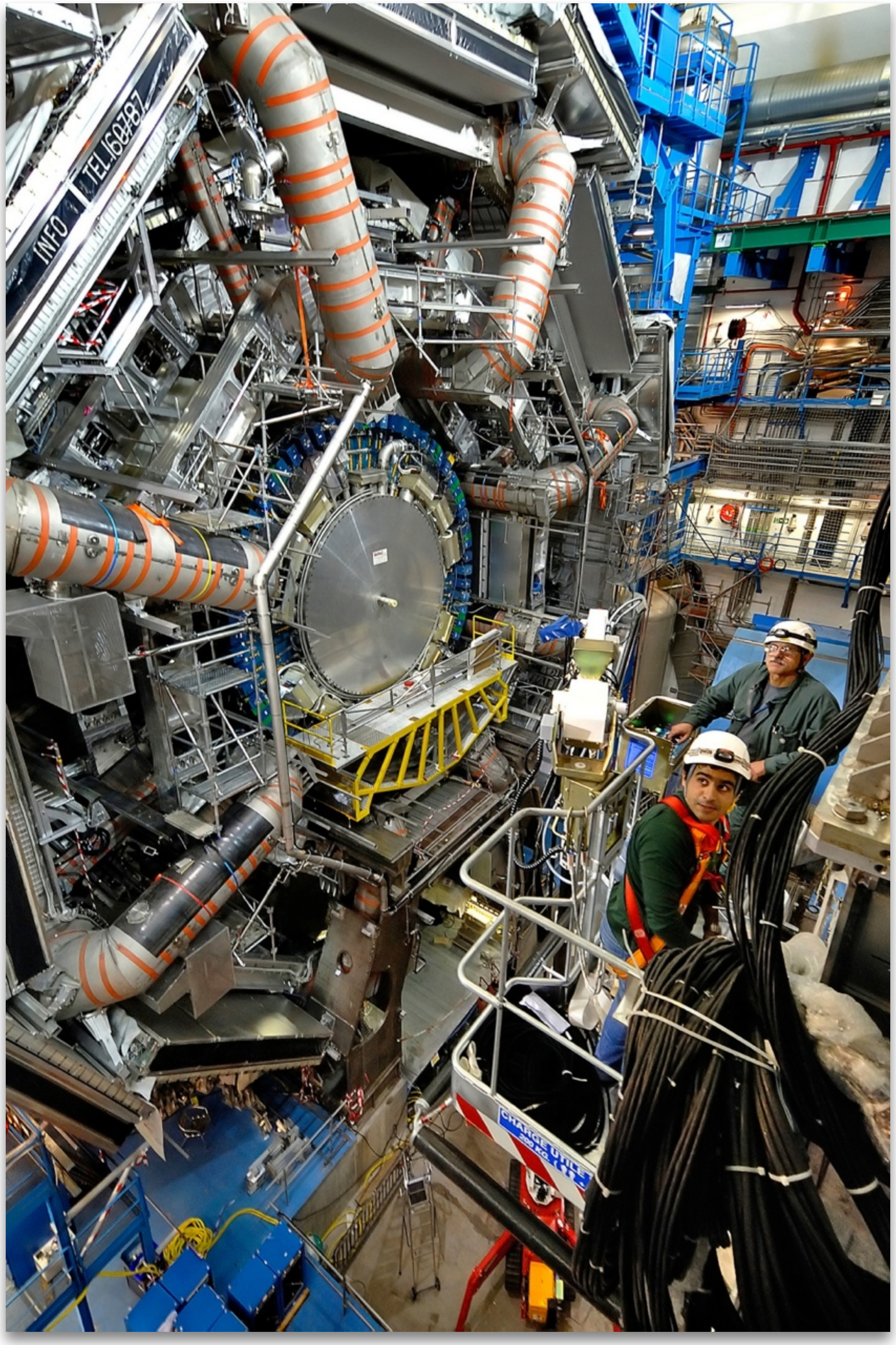

General role and uses of particle detectors

- Nuclear and particle
- Astronomy
- Medicine
- Industry
- . . .

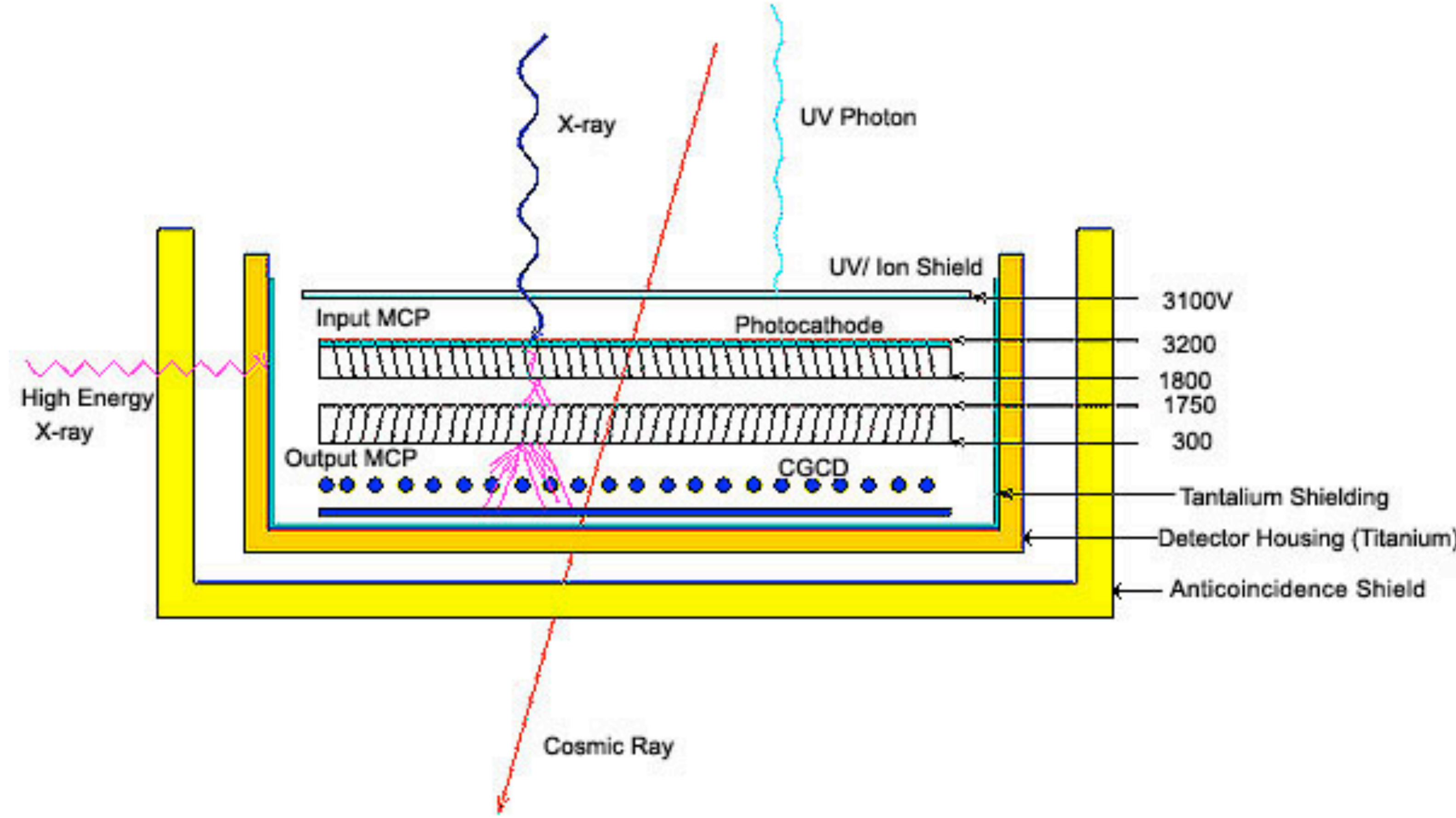

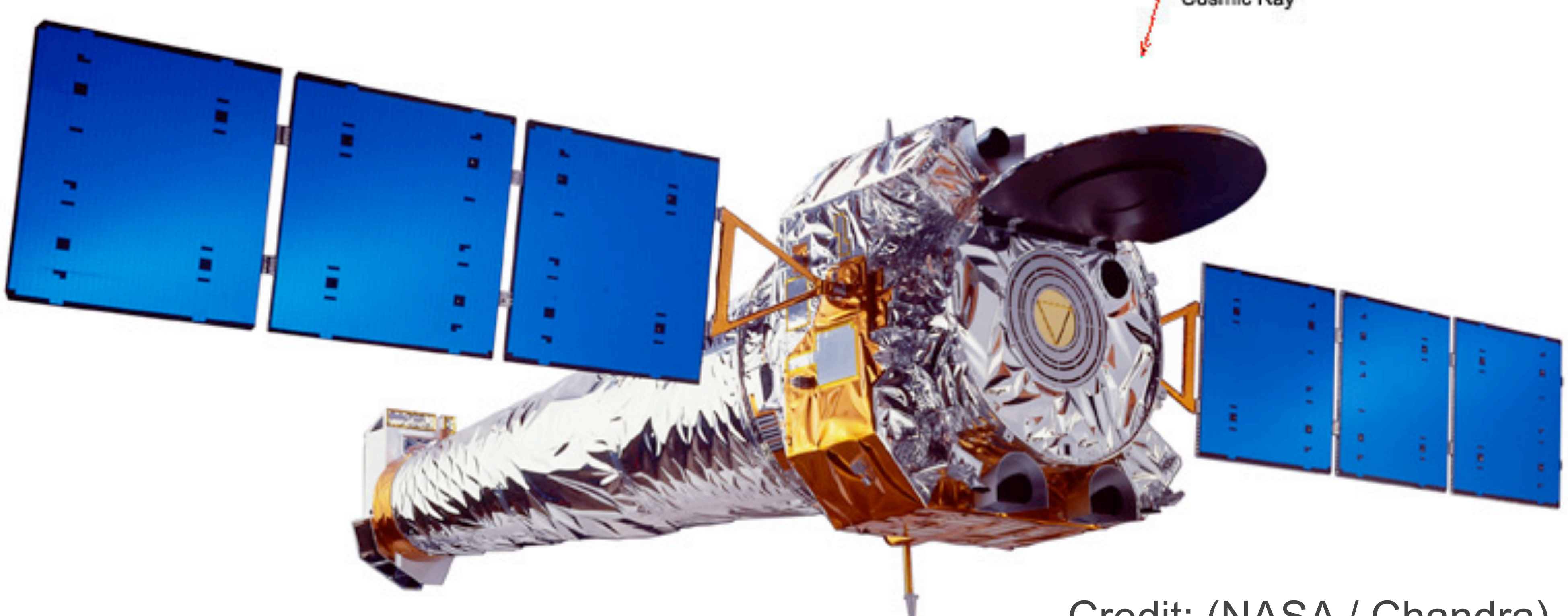

Credit: (NASA / Chandra)

General role and uses of particle detectors

- Nuclear and particle physics.
- Astronomy
- Medicine
- Industry
- . . .

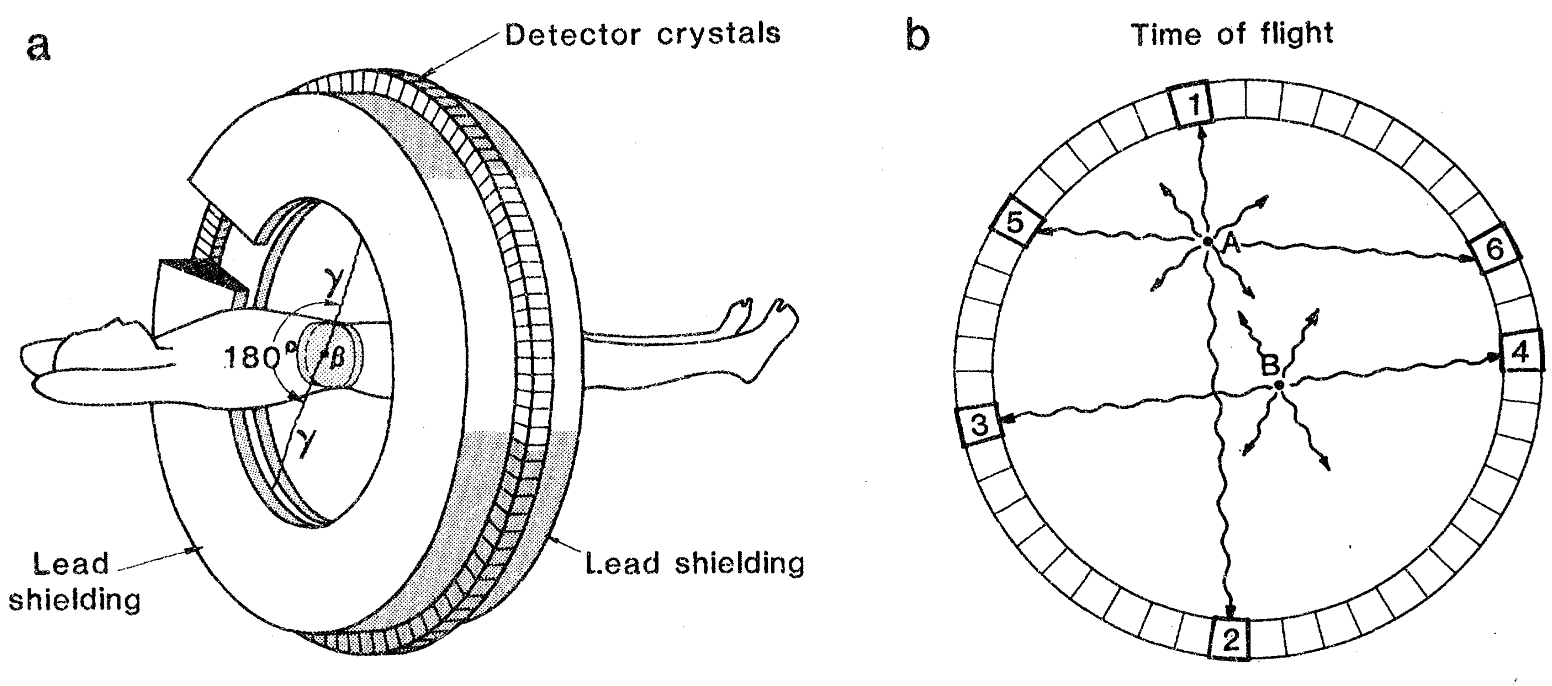

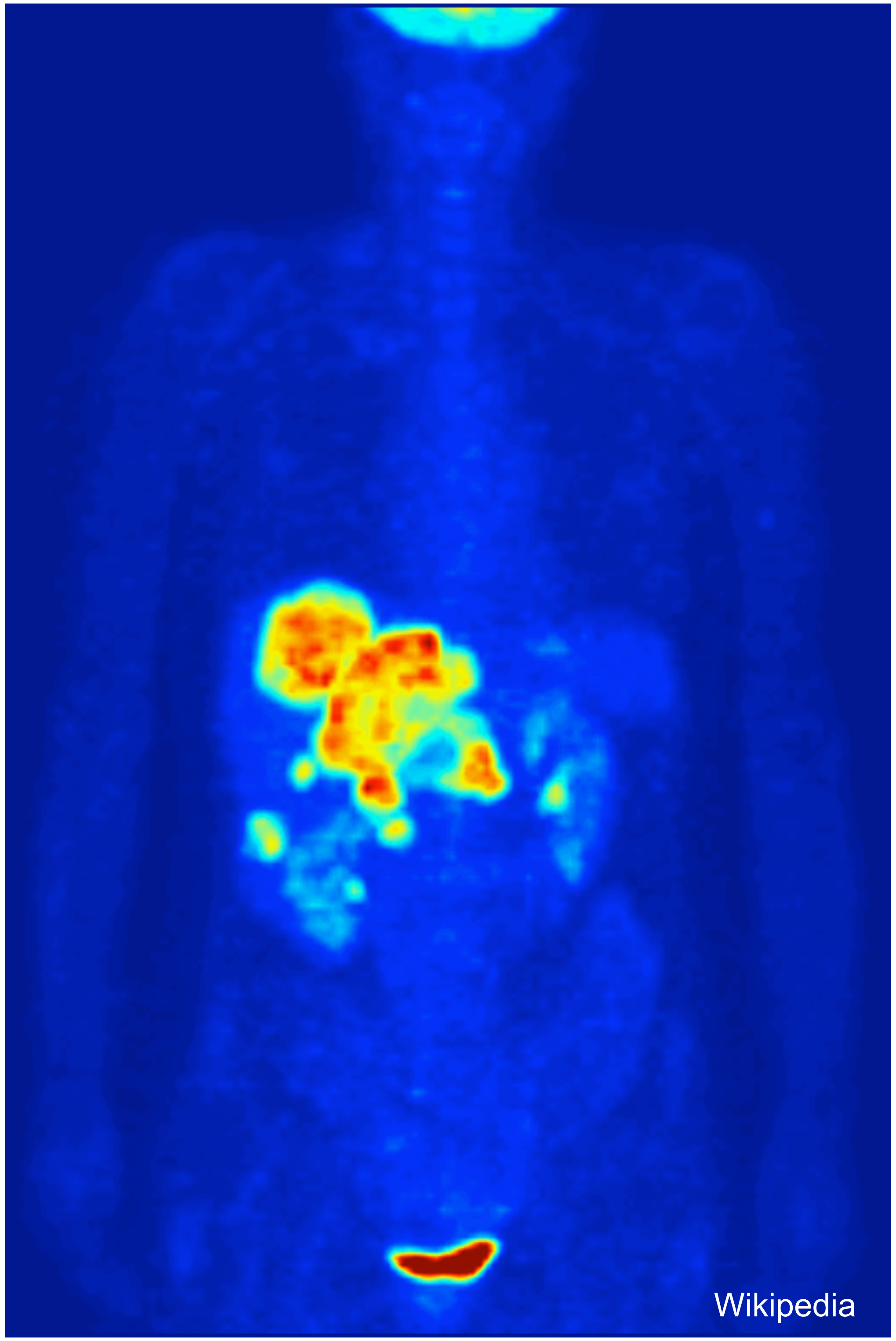

Interaction of radiation with matter

We detect particles through their direct and indirect interactions within a detector volume.

Charged Particles	Neutral Particles
Heavy charged particles (*p*, α, ions)	**Neutrons**
Fast electrons / positrons	**X-rays and γ-rays**

Interaction of radiation with matter

We detect particles through their direct and indirect interactions within a detector volume.

Charged Particles	Neutral Particles
Heavy charged particles (p, α, ions)	**Neutrons**
Fast electrons / positrons	**X-rays and γ-rays**

Charged particles undergo continuous interaction through the coulomb force.

Many orbital electron interactions,

- Excitation
- Ionization

Interaction of radiation with matter

We detect particles through their direct and indirect interactions within a detector volume.

Charged Particles	**Neutral Particles**
Heavy charged particles (p, α, ions)	**Neutrons**
Fast electrons / positrons	**X-rays and γ-rays**

Charged particles undergo continuous interaction through the coulomb force.

Many orbital electron interactions,

- Excitation
- Ionization

Conversion of particle energy primarily through localized interactions

Energy loss of heavy charged particles

$$-\frac{dE}{dx} = \frac{4\pi e^4 z^2}{m_0 v^2} NZ \left[\ln \frac{2m_0 v^2}{I} - \ln\left(1 - \frac{v^2}{c^2}\right) - \frac{v^2}{c^2} \right]$$

- **Bethe formula (1930 Hans Bethe):**
  - z = incident-particle charge
  - v = incident-particle velocity
  - N = absorber number density
  - Z = absorber atomic number
  - m_0 = electron mass
  - e = electron charge
  - I = Mean excitation potential (Carbon: 73.8 eV, Silicon: 174.5 eV, Lead: 818.8 eV)

- Proportional to z^2
- Proportional to NZ

Energy loss of heavy charged particles

$$-\frac{dE}{dx} = \frac{4\pi e^4 z^2}{m_0 v^2} NZ \left[\ln \frac{2m_0 v^2}{I} - \underbrace{\ln\left(1 - \frac{v^2}{c^2}\right) - \frac{v^2}{c^2}}_{\substack{\text{For low kinetic energies} \\ v \ll c}} \right]$$

- **Bethe formula (1930 Hans Bethe):**

  z = incident-particle charge ***v*** = incident-particle velocity
  N = absorber number density ***Z*** = absorber atomic number
  m_0 = electron mass ***e*** = electron charge
  I = Mean excitation potential (Carbon: 73.8 eV, Silicon: 174.5 eV, Lead: 818.8 eV)

- Proportional to z^2
- Proportional to NZ

Energy loss of heavy charged particles

$$-\frac{dE}{dx} = \frac{4\pi e^4 z^2}{m_0 v^2} NZ \left[\ln\frac{2m_0 v^2}{I} \underbrace{- \ln\left(1 - \frac{v^2}{c^2}\right) - \frac{v^2}{c^2}}_{\substack{\text{For low kinetic energies} \\ v<<c}} \right]$$

- **Bethe formula (1930 Hans Bethe):**

  z = incident-particle charge ***v*** = incident-particle velocity

  N = absorber number density ***Z*** = absorber atomic number

  $\boldsymbol{m_0}$ = electron mass ***e*** = electron charge

  I = Mean excitation potential (Carbon: 73.8 eV, Silicon: 174.5 eV, Lead: 818.8 eV)

- Proportional to z^2
- Proportional to *NZ*

$$\frac{dE}{dx} \propto \frac{m_z z^2}{E} \ln(C\frac{E}{m_z})$$

Gaseous ionization chambers

- Ionization and excitation of detector gas.
- Energy to produce an electron-ion pair is ~30eV.
- Collection times for electrons and ions differ greatly, of order μs for electrons compared to ms for ions.
- Relatively simple detectors and can have large dimensions.

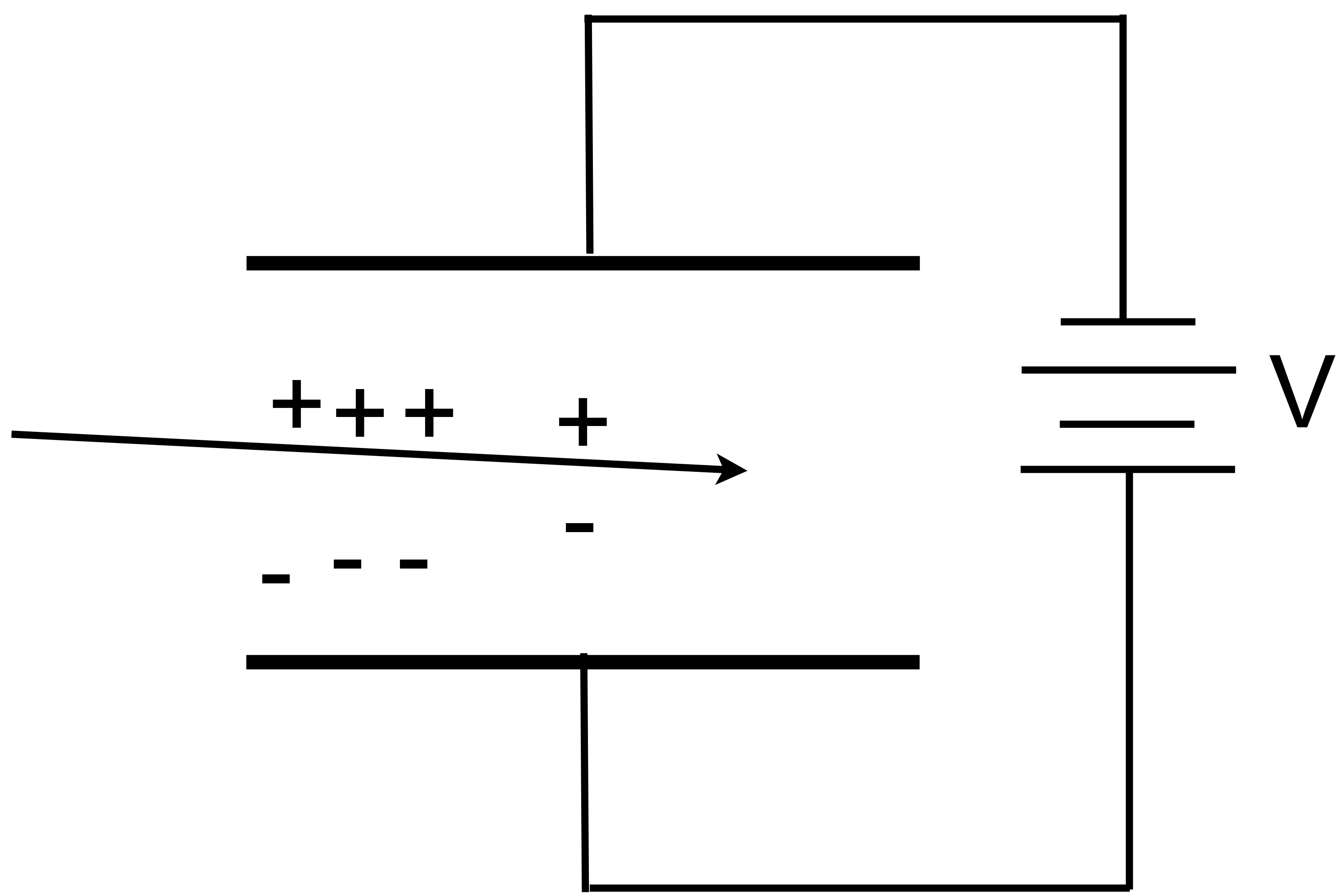

Gaseous ionization chambers

- Ionization and excitation of detector gas.
- Energy to produce an electron-ion pair is ~30eV.
- Collection times for electrons and ions differ greatly, of order μs for electrons compared to ms for ions.
- Relatively simple detectors and can have large dimensions.

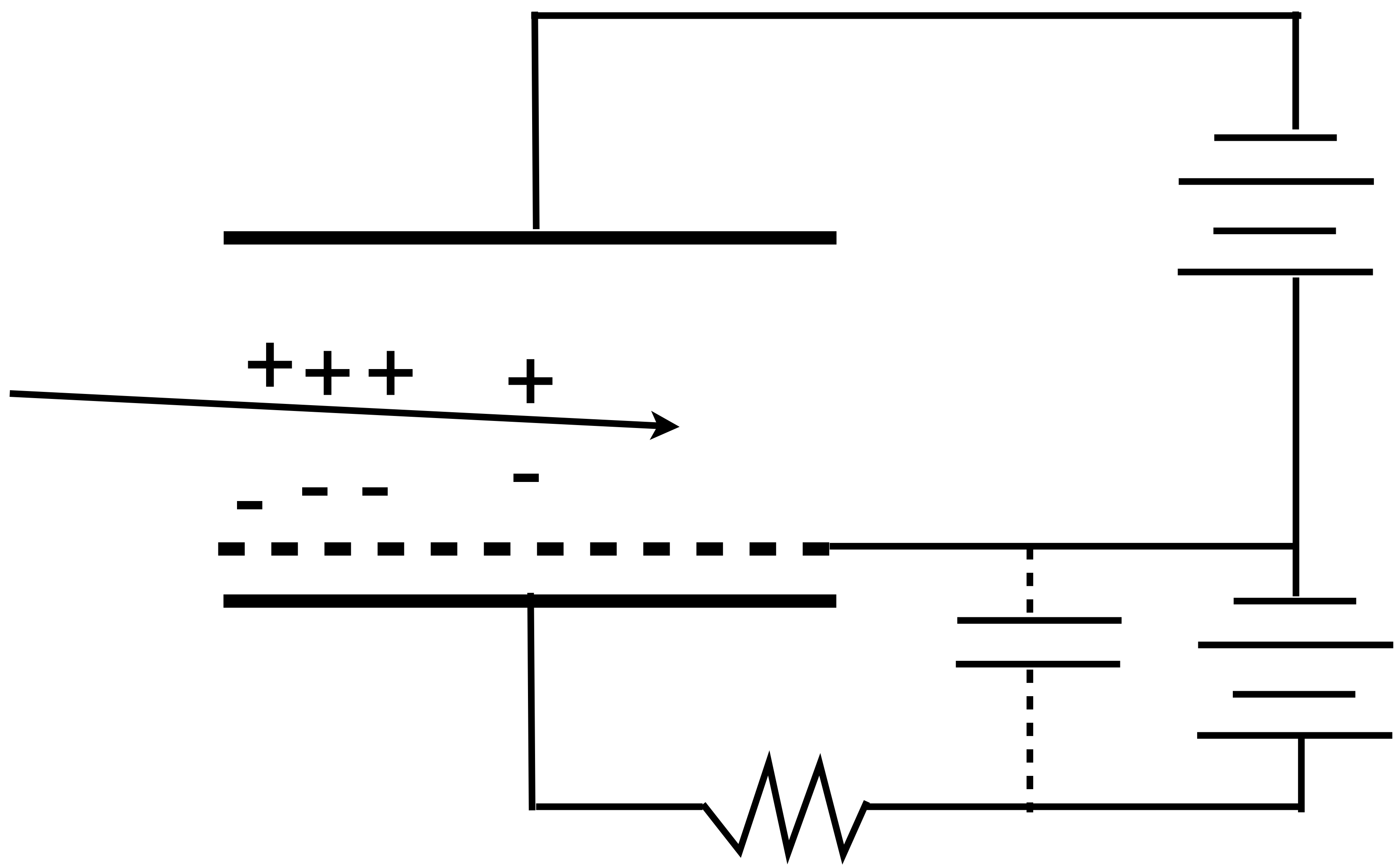

Frisch grid ion chamber

Gaseous chambers in the NSCL S800

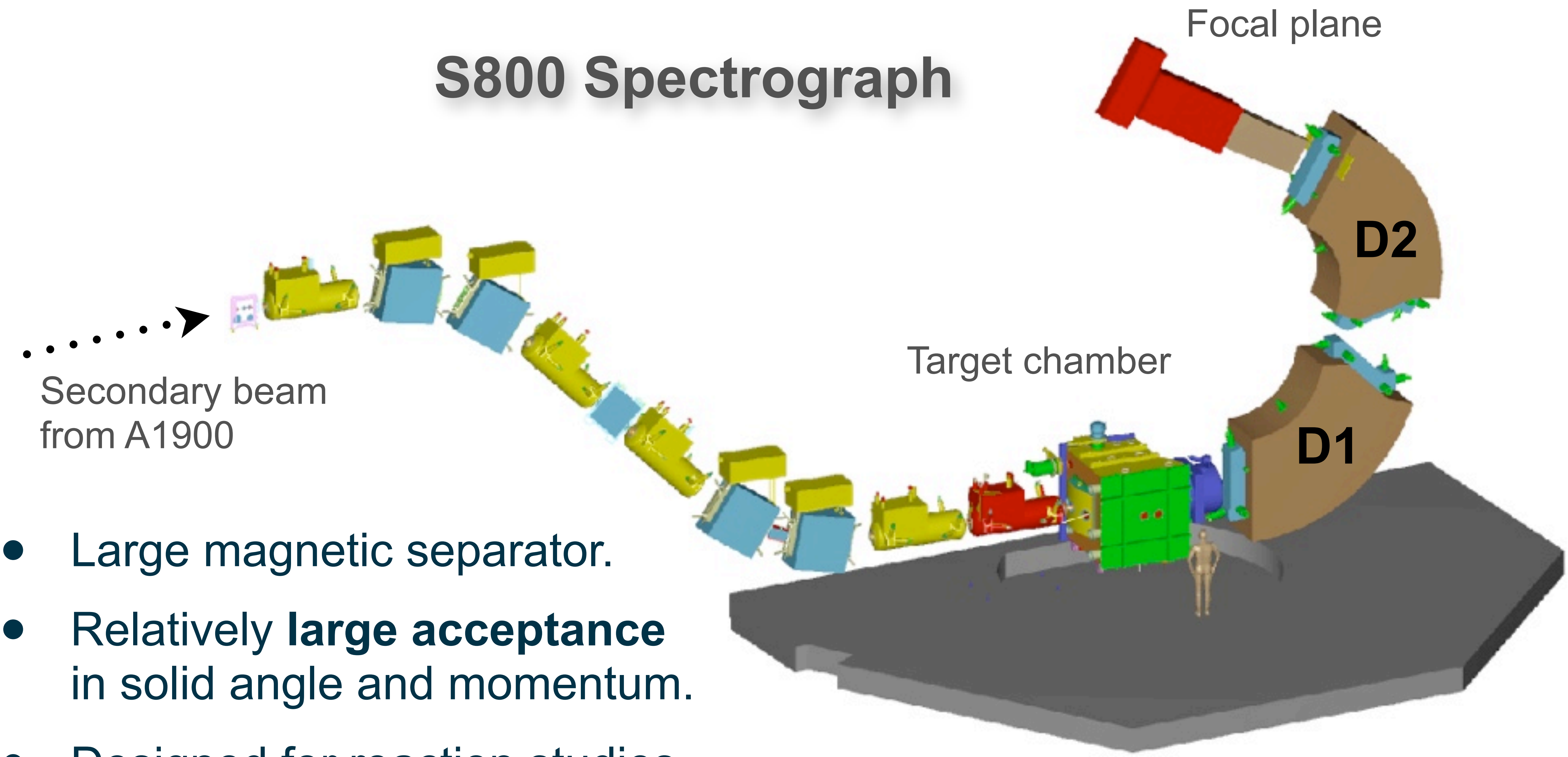

- Large magnetic separator.
- Relatively **large acceptance** in solid angle and momentum.
- Designed for reaction studies with exotic beams produced through projectile fragmentation at NSCL.

Gaseous chambers in the NSCL S800

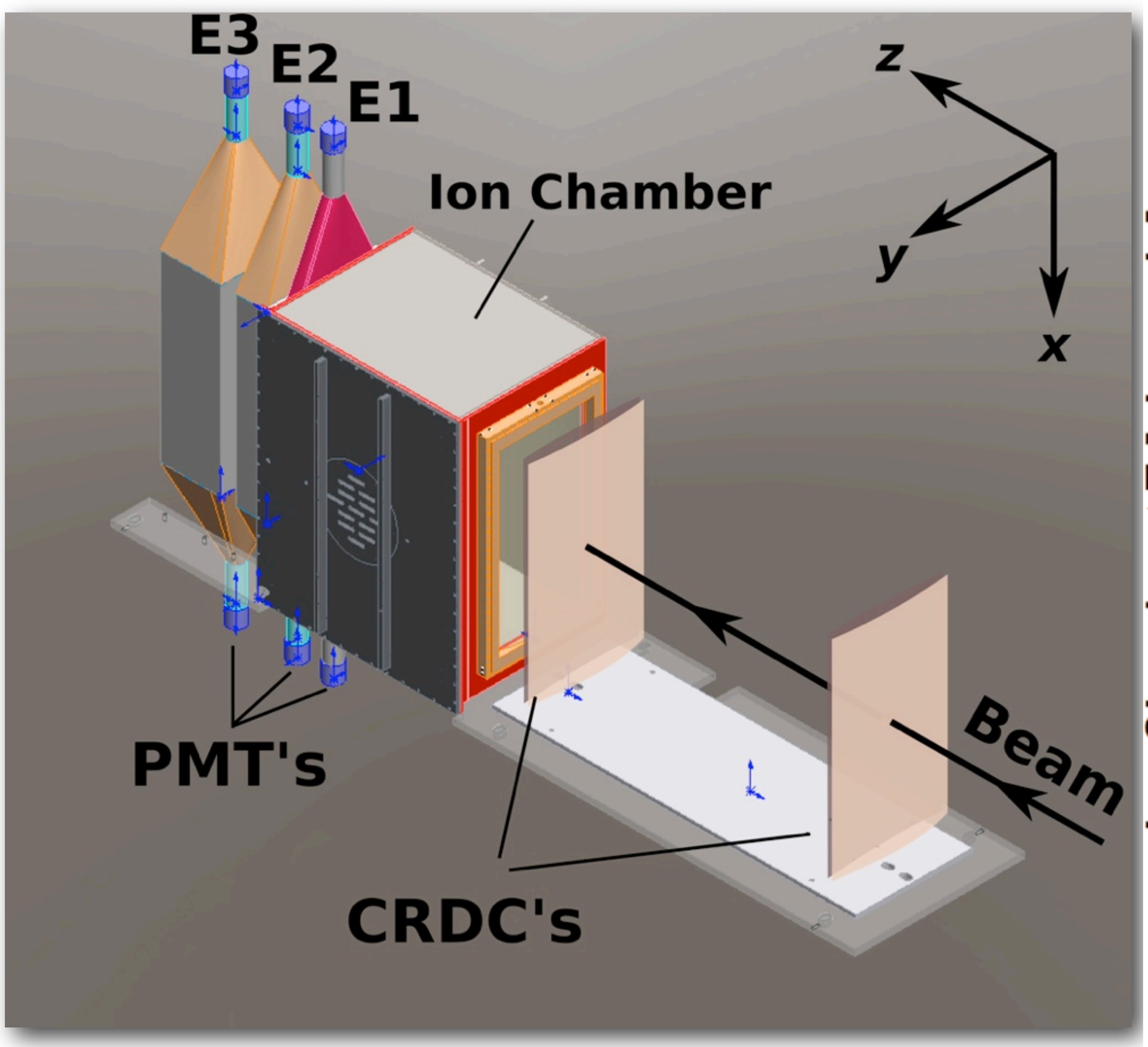

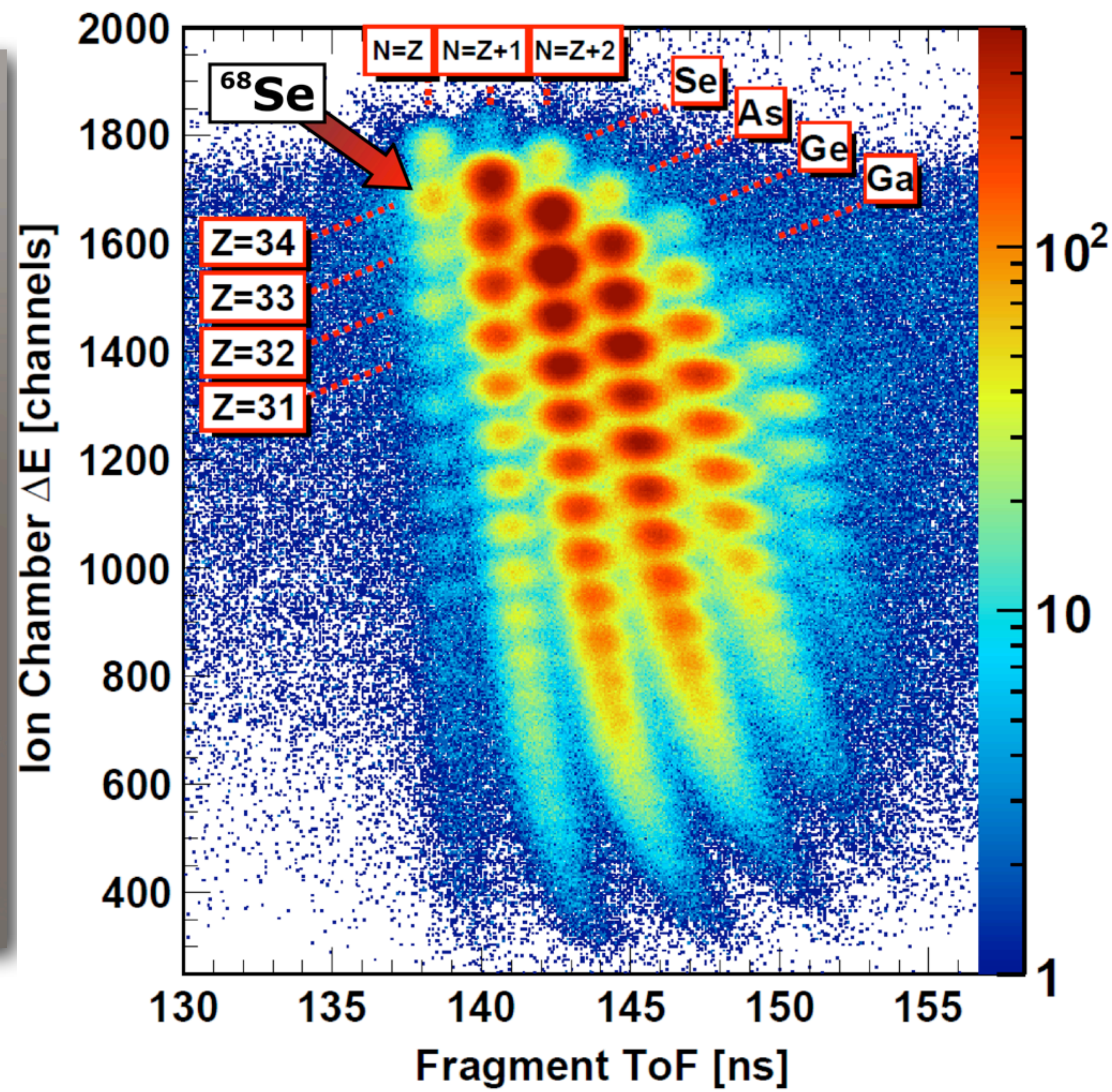

Silicon Detectors

Silicon

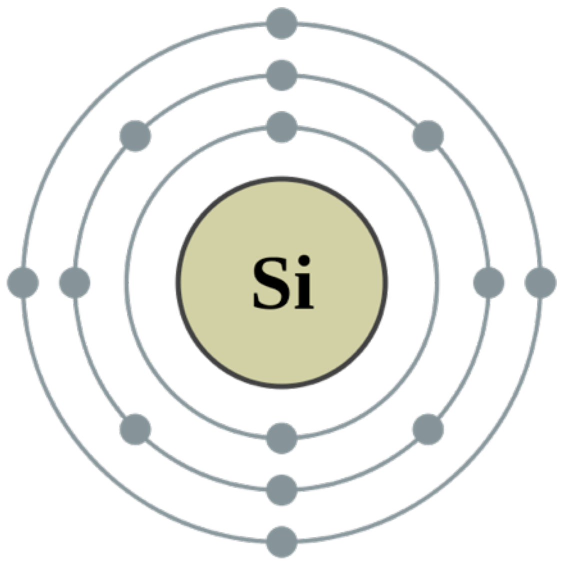

3A	4A	5A	6A	7A	8A
					2 He $1s^2$ helium 4.003
5 B $[He]2s^2 2p^1$ boron 10.81	6 C $[He]2s^2 2p^2$ carbon 12.01	7 N $[He]2s^2 2p^3$ nitrogen 14.01	8 O $[He]2s^2 2p^4$ oxygen 16.00	9 F $[He]2s^2 2p^5$ fluorine 19.00	10 Ne $[He]2s^2 2p^6$ neon 20.18
13 Al $[Ne]3s^2 3p^1$ aluminum 26.98	14 Si $[Ne]3s^2 3p^2$ silicon 28.09	15 P $[Ne]3s^2 3p^3$ phosphorus 30.97	16 S $[Ne]3s^2 3p^4$ sulfur 32.06	17 Cl $[Ne]3s^2 3p^5$ chlorine 35.45	18 Ar $[Ne]3s^2 3p^6$ argon 39.95
31 Ga $[Ar]4s^2 3d^{10} 4p^1$ gallium 69.72	32 Ge $[Ar]4s^2 3d^{10} 4p^2$ germanium 72.64	33 As $[Ar]4s^2 3d^{10} 4p^3$ arsenic 74.92	34 Se $[Ar]4s^2 3d^{10} 4p^4$ selenium 78.96	35 Br $[Ar]4s^2 3d^{10} 4p^5$ bromine 79.90	36 Kr $[Ar]4s^2 3d^{10} 4p^6$ krypton 83.79

(From LANL Chem. Div.)

The Avogadro Project

4 valence electrons that participate in covalent bonding.

Electronic band structure

- Atoms have discrete energy levels.
- Electrons in crystals are arranged in energy bands.
- Forbidden regions, where no wavelike electron orbitals exist, are known as ***bandgaps***.

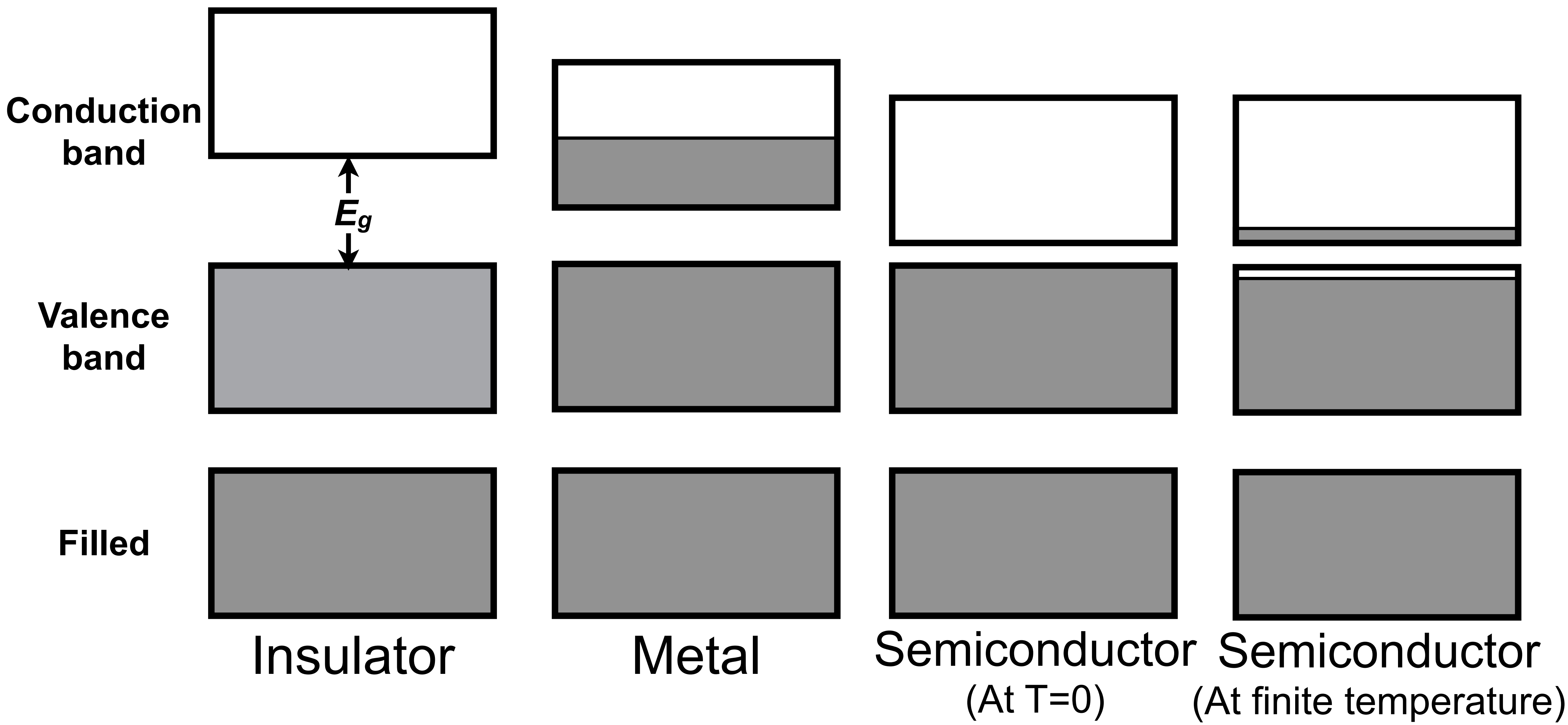

Insulator band structure

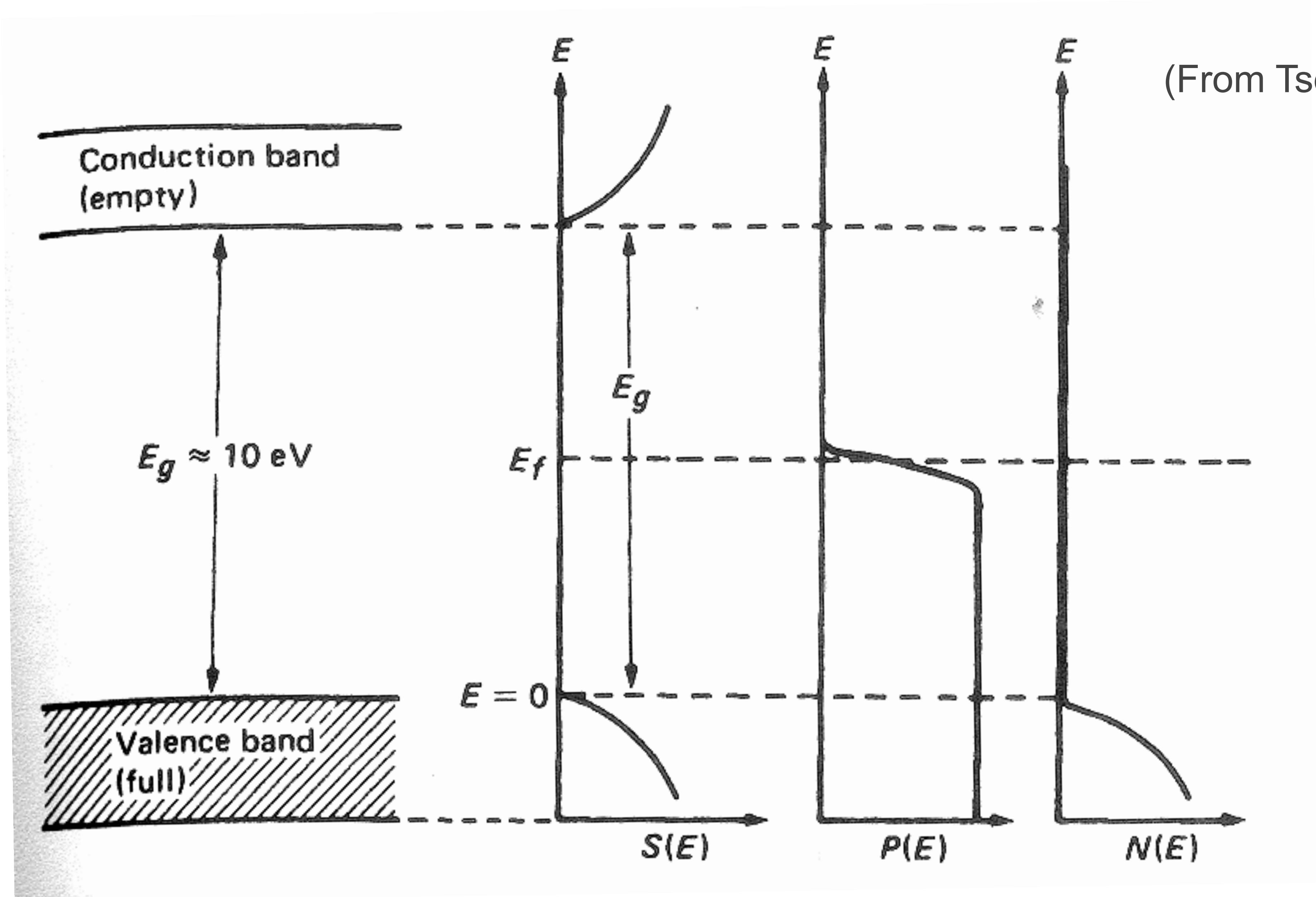

(From Tsoulfanidis)

- The probability that a state of energy *E* is occupied is given by the Fermi distribution function.
- In an ***insulator*** the band gap is relatively large.
- Even at large finite temperature the number of electrons in the conduction band is **zero.**

$$P(E) = \frac{1}{1 + e^{(E - E_f)/kT}}$$

Semiconductor band structure

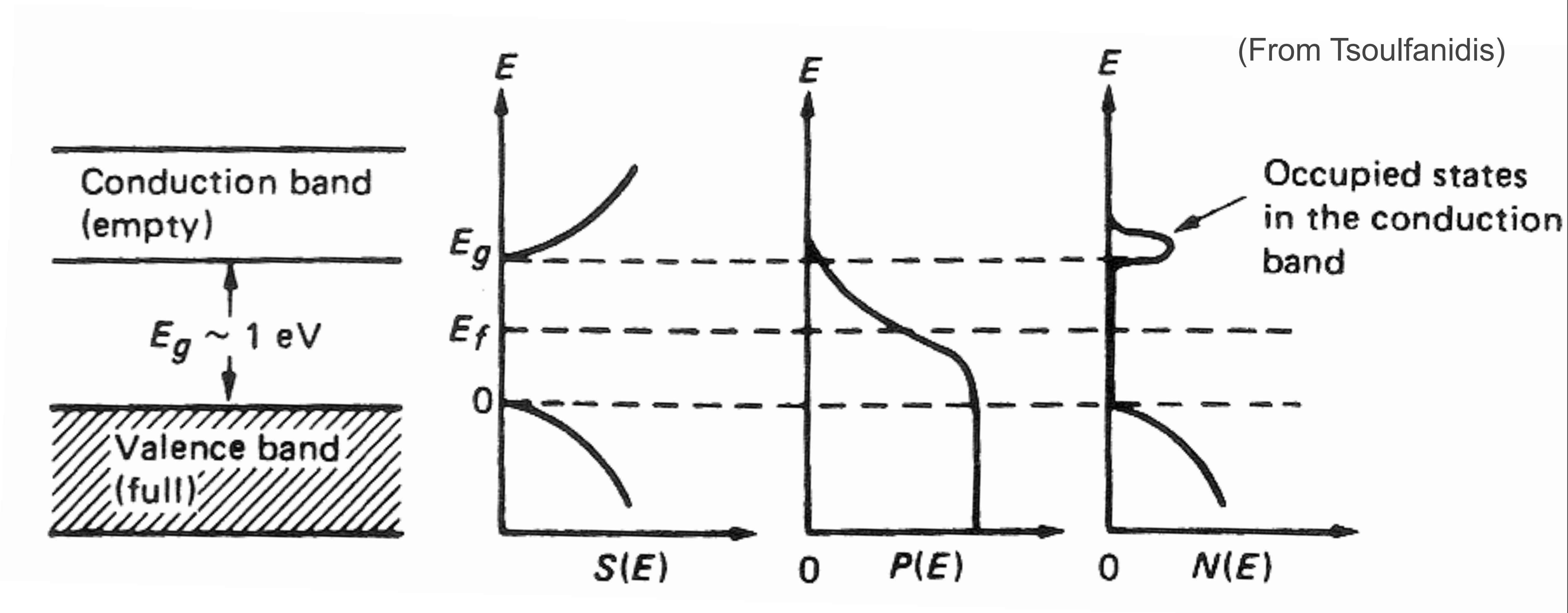

- In an ***semiconductor*** the band gap is relatively small.
- At finite temperature the number of electrons in the conduction band is **finite** but small compared to a metal**.** If an electric field is applied a current will flow.
- At T=0, states can be filled up to the Fermi energy and the number of electrons in the conduction band is zero. At T=0 the semiconductor is an ***insulator***.

Intrinsic (pure) silicon

- At finite temperature there are on the order $n_i \sim 10^{10}$ electrons/cm^3 in the conduction band that are free to move through the lattice.
- An equilibrium concentration of ***electron-hole pairs*** is created and the intrinsic-carrier densities are equal,

$$n_i = p_i$$

- These electron-hole pairs diffuse randomly, if we apply an electric field we can collect these charges.
- There are always impurities and defects in real crystalline silicon.

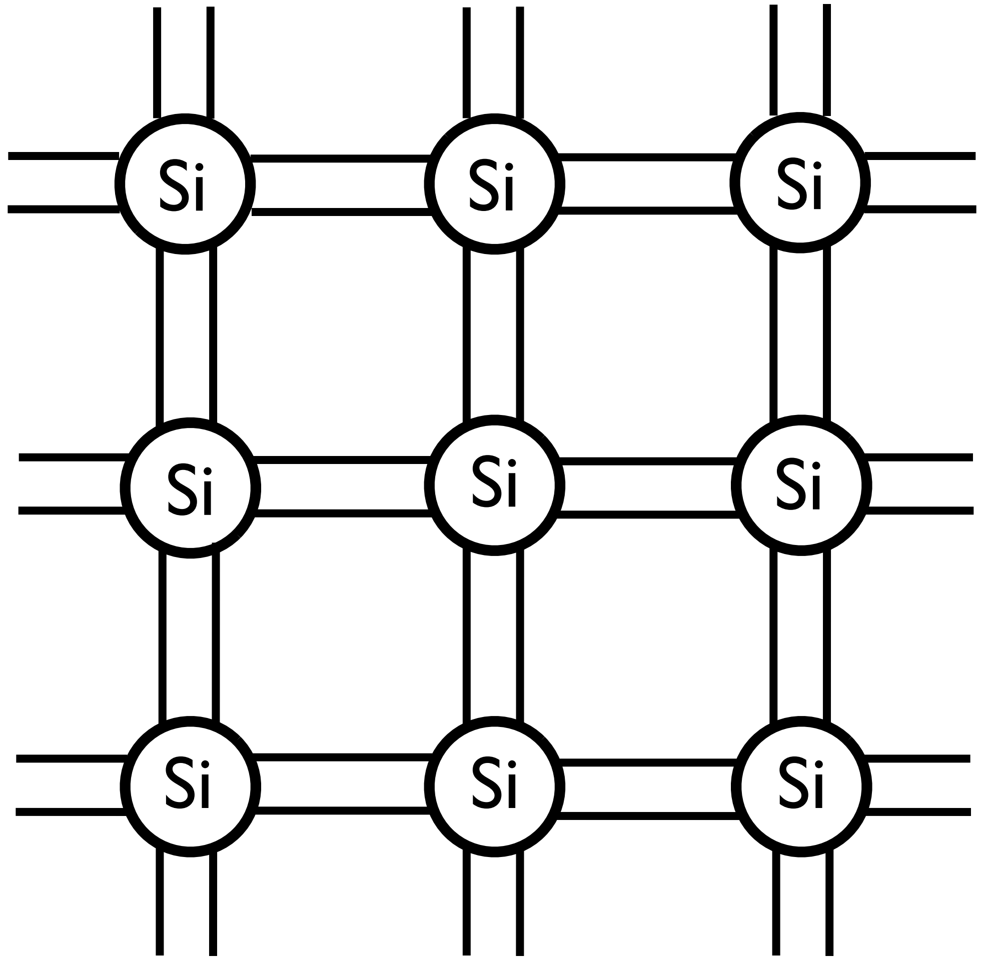

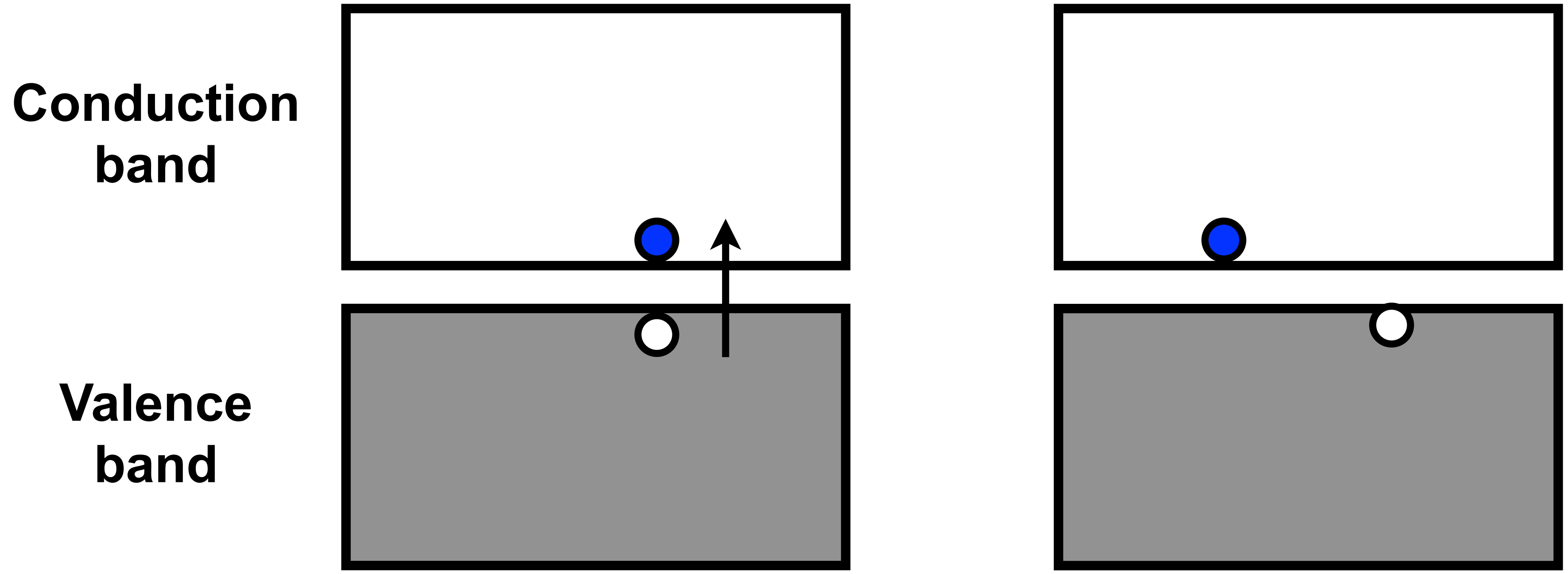

Impurities: n-type silicon

- We can dope a semiconductor in order to control the number of electrons and holes, thus altering the resistivity.
- ***n-type*** silicon is doped with atoms that ***add electrons*** to the conduction band.
- The extra electron does not participate in bonding.
- Typically come from Group V when added to Si or Ge and have a weakly-bound electron.
- The wavefunction of the impurity extends over many of its neighbor atoms.

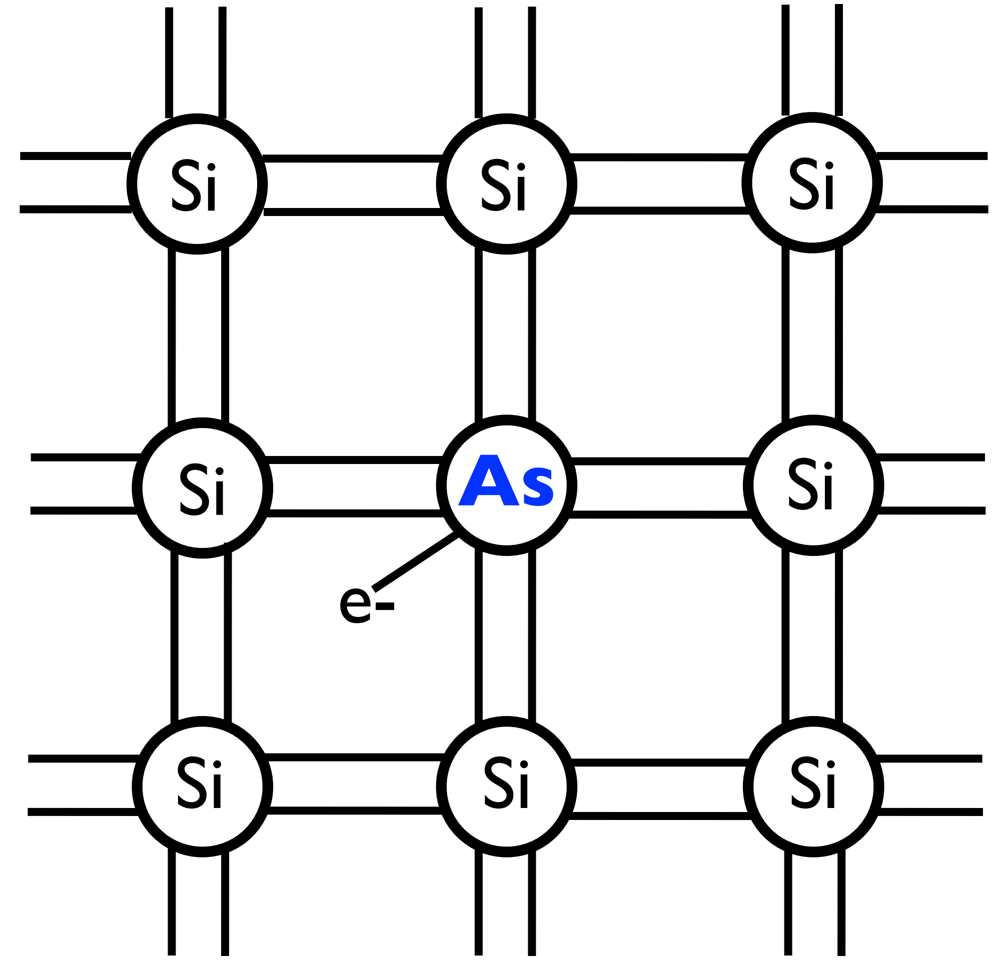

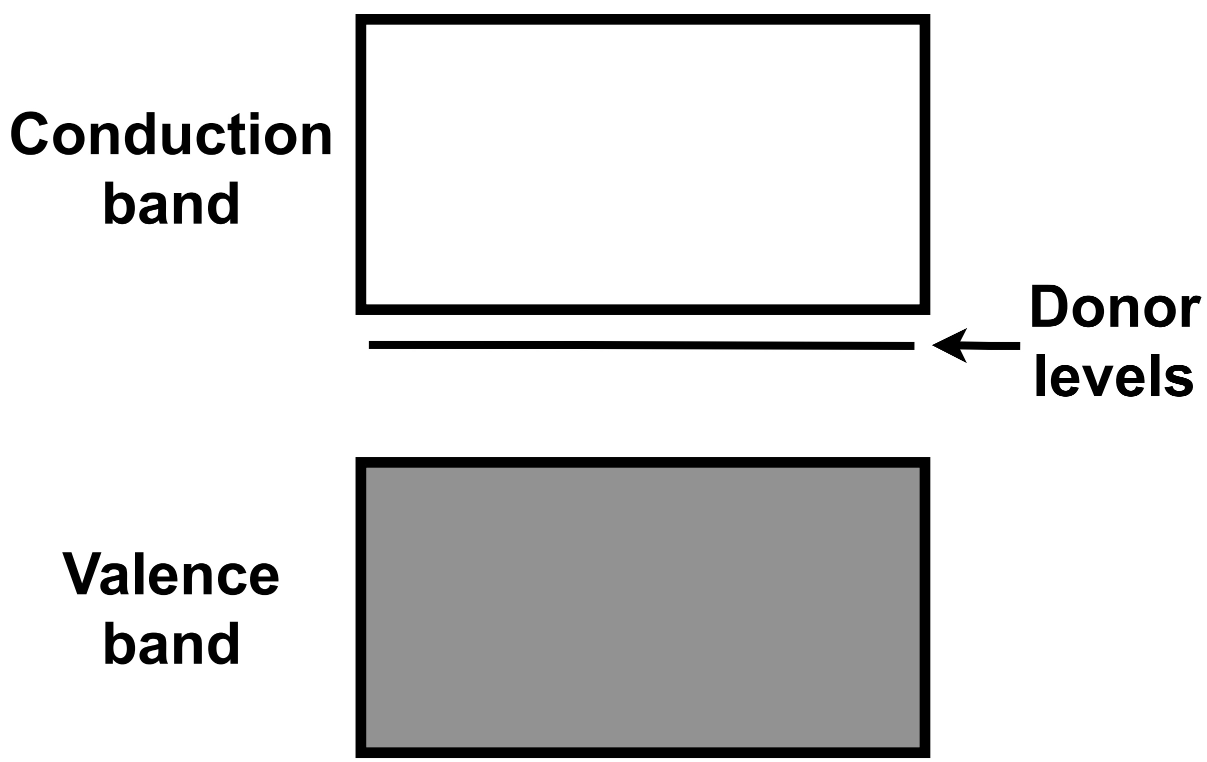

- ***Electrons*** are the majority carrier.
- Energy gap between the donor levels and the conduction band is small.
- Contributes to the electron concentration without adding holes to the valence band of the lattice.

Impurities: n-type silicon

- We can dope a semiconductor in order to control the number of electrons and holes, thus altering the resistivity.
- ***n-type*** silicon is doped with atoms that ***add electrons*** to the conduction band.
- The extra electron does not participate in bonding.
- Typically come from Group V when added to Si or Ge and have a weakly-bound electron.
- The wavefunction of the impurity extends over many of its neighbor atoms.

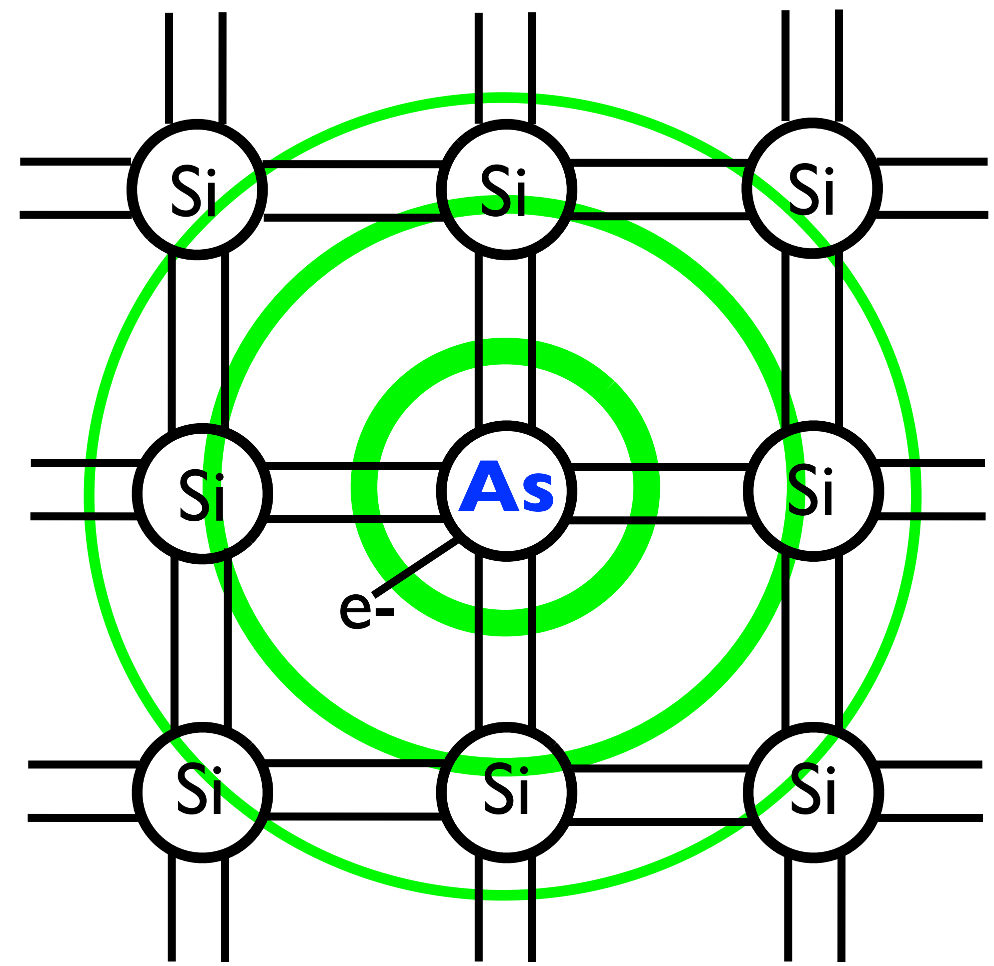

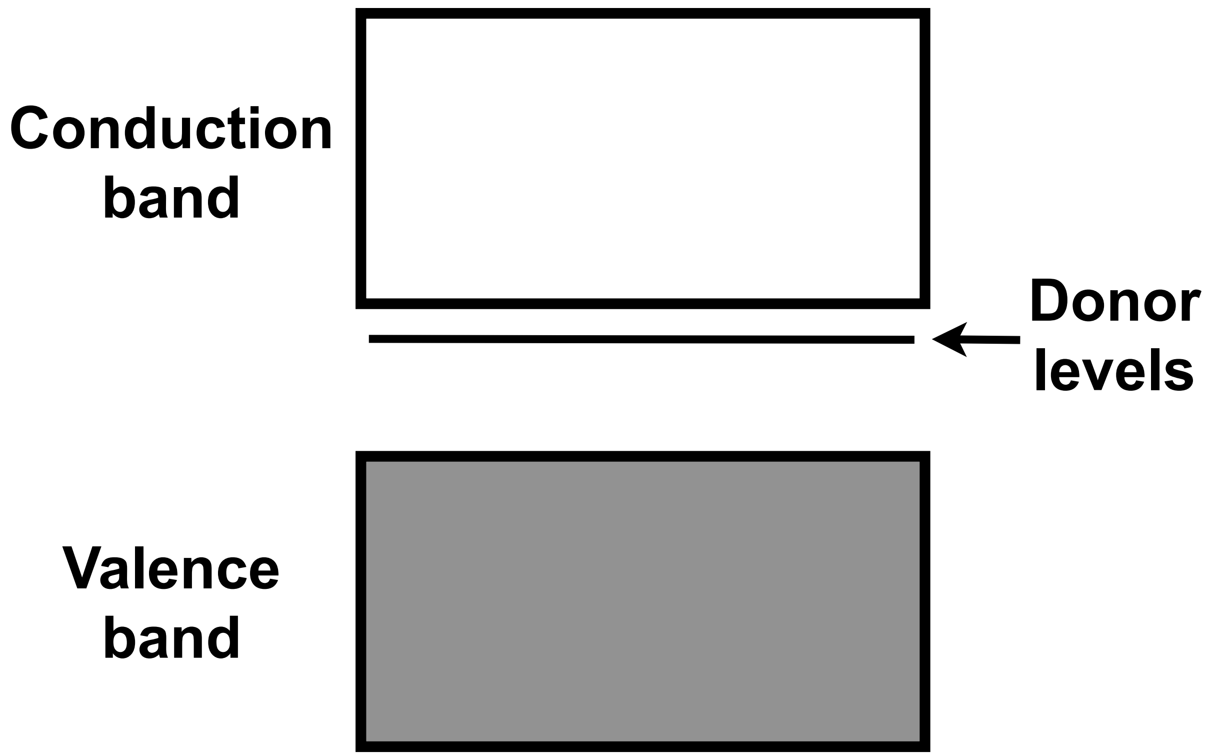

- ***Electrons*** are the majority carrier.
- Energy gap between the donor levels and the conduction band is small.
- Contributes to the electron concentration without adding holes to the valence band of the lattice.

Impurities: p-type silicon

- ***p-type*** silicon is doped with atoms that ***add holes*** to the valence band.
- Typically come from Group III when added to Si or Ge and are missing a valence electron.

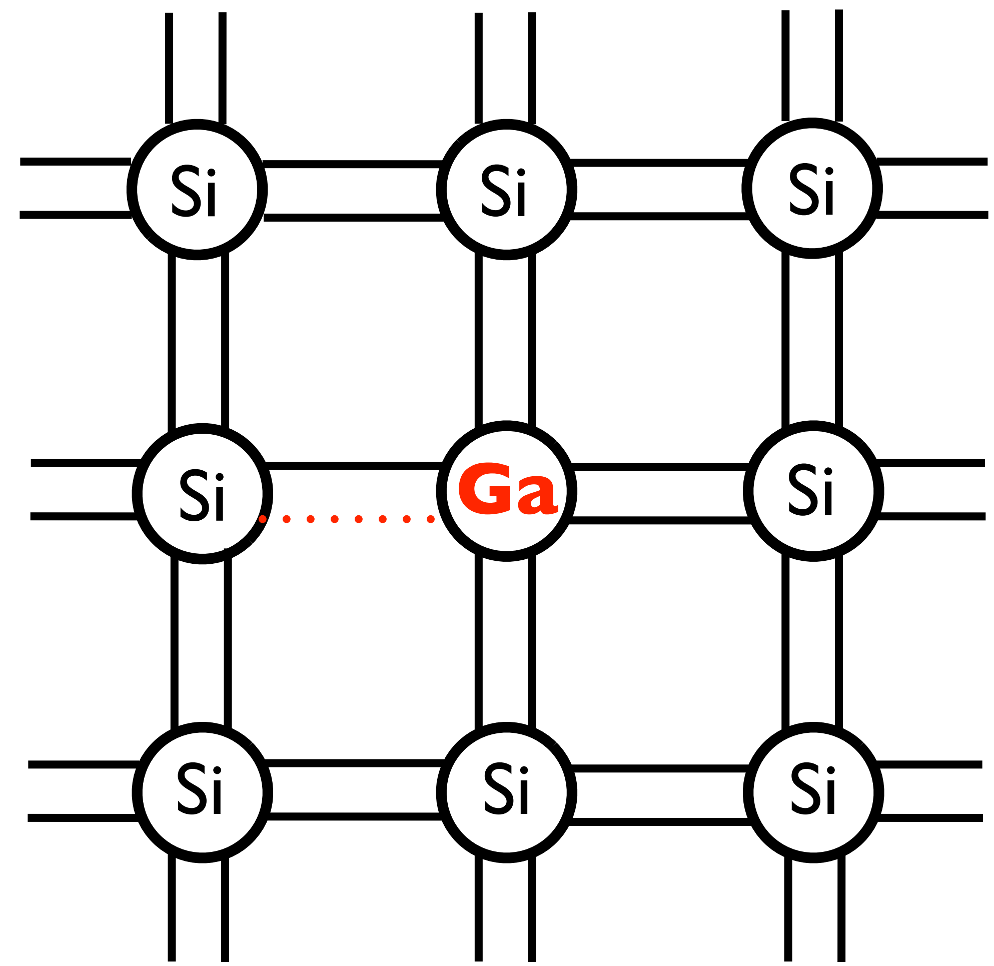

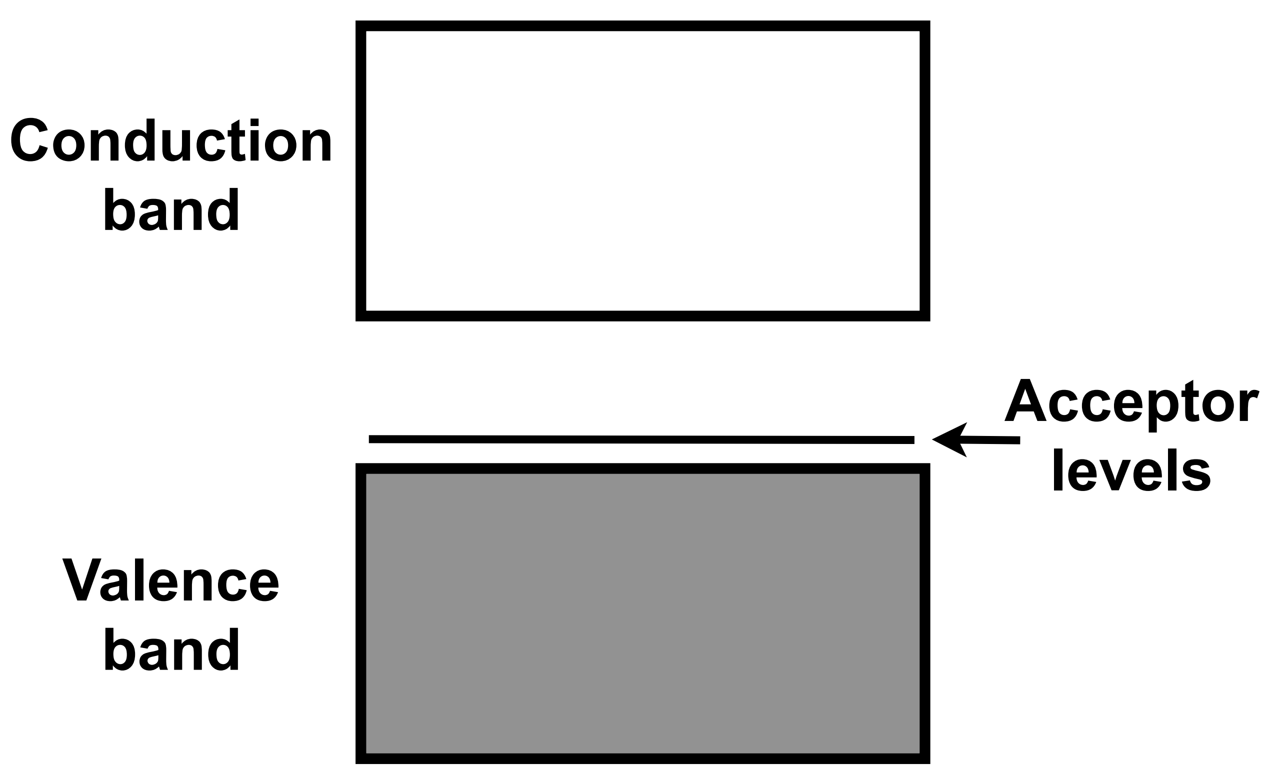

- ***Holes*** are the majority carrier.
- Energy gap between the acceptor levels and the valence band is small.
- Contributes to the hole concentration without adding electrons to the conduction band of the lattice.

Crystalline inorganic scintillators

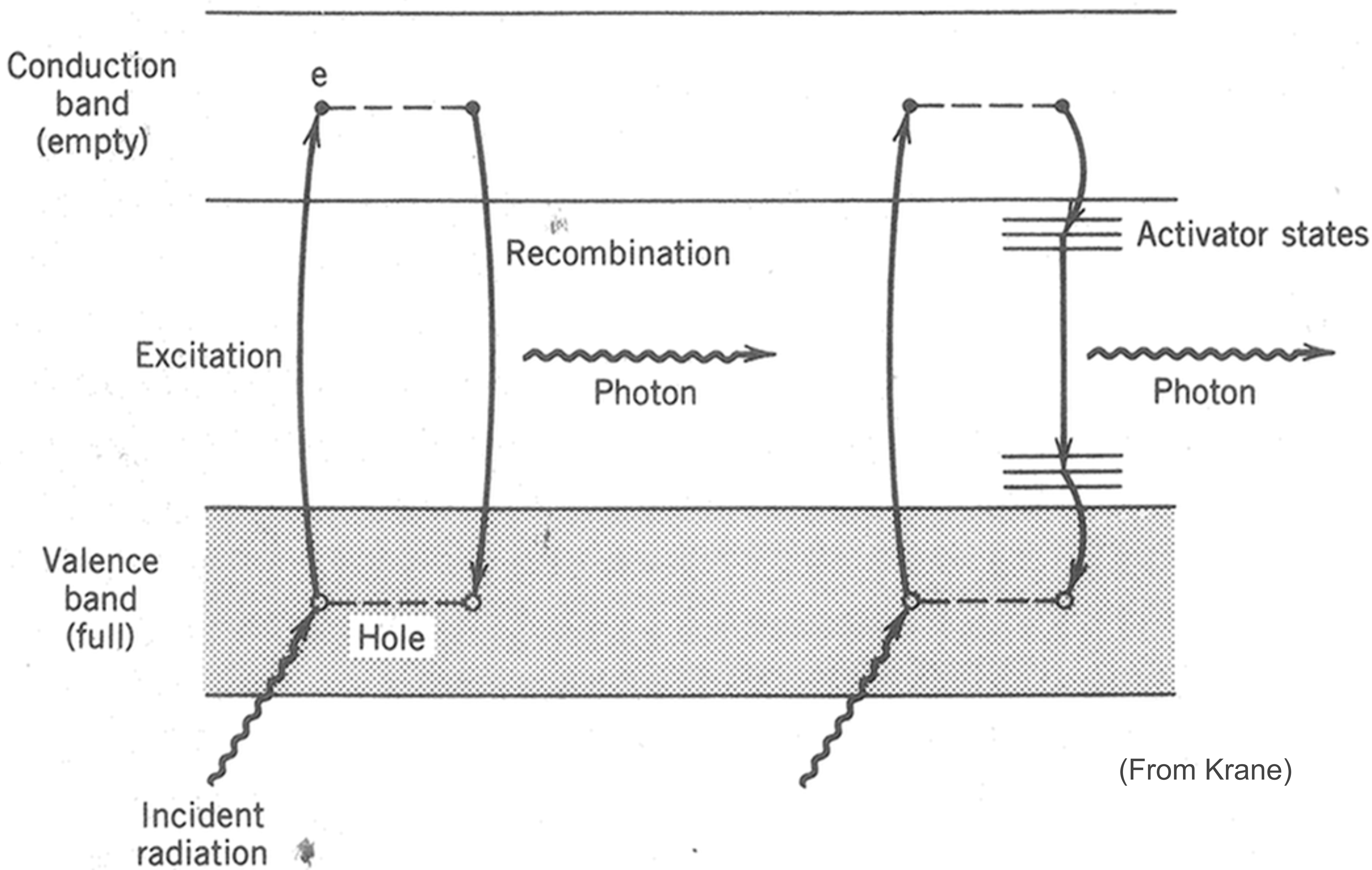

(From Krane)

The p-n junction

- Silicon detectors are based on the p-n junction.
- Formed by starting with a bulk n/p material and usually diffusing or implanting p/n impurities.
- Near the n-type region the concentration is dominated by the donor impurities.
- At the junction interface N_A=N_D and the silicon is intrinsic.

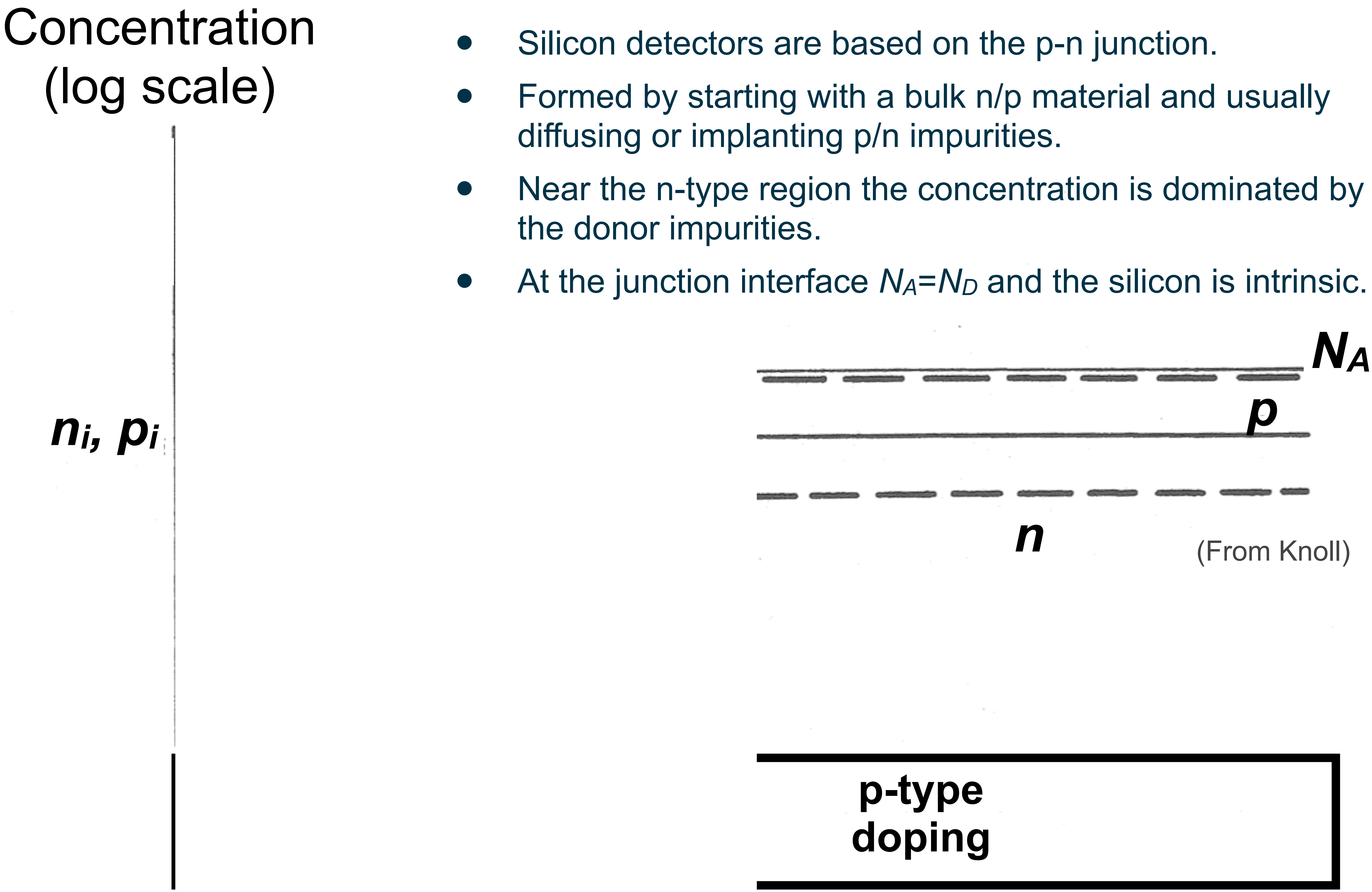

(From Knoll)

The p-n junction

- Silicon detectors are based on the p-n junction.
- Formed by starting with a bulk n/p material and usually diffusing or implanting p/n impurities.
- Near the n-type region the concentration is dominated by the donor impurities.
- At the junction interface N_A=N_D and the silicon is intrinsic.

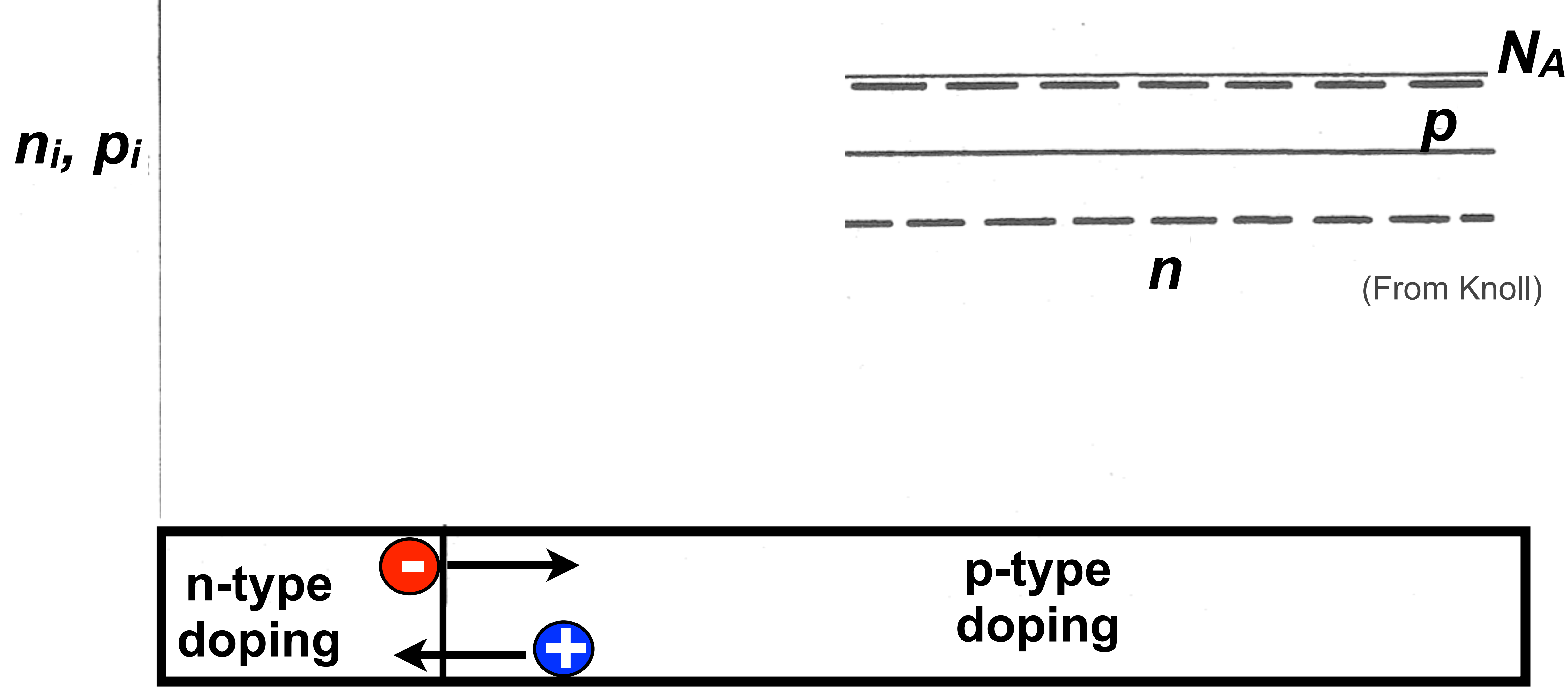

The p-n junction

- Silicon detectors are based on the p-n junction.
- Formed by starting with a bulk n/p material and usually diffusing or implanting p/n impurities.
- Near the n-type region the concentration is dominated by the donor impurities.
- At the junction interface $N_A = N_D$ and the silicon is intrinsic.

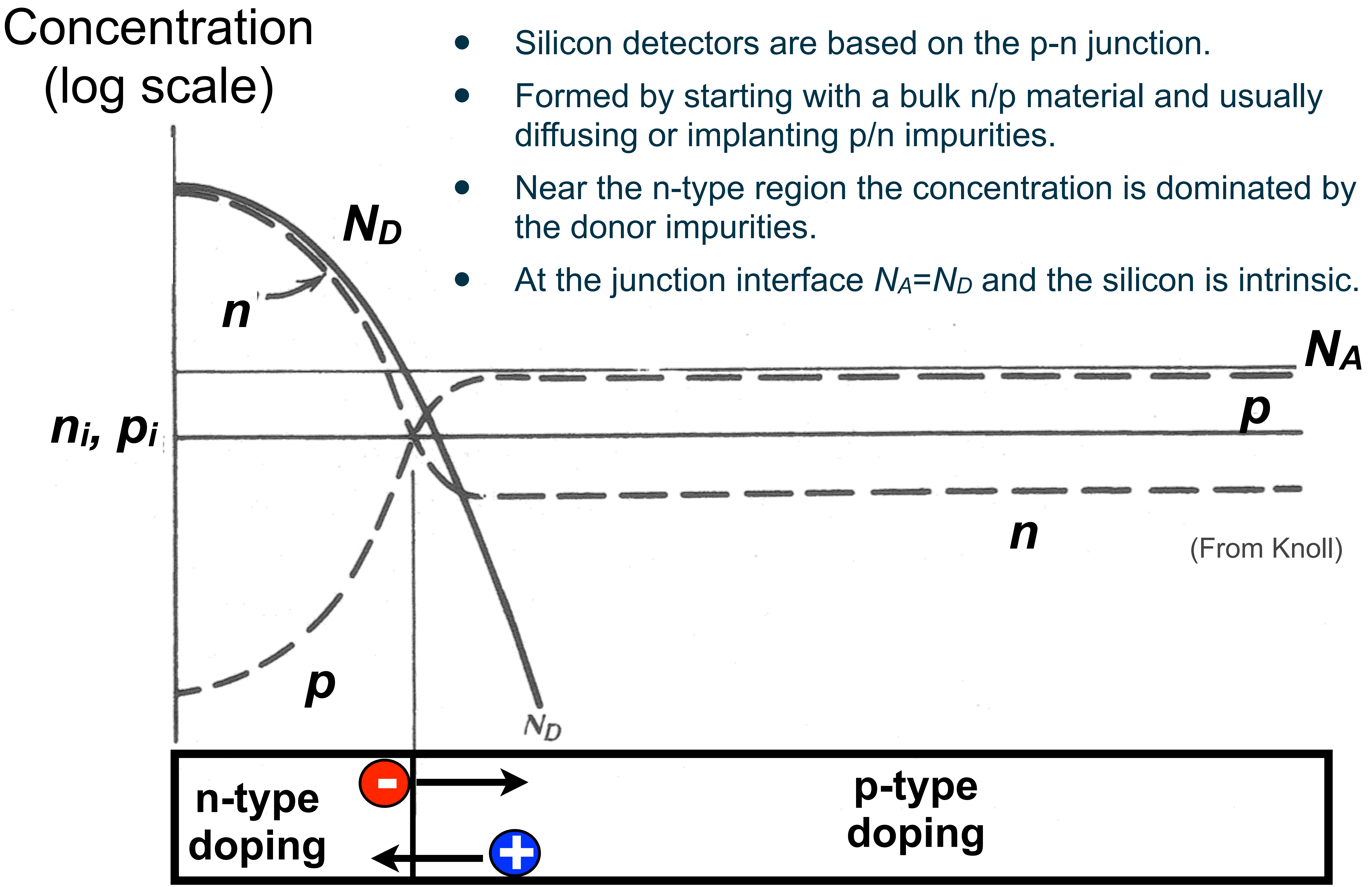

(From Knoll)

The p-n junction

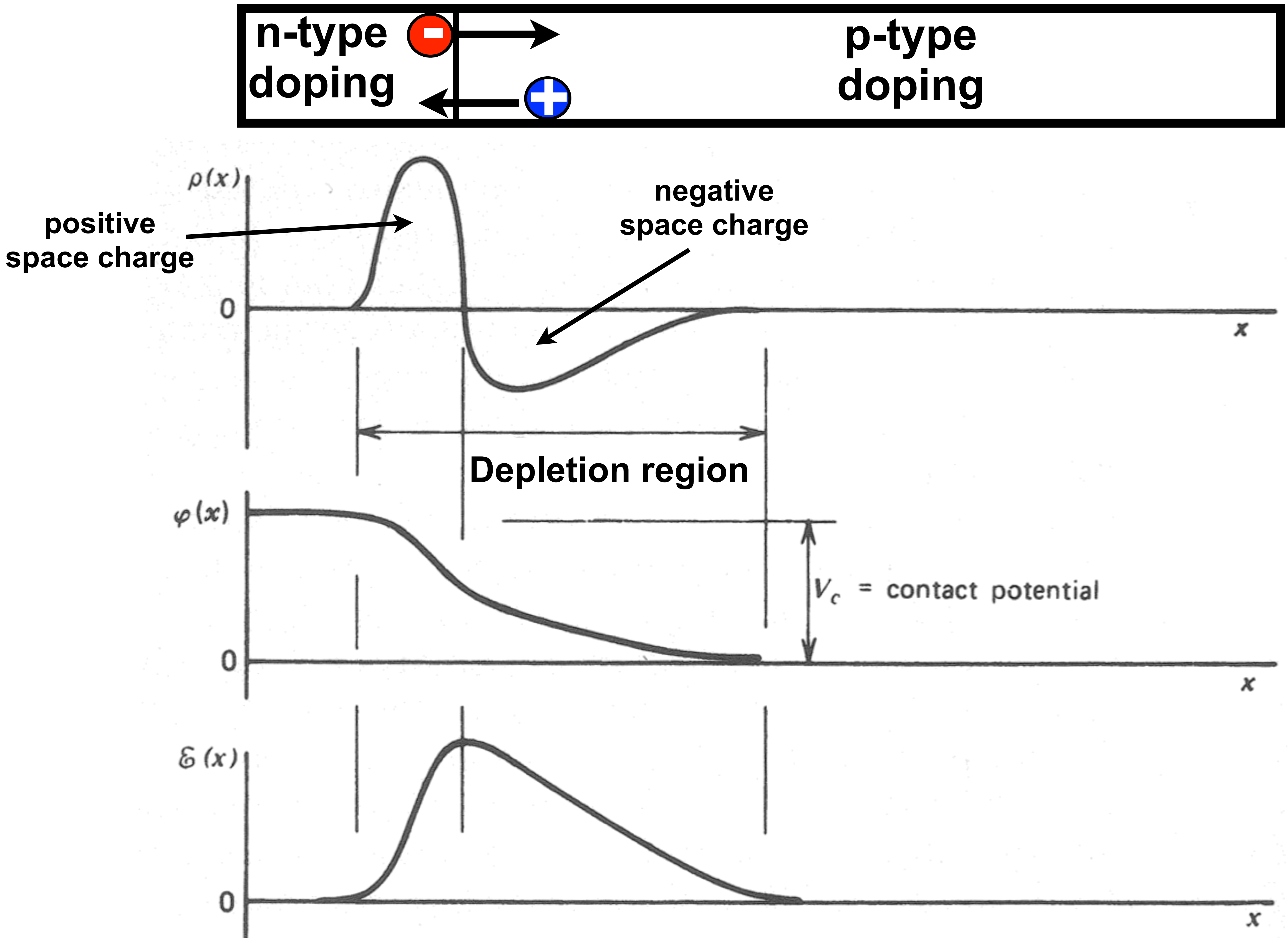

(From Knoll)

Fully depleted detector

- In the ***depletion region*** any electron-hole pairs are swept away by the electric field generated by the contact potential.
- **THIS IS VERY SIMILAR TO AN IONIZATION CHAMBER.**
- A detector is ***fully depleted*** when the electric field extends across the entire thickness of the detector.

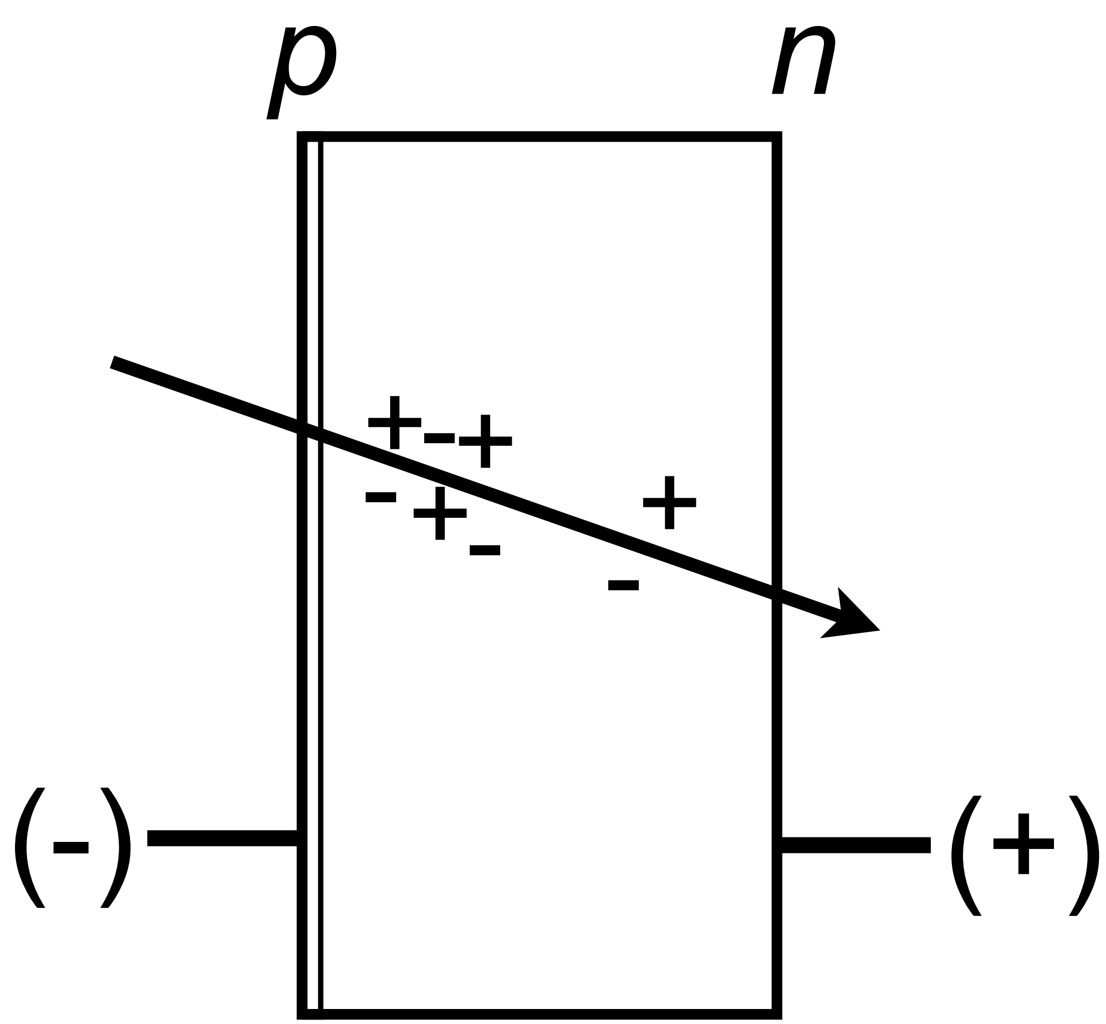

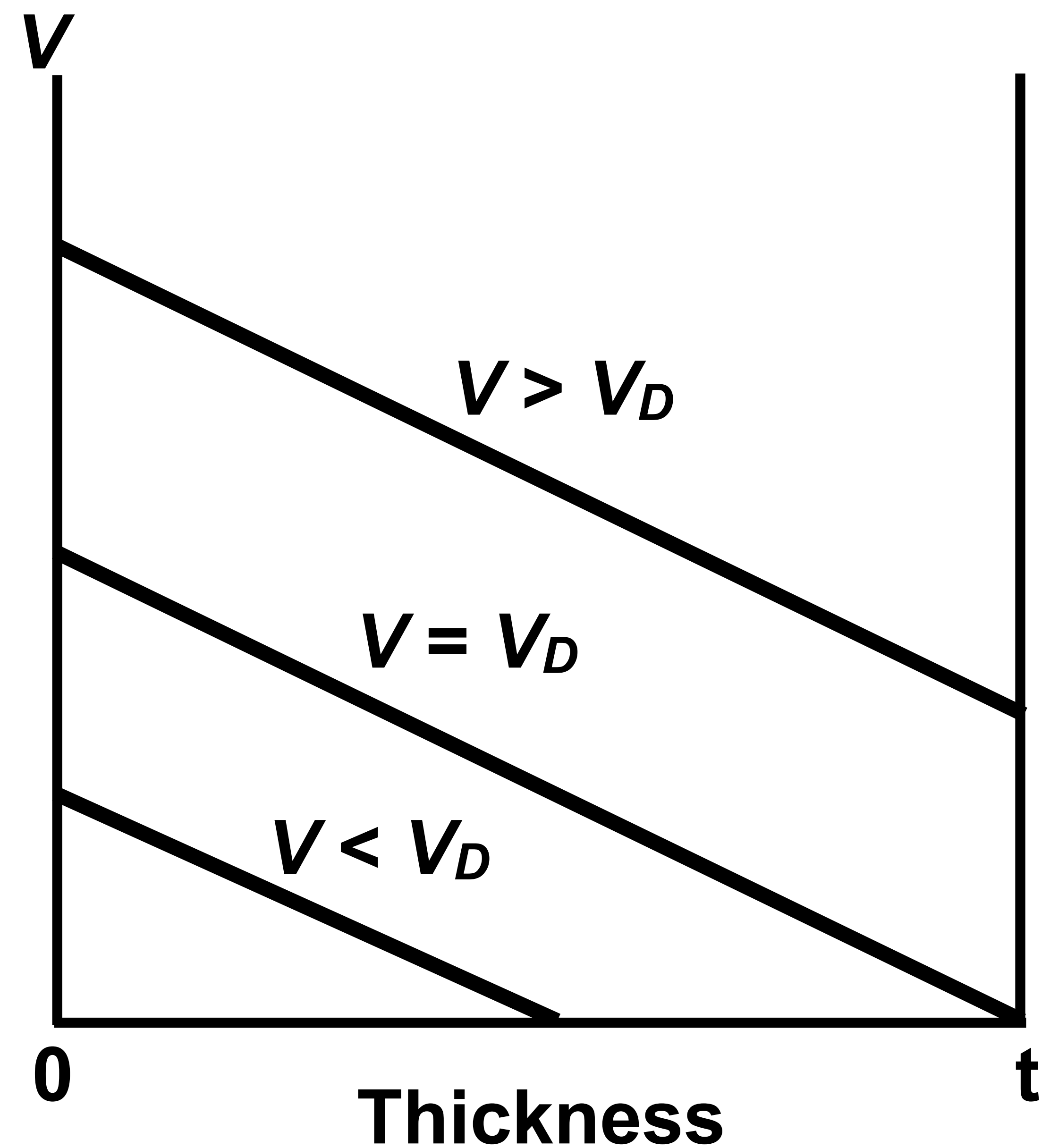

Silicon as a detector

- Silicon detectors are solid-state analogs of the ionization chamber.
- ***Unlike*** an ionization chamber, the mobility of the charge carriers (electrons and holes) are of the same order.
- At high enough voltages the charge-carrier velocity saturates and is on the order of,

$$10^7\mathrm{cm/s} \implies < 10 \text{ ns collection time}$$

for a detector 1mm thick.
- The amount of time it takes to collect the charge is effects the ***rise time*** of the signal and thus the timing response.
- Ionization energy of order 3eV compared to 30 eV for an ionization chamber.

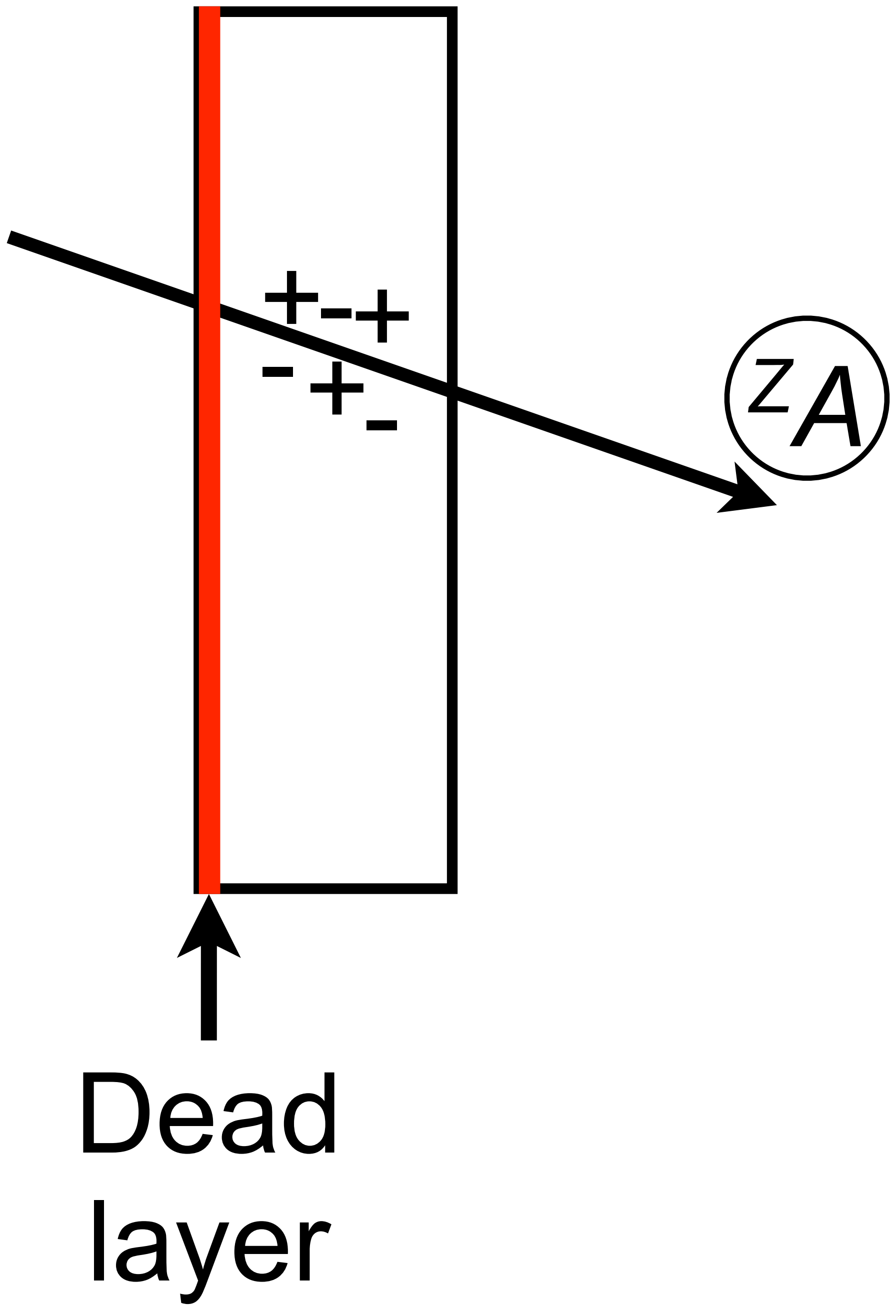

Dead layers

- We can control the active volume of a detector by controlling the depletion region.
- In a fully depleted detector almost the entire volume is active.
- However, there is always an inactive region of the detector called the ***dead layer.***
- This may be a non-negligible source of energy loss.

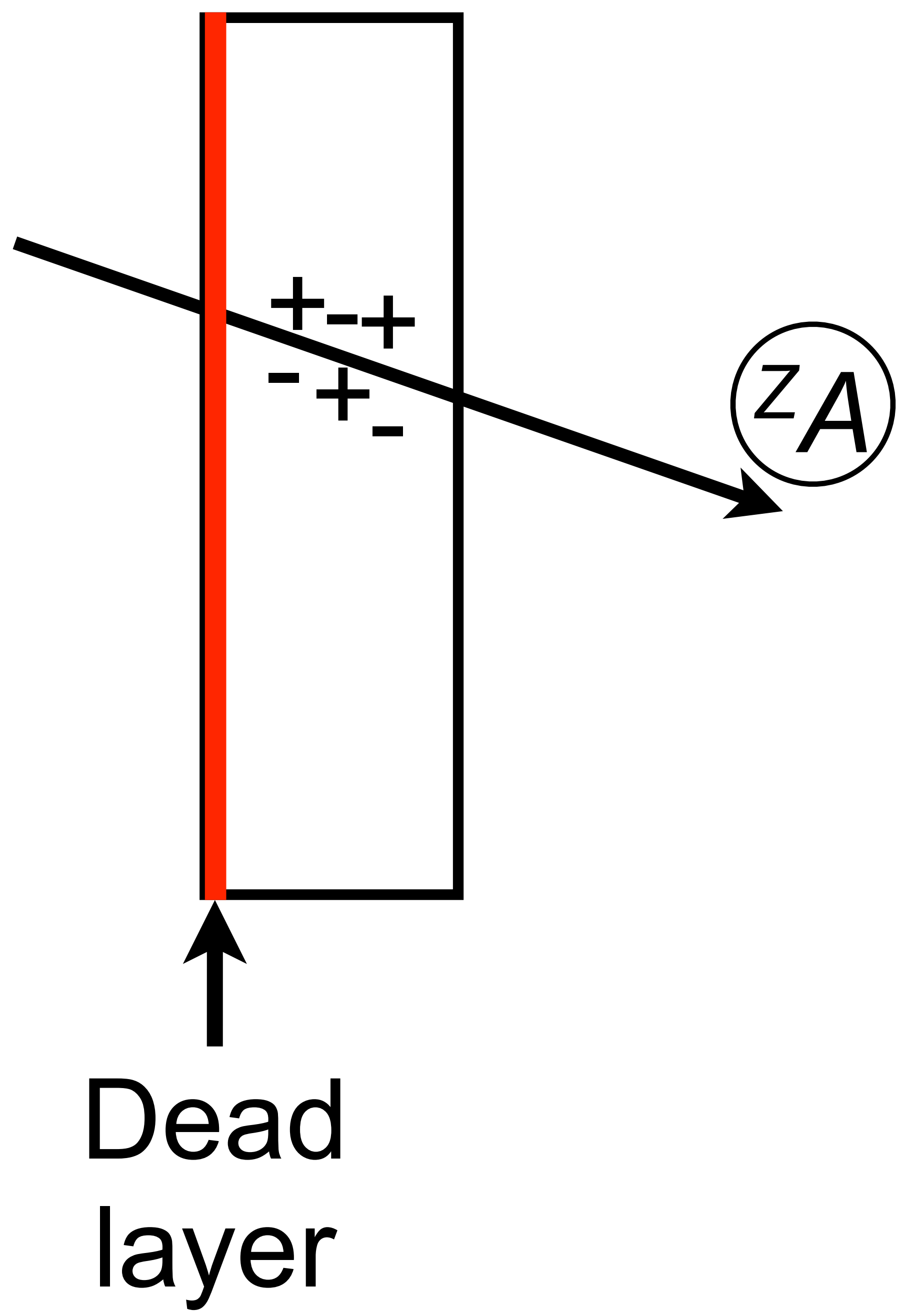

Silicon detectors

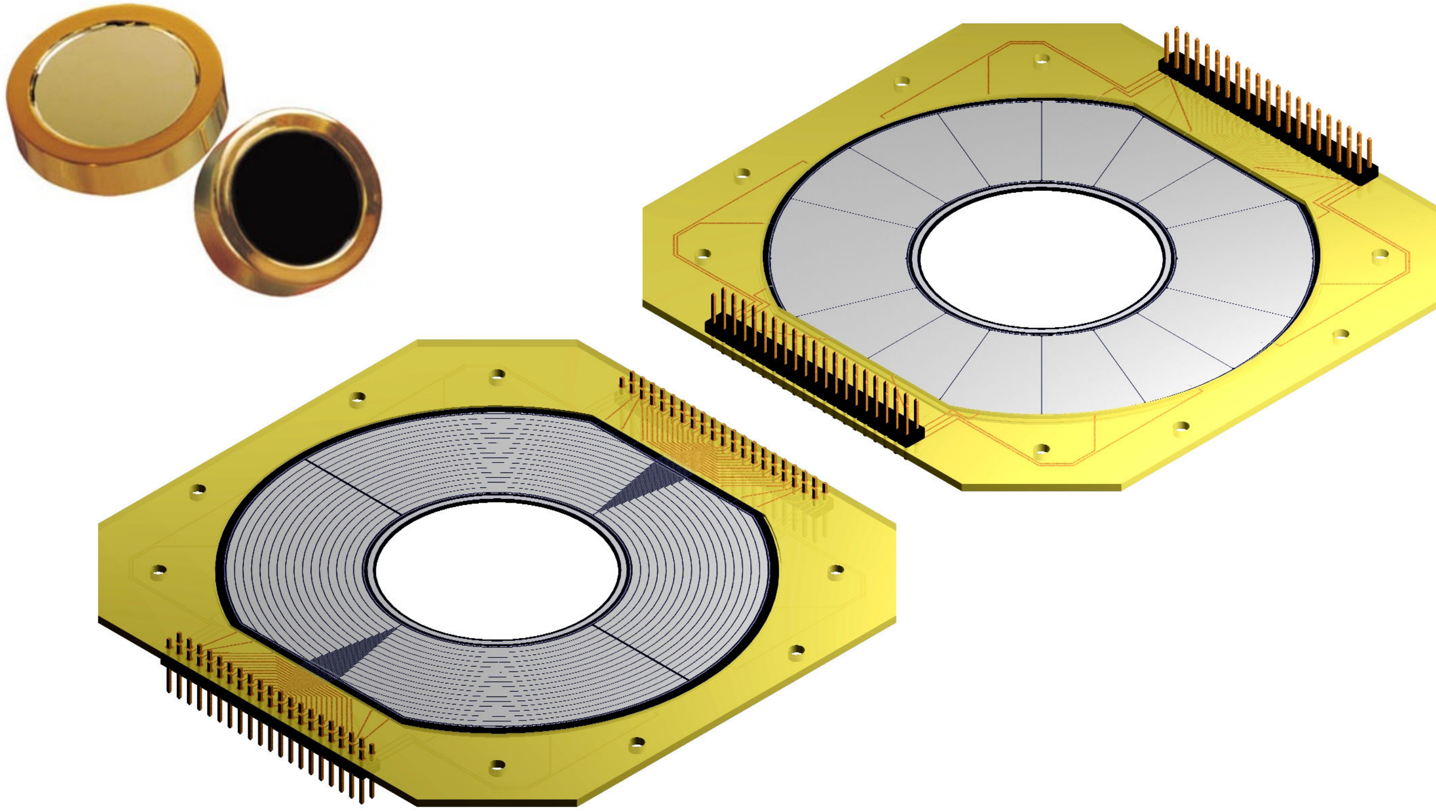

S1 detector and PCB as viewed from the p- and n-side.

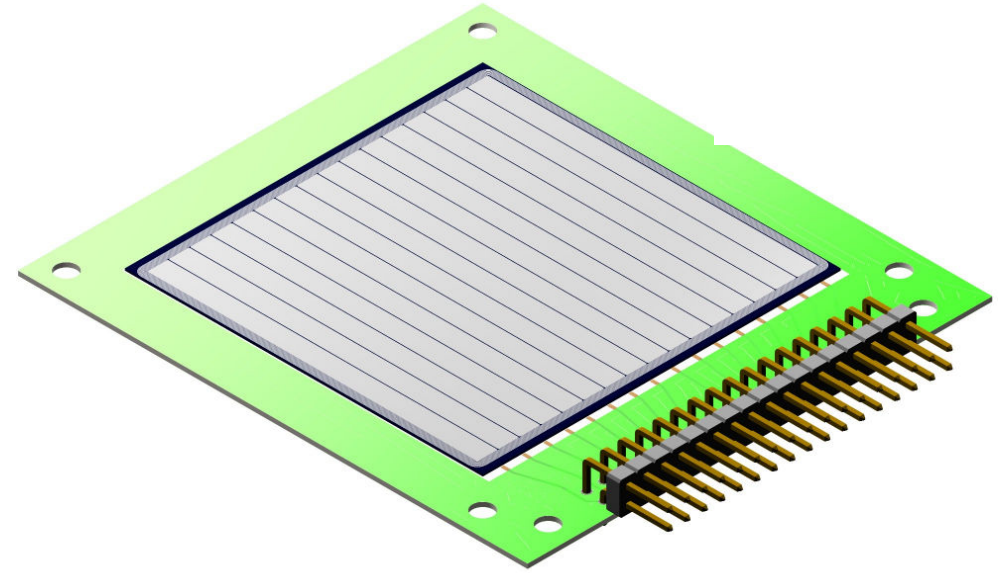

Design W1(DS)-300 2M/2M on a standard ceramic transmission package.

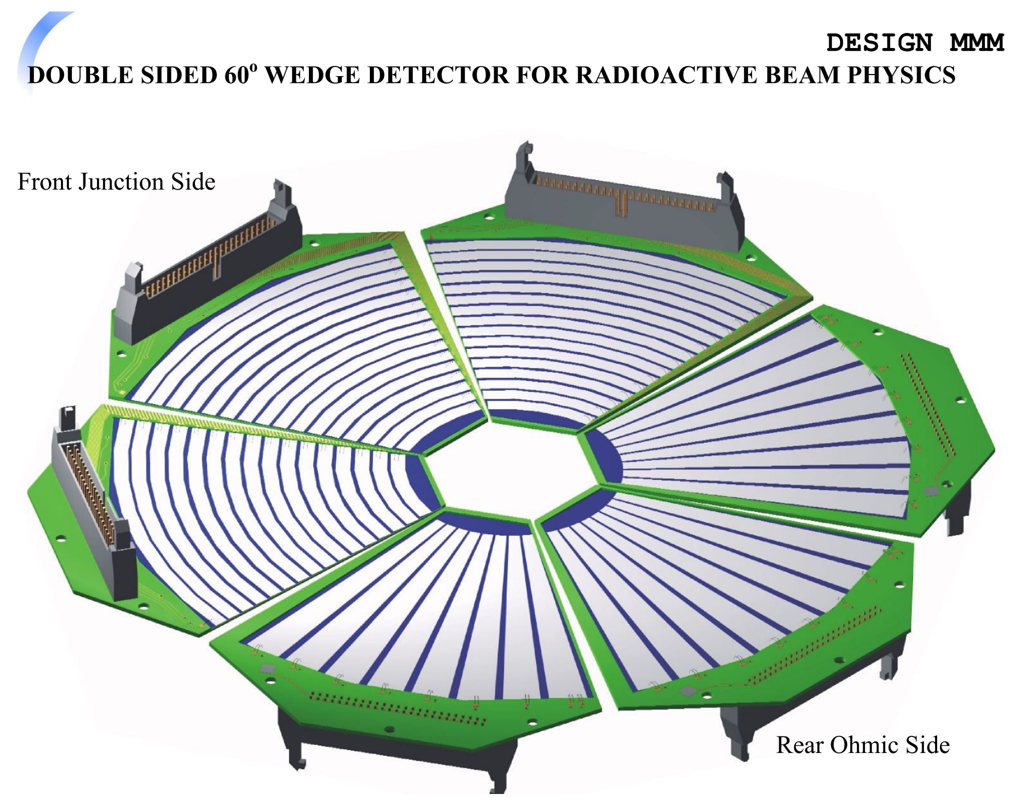

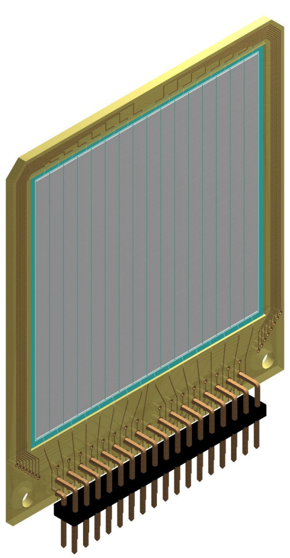

X1 Assembly

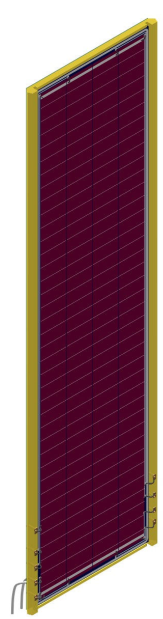

X2 Assembly

X3 Assembly

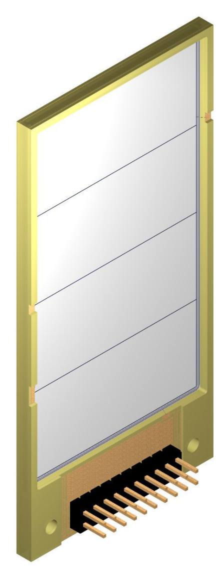

Super X3 with standard Pads on Rear

Spectroscopy with silicon

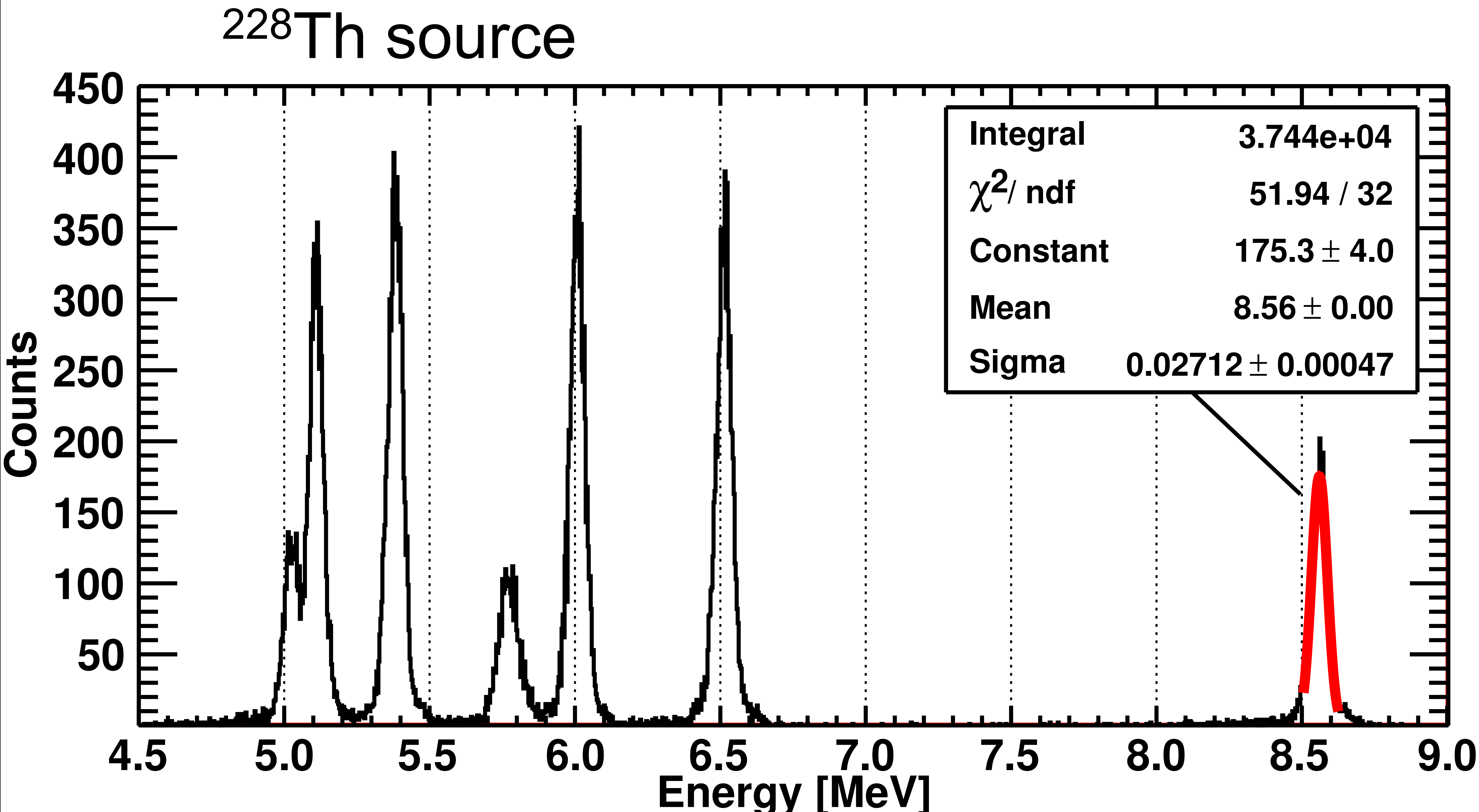

ΔE-E particle identification

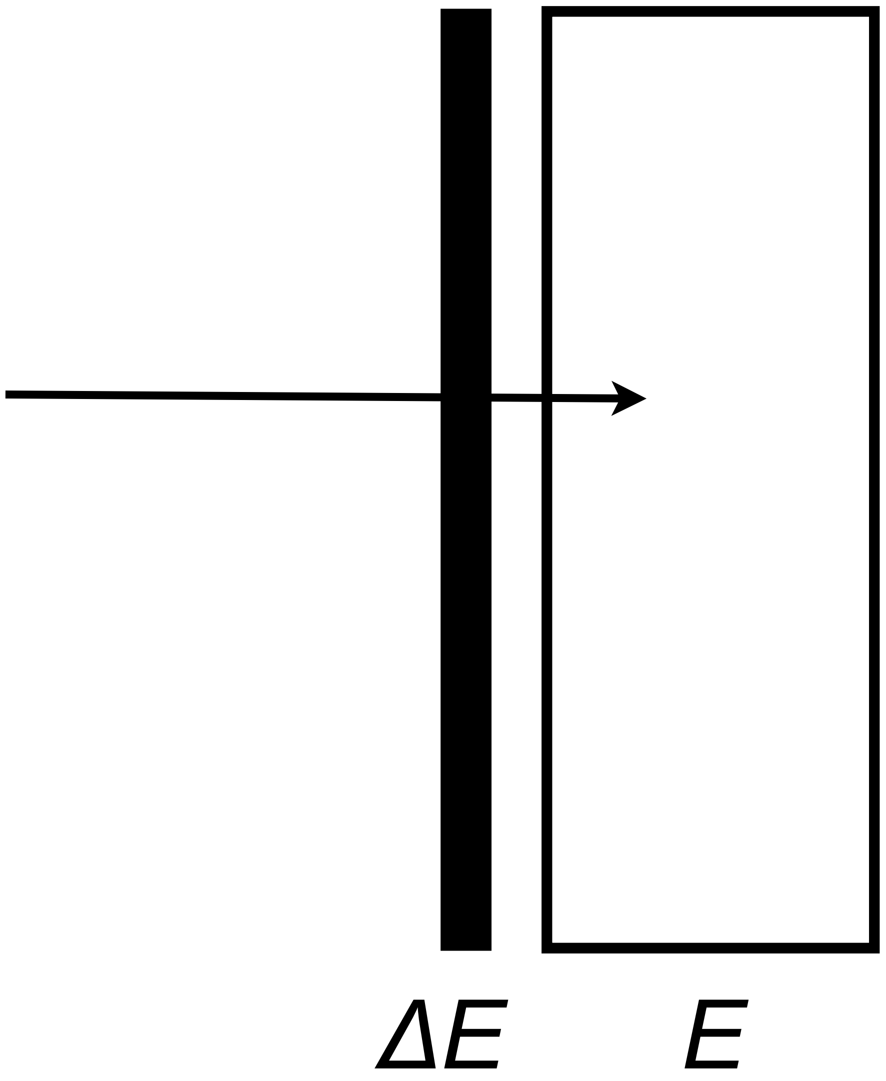

- **If you remember back to the Bethe equation . . .**

$$\frac{dE}{dx} \propto \frac{m_z z^2}{E} \ln(C \frac{E}{m_z})$$

Δ*E*-*E* particle identification

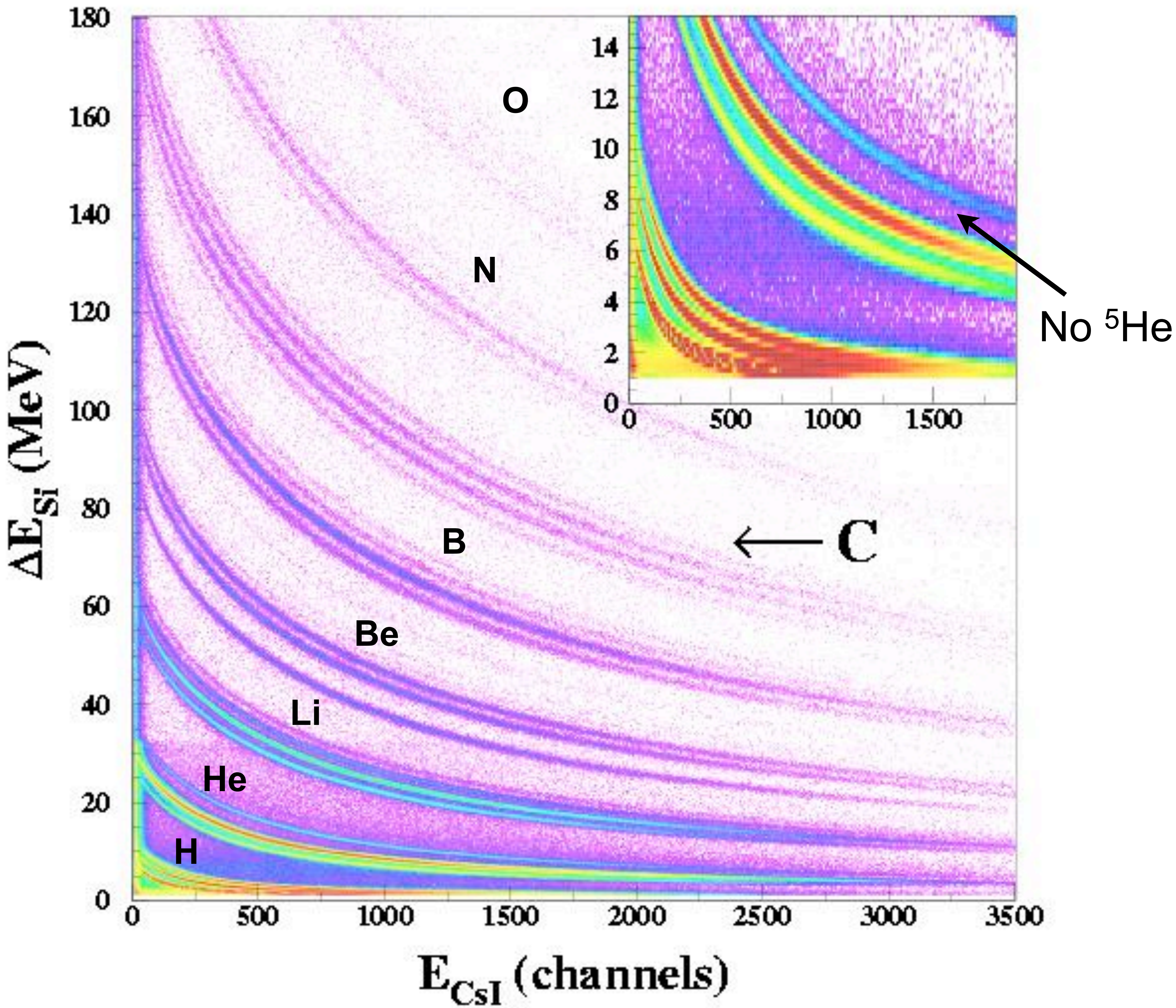

Science with EXOTIC BEAMS

Exotic-beam decay spectroscopy

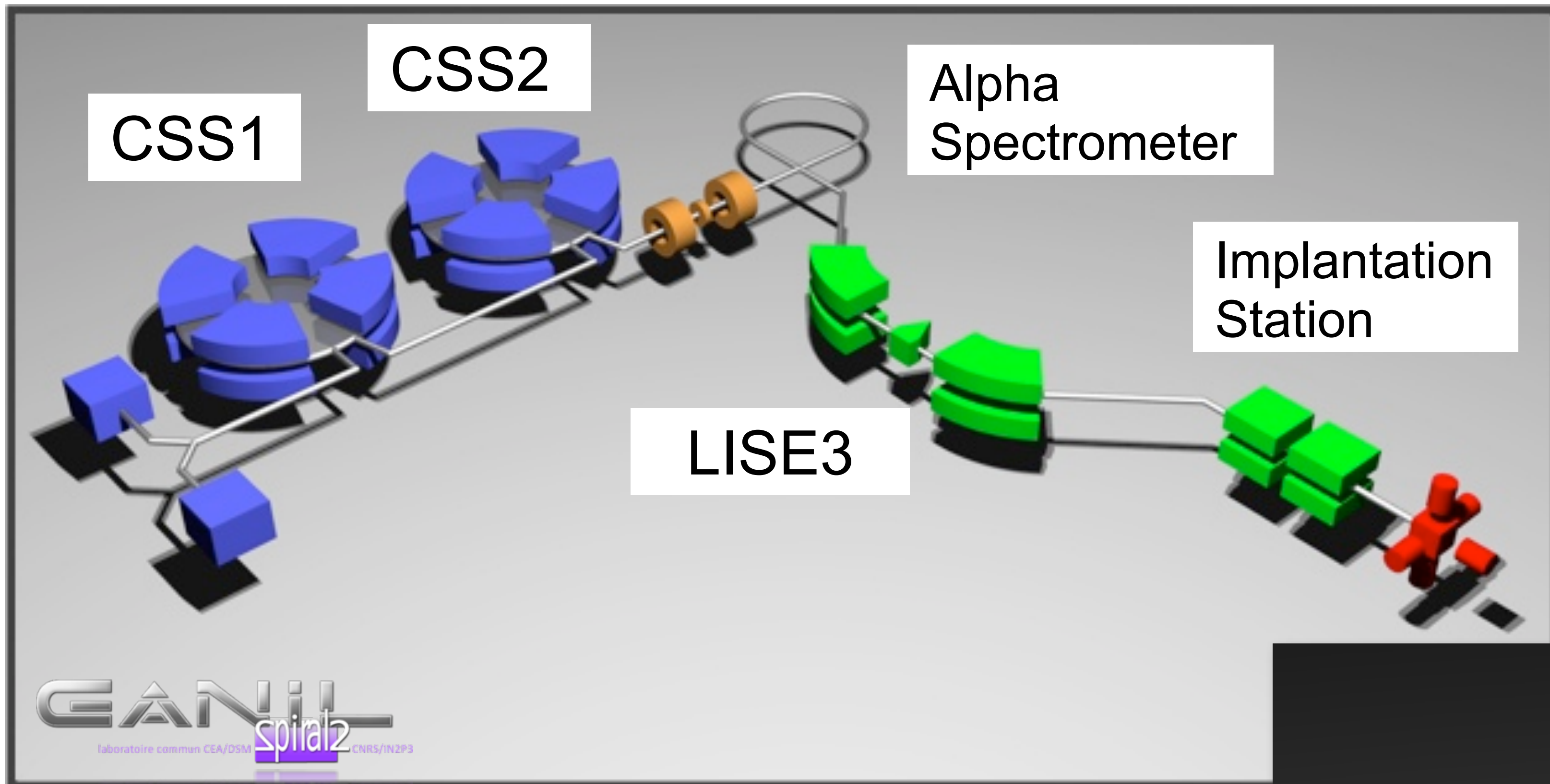

- Fragmentation of ^{78}Kr primary beam on a ^{nat}Ni target.
- ***E* = 70 MeV/u**
- Implant-decay experiment using ***β-p*** and ***β-γ*** event tagging.

- ToF from RF and MCP's.
- **300-μm Si Δ*E*** detector and **300-μm Si degrader**.
- Heavy ions are implanted into a **16x16 strip DSSD** (3-mm pitch, 300 μm thick).
- γ's are measured using four high-purity germanium clover detectors (HPGe).

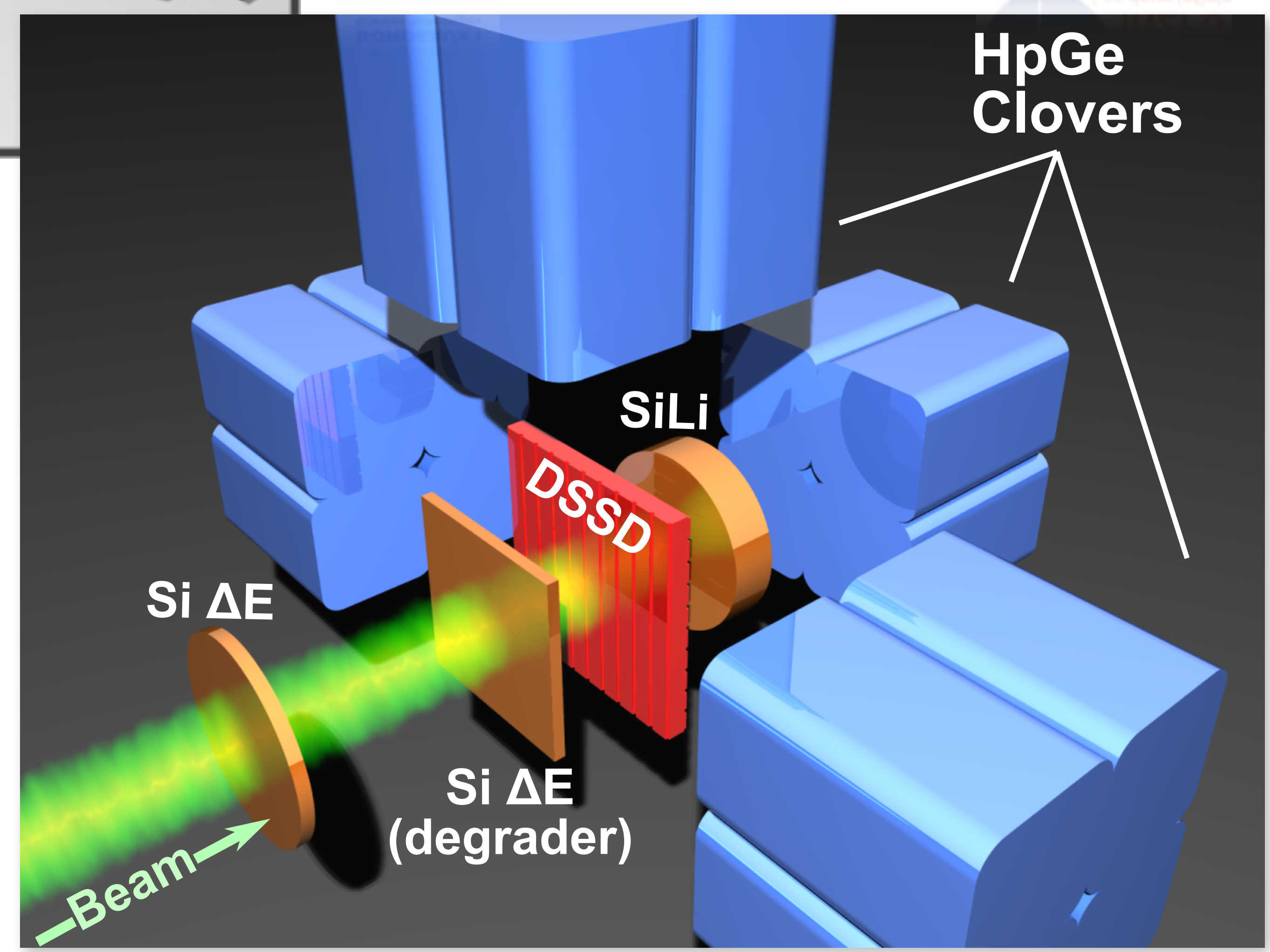

Exotic-beam decay spectroscopy

- **PID**
  - Energy loss from silicon
  - ToF from RF and MCP
- **Energy Degrader**
  - Decreases heavy ion energy
  - Optimized to stop nuclei in the middle of the DSSD
- **Charged-particle spectroscopy (DSSD)**
- **VETO (SiLi)**
- **Gamma spectroscopy**
  - 4 HPGe clovers
  - Detect coincident gamma rays

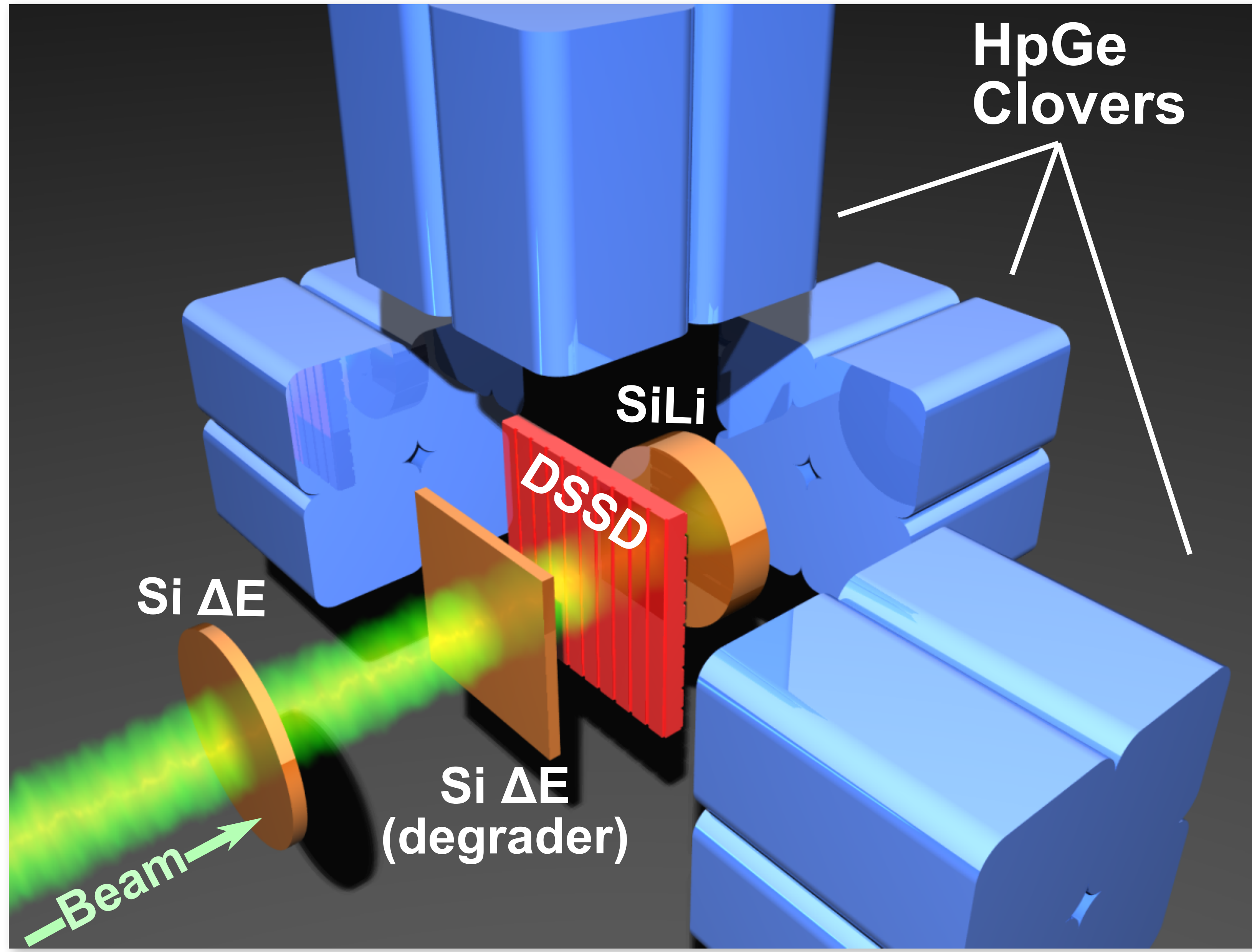

Exotic-beam decay spectroscopy

- **PID**
  - Energy loss from silicon
  - ToF from RF and MCP
- **Energy Degrader**
  - Decreases heavy ion energy
  - Optimized to stop nuclei in the middle of the DSSD
- **Charged-particle spectroscopy (DSSD)**
- **VETO (SiLi)**
- **Gamma spectroscopy**
  - 4 HPGe clovers
  - Detect coincident gamma rays

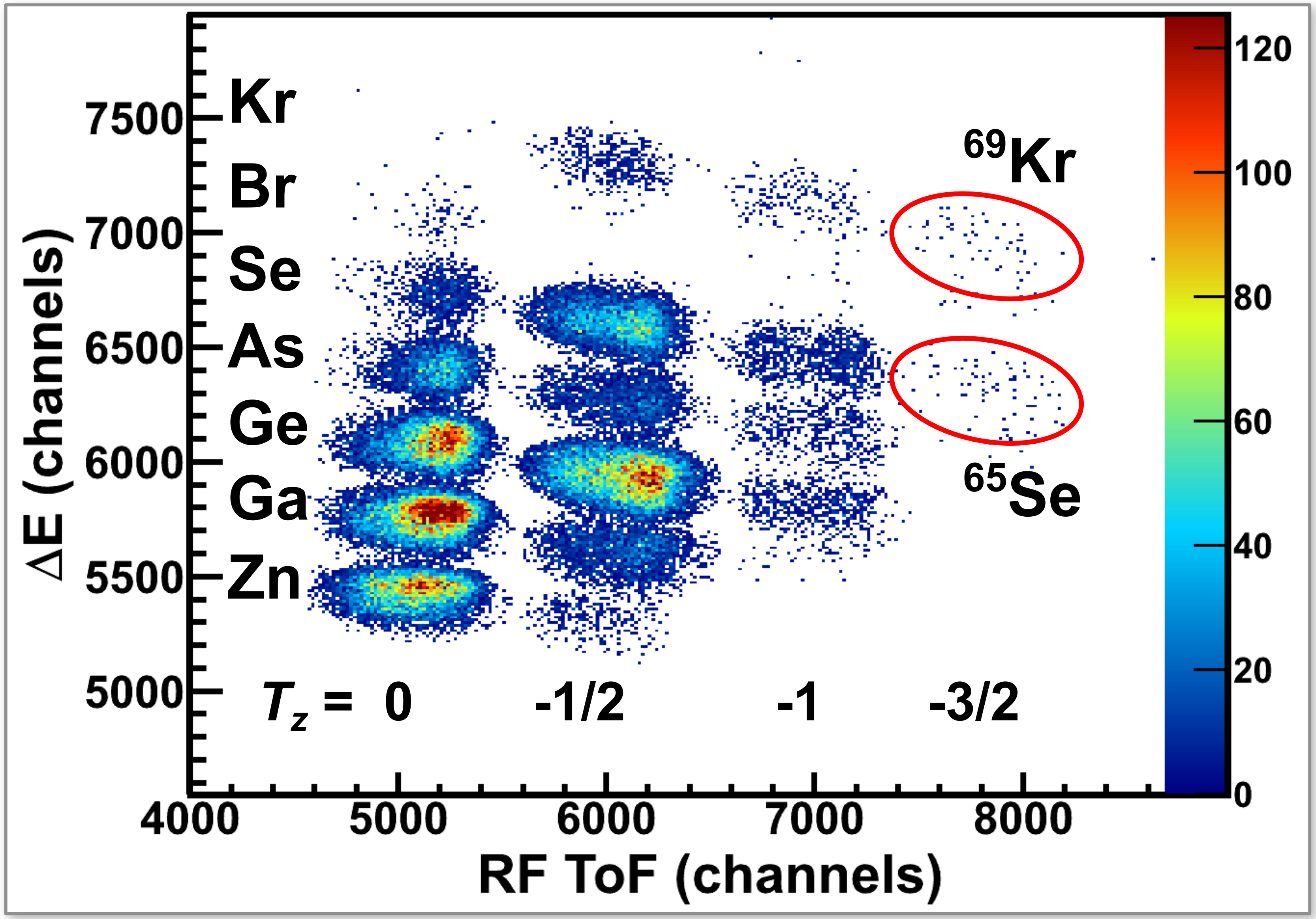

Exotic-beam decay spectroscopy

- **PID**
  - Energy loss from silicon
  - ToF from RF and MCP
- **Energy Degrader**
  - Decreases heavy ion energy
  - Optimized to stop nuclei in the middle of the DSSD
- **Charged-particle spectroscopy (DSSD)**
- **VETO (SiLi)**
- **Gamma spectroscopy**
  - 4 HPGe clovers
  - Detect coincident gamma rays

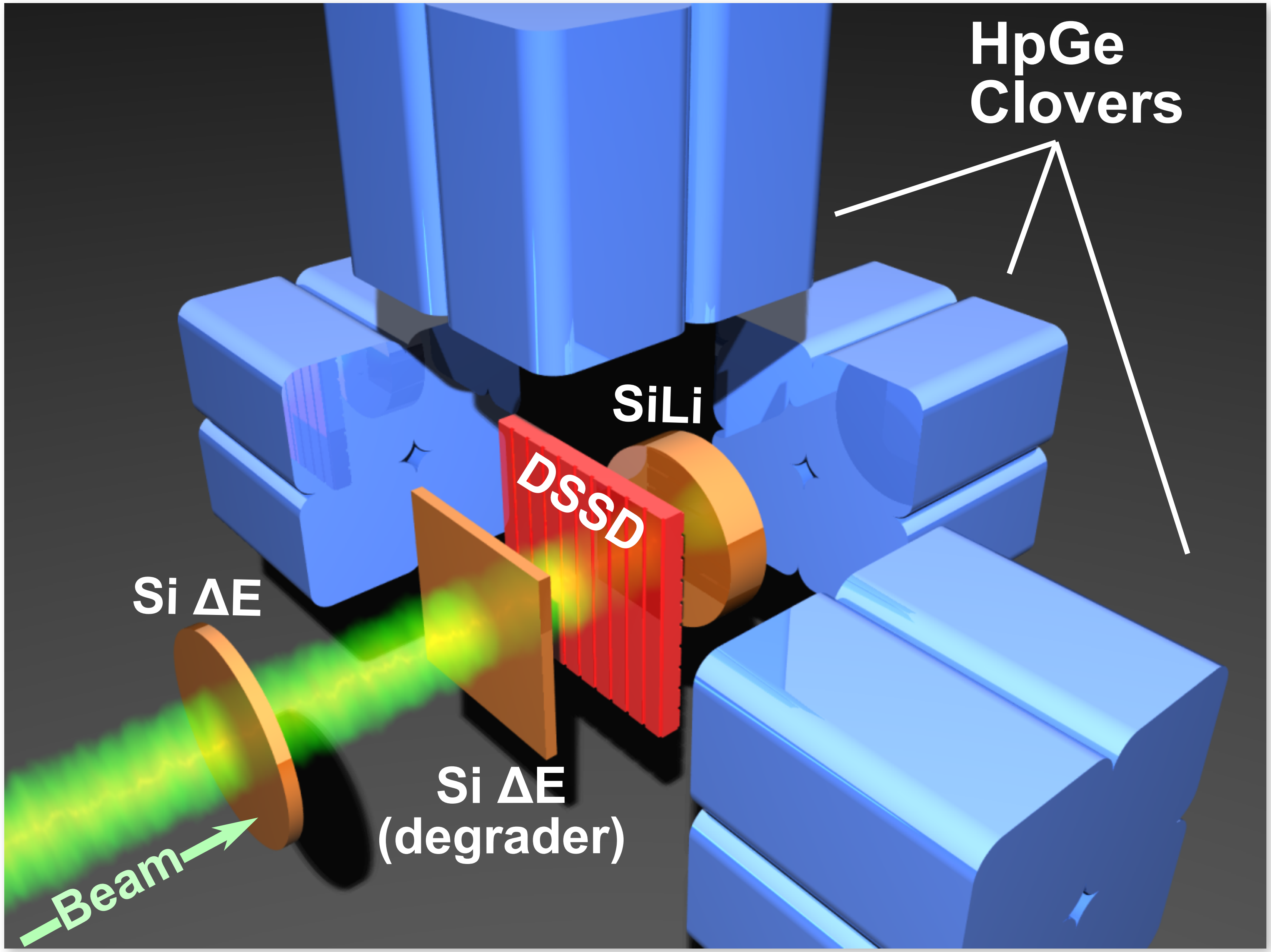

Exotic-beam decay spectroscopy

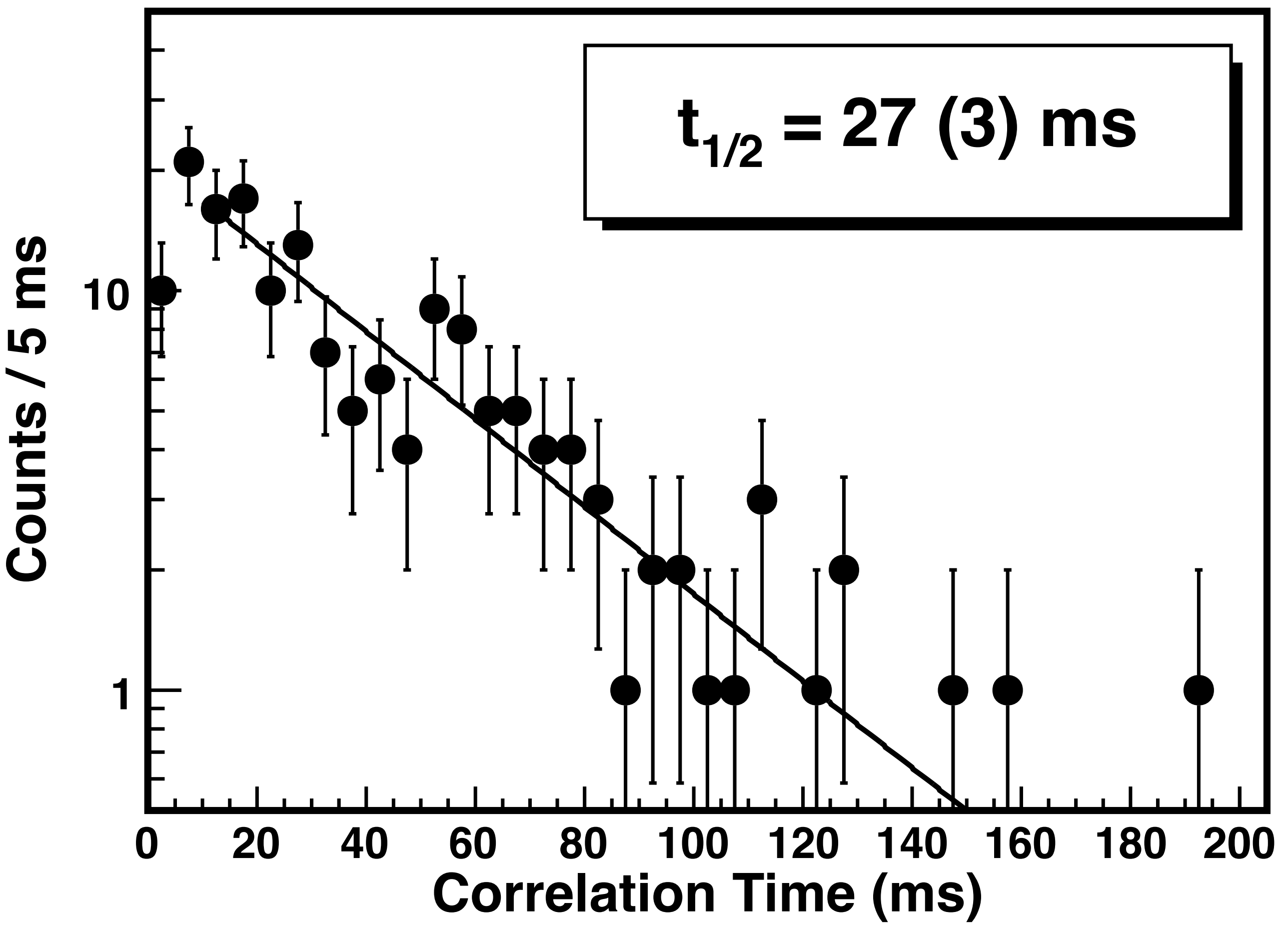

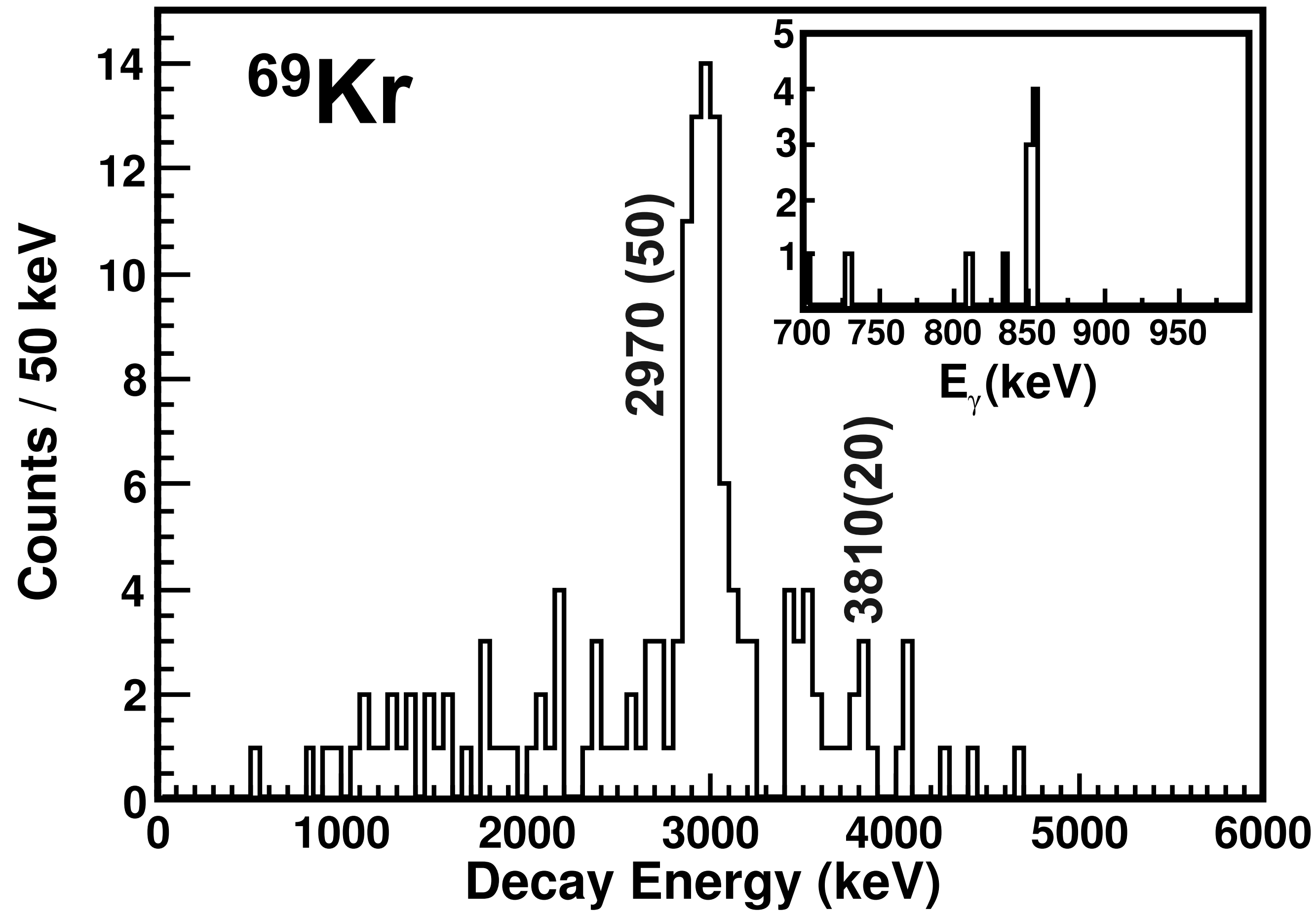

- **Time** between heavy-ion implantation event and decay event in DSSD allows us to measure the **decay curve**.
- **Charged-particle spectroscopy** in the DSSD allows us to observe proton emission.
- **DSSD pixelation** allows us to spatially correlate the correct heavy ion with it’s charged-particle decay.

Exotic-beam decay spectroscopy

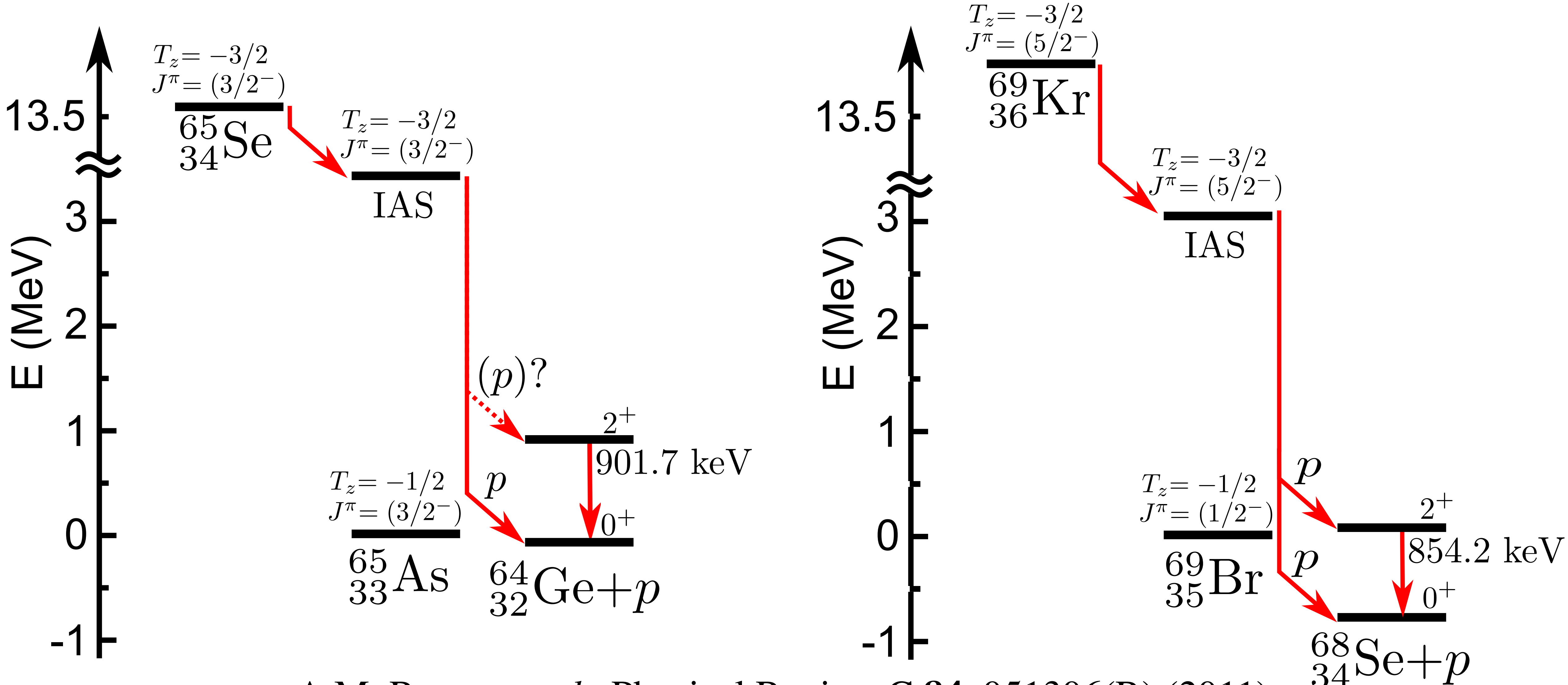

A.M. Rogers *et al.*, Physical Review C **84**, 051306(R) (2011)

Nucleus	$t_{1/2}$ (ms)	Feeding to IAS (%)	log(*ft*)	ME (keV)	ΔME_{AME}(keV)
^{65}Se	33(4)	52(18)	3.44(17)	−33358(141)	+438
^{69}Kr	27(3)	50(19)	3.53(18)	−32128(96)	−312

- Upper limit on proton-branching ratio to the ^{69}Br ground state of < 5%.

HELIcal Orbit Spectrometer (HELIOS)

- Novel spectrometer designed for reaction studies in inverse kinematics.
- ATLAS and future CARIBU beams.

$$r = \frac{mv_\perp}{qeB}$$

$$T_{\rm cyc} = \frac{2\pi r}{v_\perp} = \frac{2\pi}{B}\frac{m}{qe}$$

$$E_{\rm cm} = E_{\rm lab} + \frac{m}{2}V_{\rm cm}^2 - \frac{mV_{\rm cm}}{T_{\rm cyc}}z$$

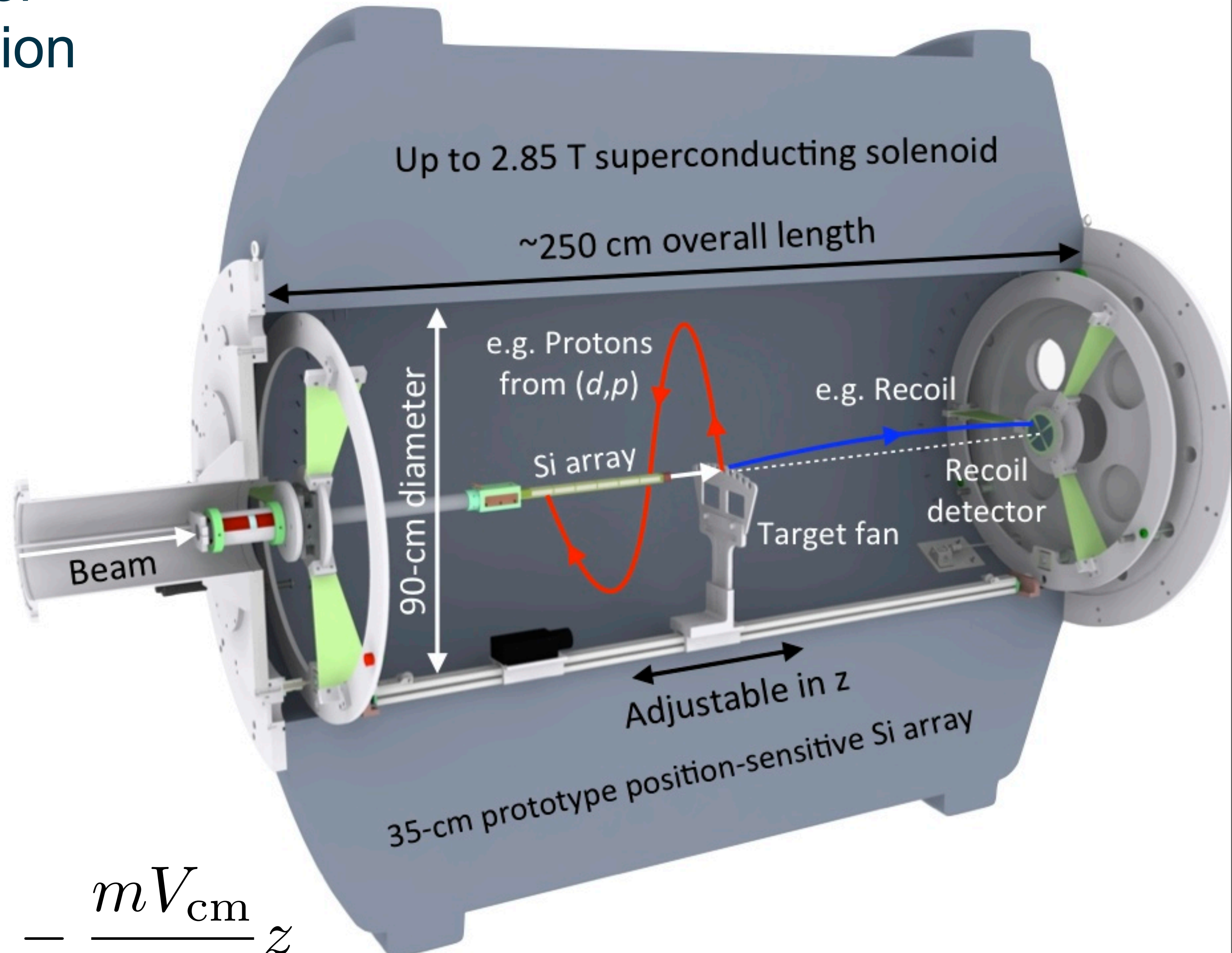

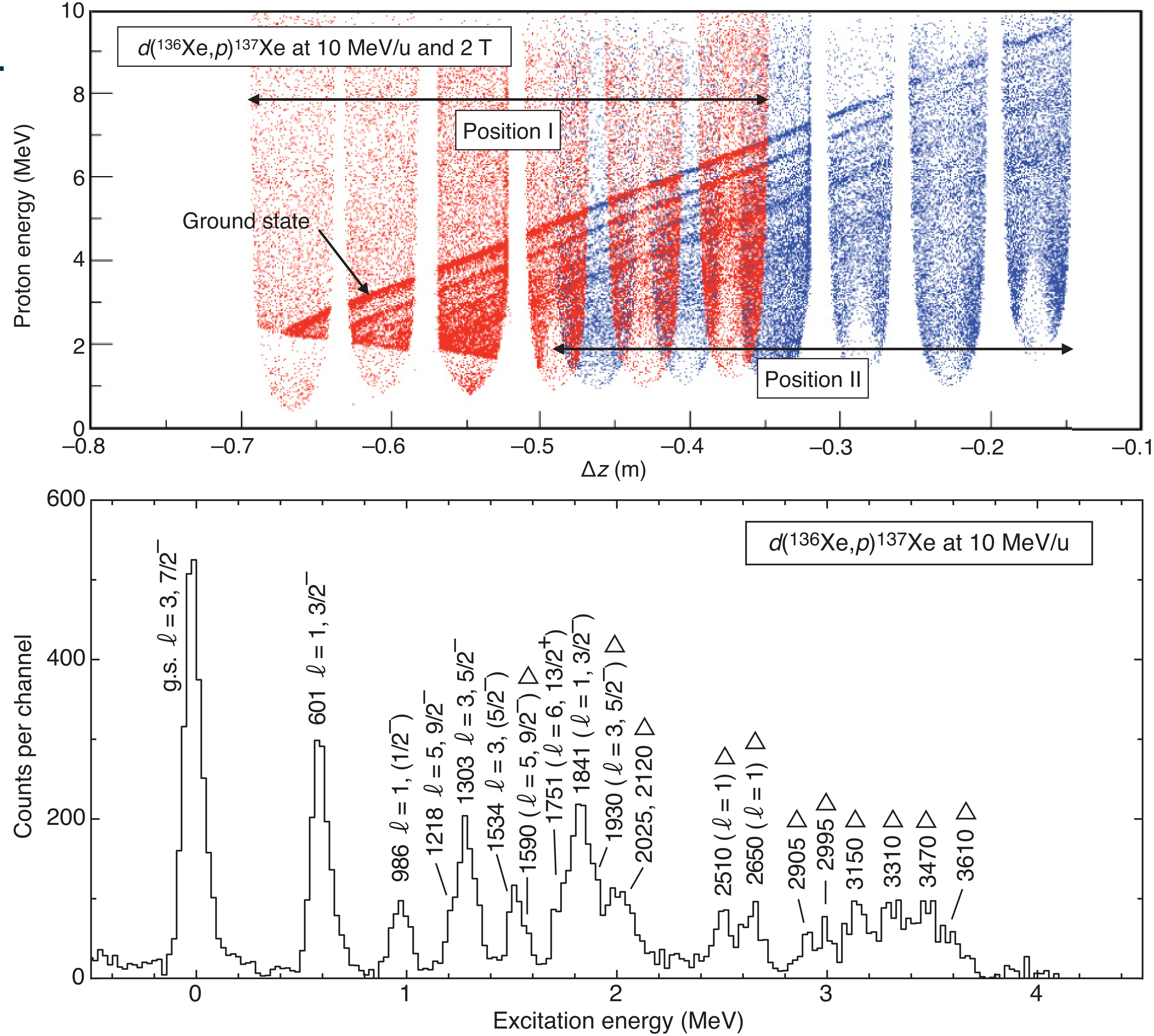

d(136Xe,p)137Xe at 10 MeV/u and 2 T
Position I
Position II
Ground state
Proton energy (MeV)
Δz (m)
d(136Xe,p)137Xe at 10 MeV/u
g.s. ℓ = 3, 7/2−
601 ℓ = 1, 3/2−
986 ℓ = 1, (1/2−)
1218 ℓ = 5, 9/2−
1303 ℓ = 3, 5/2−
1534 ℓ = 3, (5/2−)
1590 (ℓ = 5, 9/2−)
1751 (ℓ = 6, 13/2+)
1841 (ℓ = 1, 3/2−)
1930 (ℓ = 3, 5/2−)
2025, 2120
2510 (ℓ = 1)
2650 (ℓ = 1)
2905
2995
3150
3310
3470
3610
Counts per channel
Excitation energy (MeV)

B.P. Kay *et al.*

HELIcal Orbit Spectrometer (HELIOS)

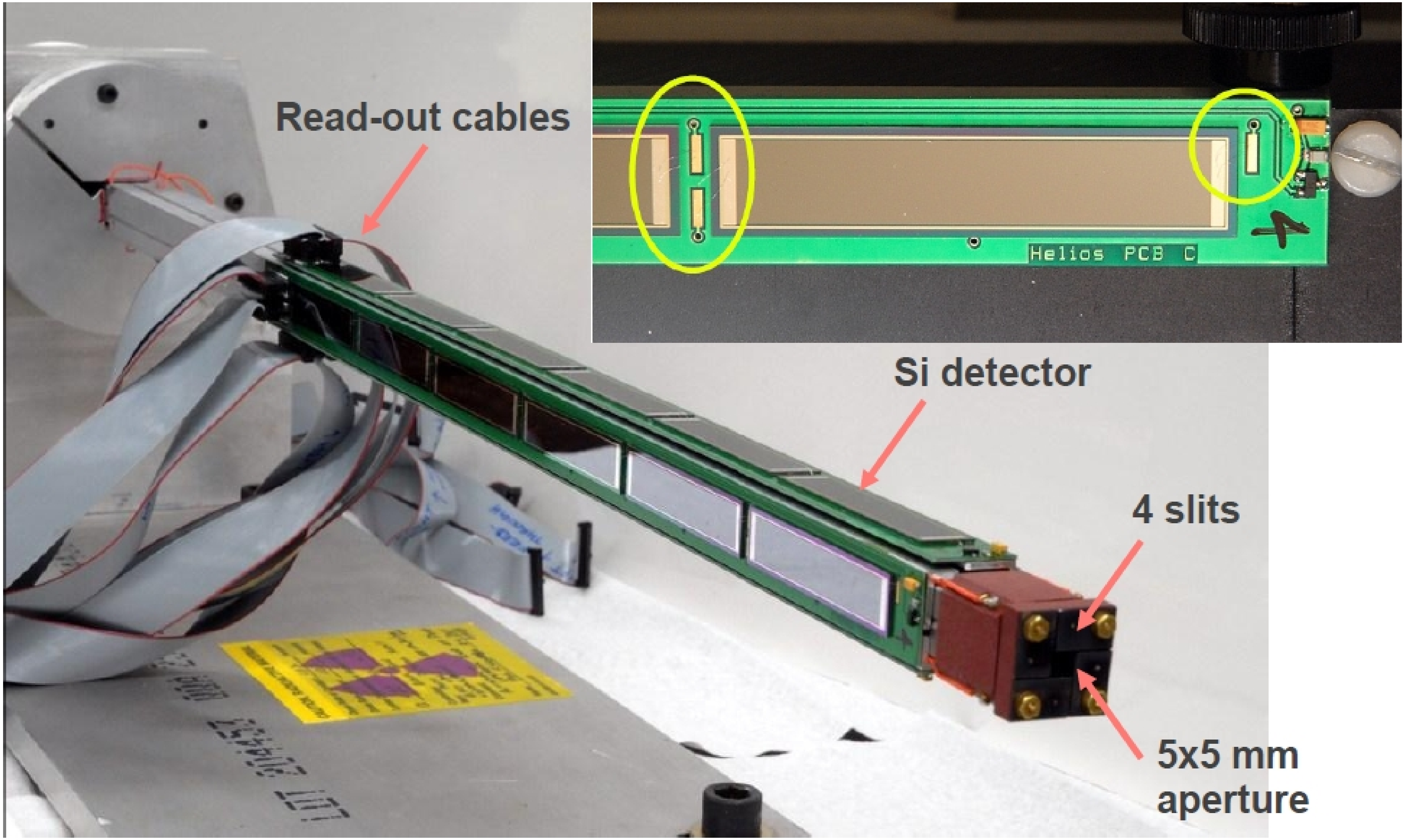

HELIcal Orbit Spectrometer (HELIOS)

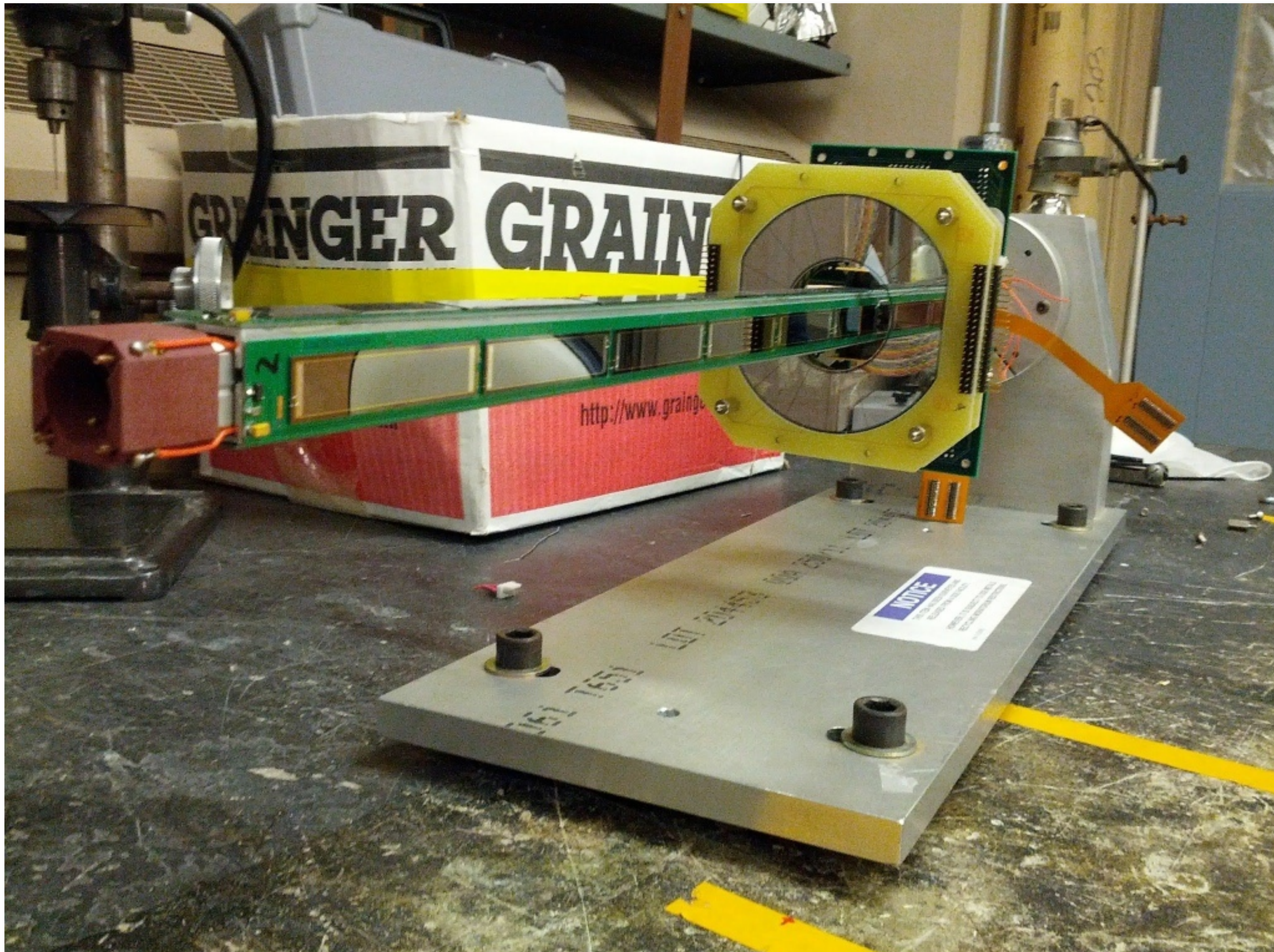

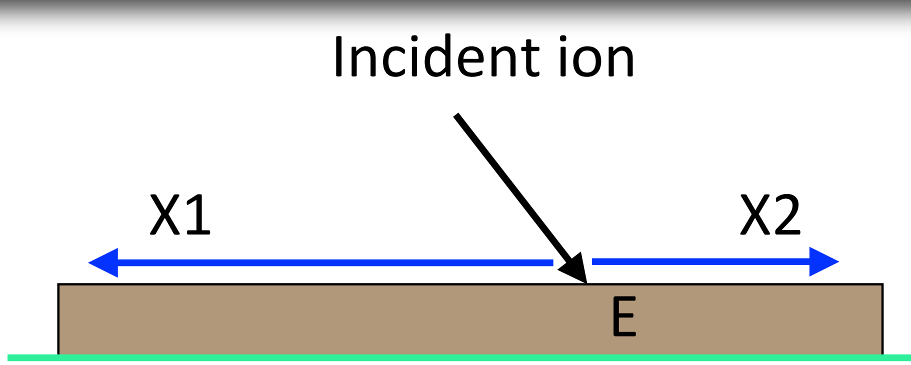

Position ≈ (X1–X2)/E

HELIcal Orbit Spectrometer (HELIOS)

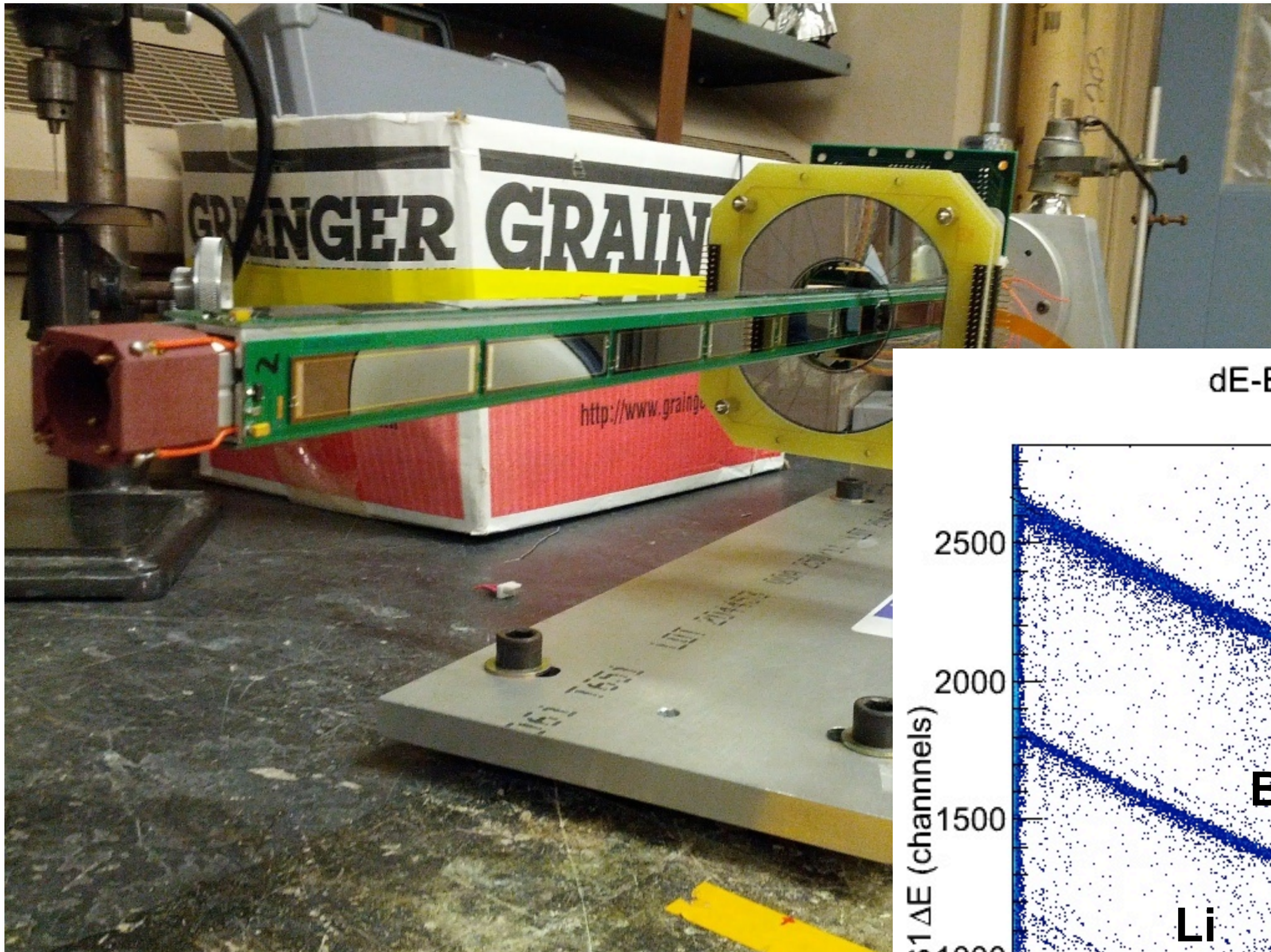

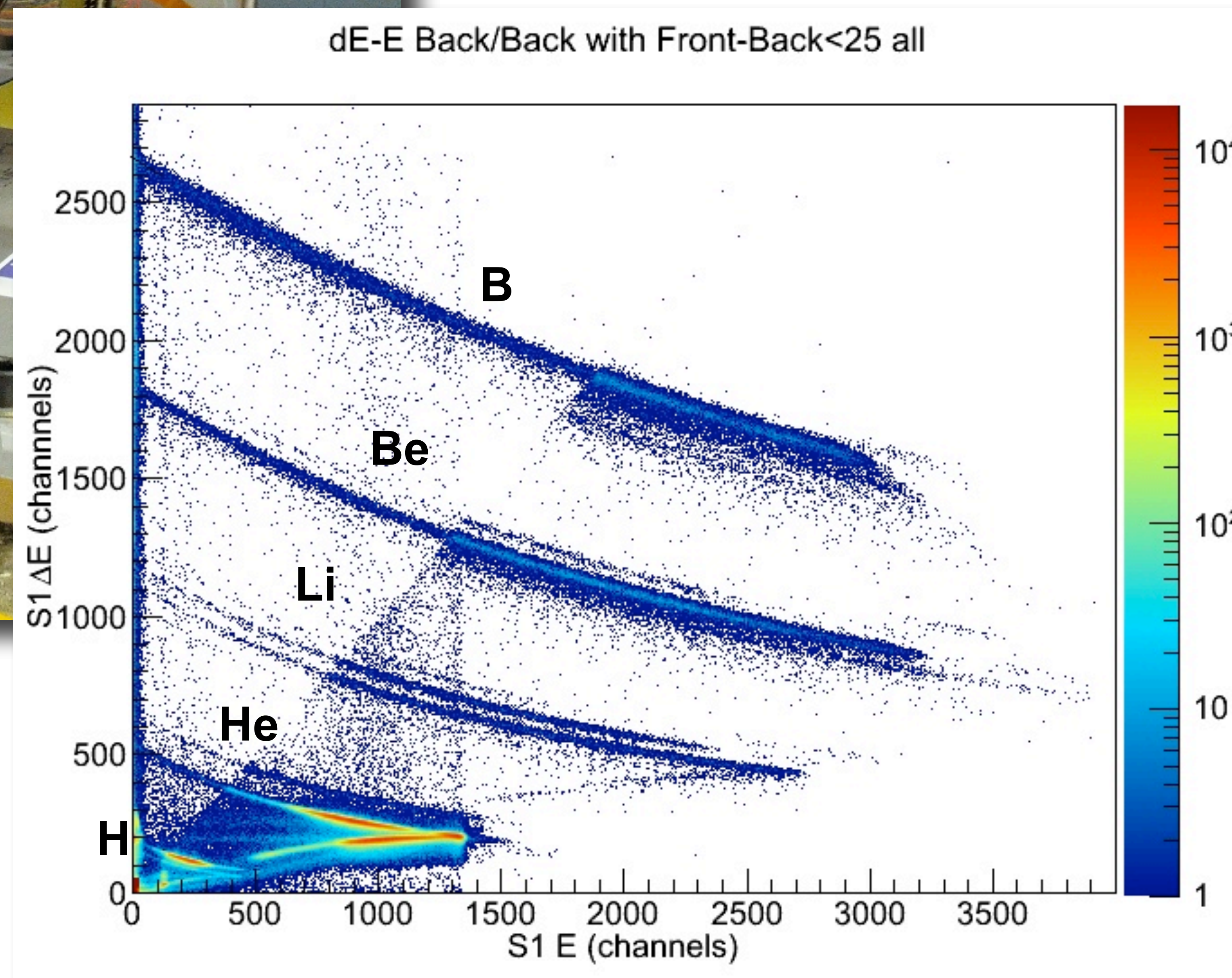

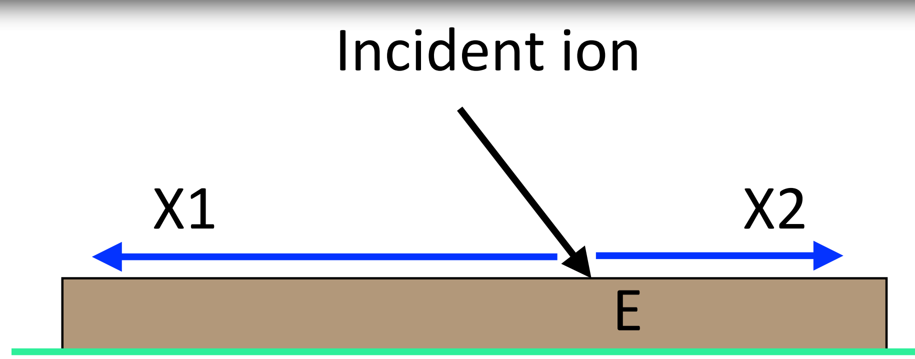

Position ≈ (X1–X2)/E

HELIcal Orbit Spectrometer (HELIOS)

Mechanical Design of NEW PSD Array (Heimsath)

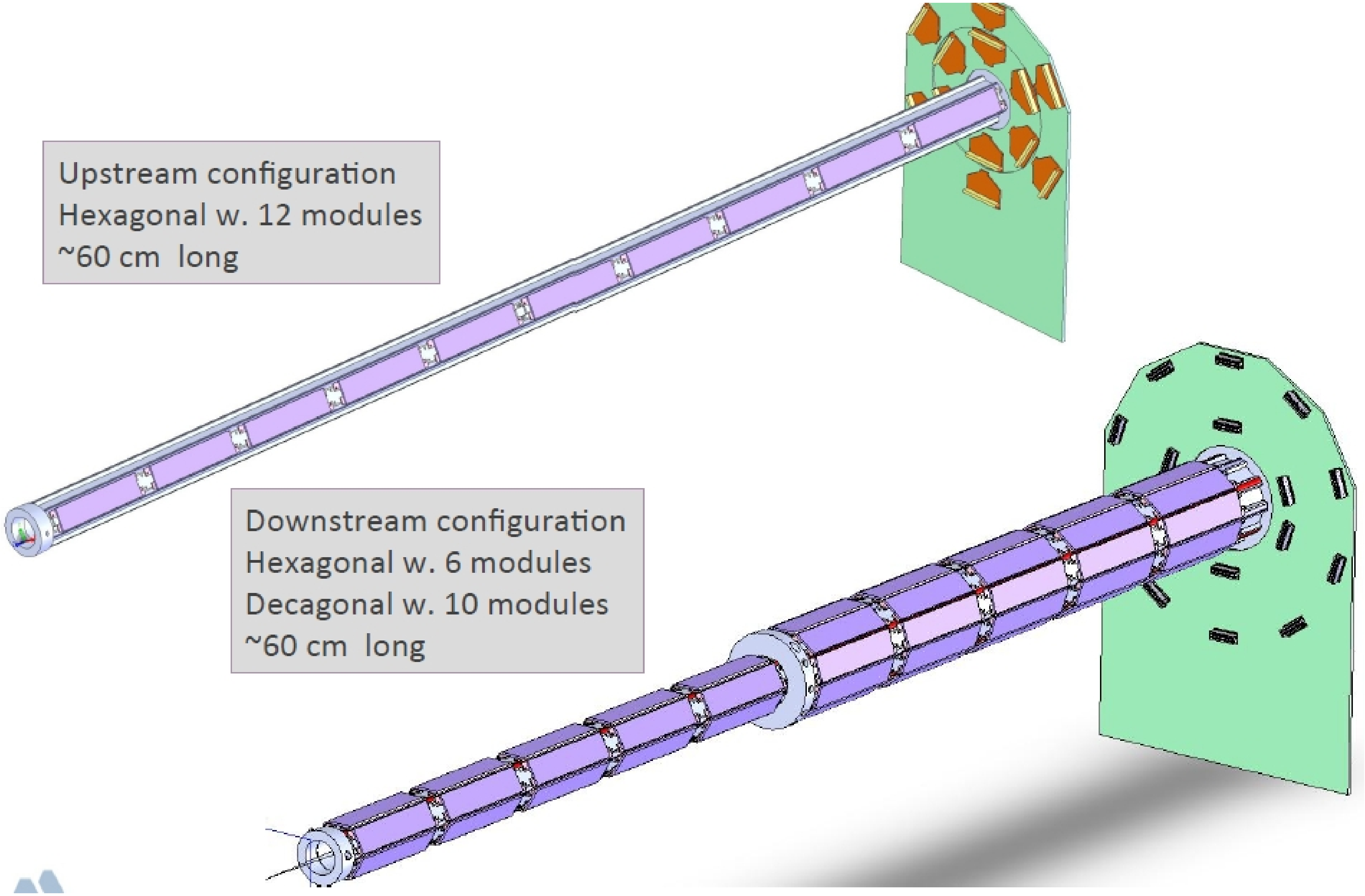

Fast-counting ionization chamber

- Entrance window (<7" diameter)
- Kapton window (25um thick)
  - Tested to 600 Torr
  - Ran between 50 – 300 Torr
  - Isobutane (C_4H_{10}) and CF_4 used
- Alternating cat – anode grids
  - gold plated W wires (20 um)
  - Spaced 2 cm apart
  - Perpendicular to beam direction
  - 1% loss for each grid
- Similar to chamber at ANASEN (ORNL, RIKEN...)
- Presently used with analog electronics

Catherine Deibel
Jianping Lai

Fast-counting ionization chamber

- Entrance window (<7” diameter)
- Kapton window (25um thick)
  - Tested to 600 Torr
  - Ran between 50 – 300 Torr
  - Isobutane (C_4H_{10}) and CF_4 used
- Alternating cat – anode grids
  - gold plated W wires (20 um)
  - Spaced 2 cm apart
  - Perpendicular to beam direction
  - 1% loss for each grid
- Similar to chamber at ANASEN (ORNL, RIKEN…)
- Presently used with analog electronics

Catherine Deibel
Jianping Lai

High Resolution Array (HiRA)

- Modular array of 20 Δ*E*-*E* telescopes
- 65-µm 32-strip SSSD
- 1.5-mm 32x32-strip DSSD
- Four 4-cm thick CsI(Tl) crystals with photodiode readout

High Resolution Array (HiRA)

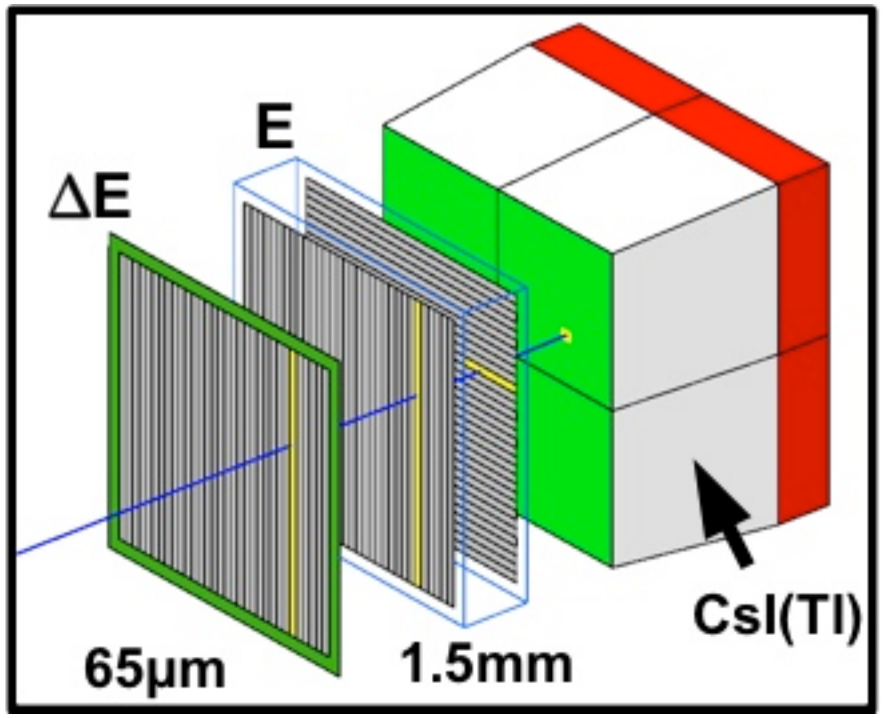

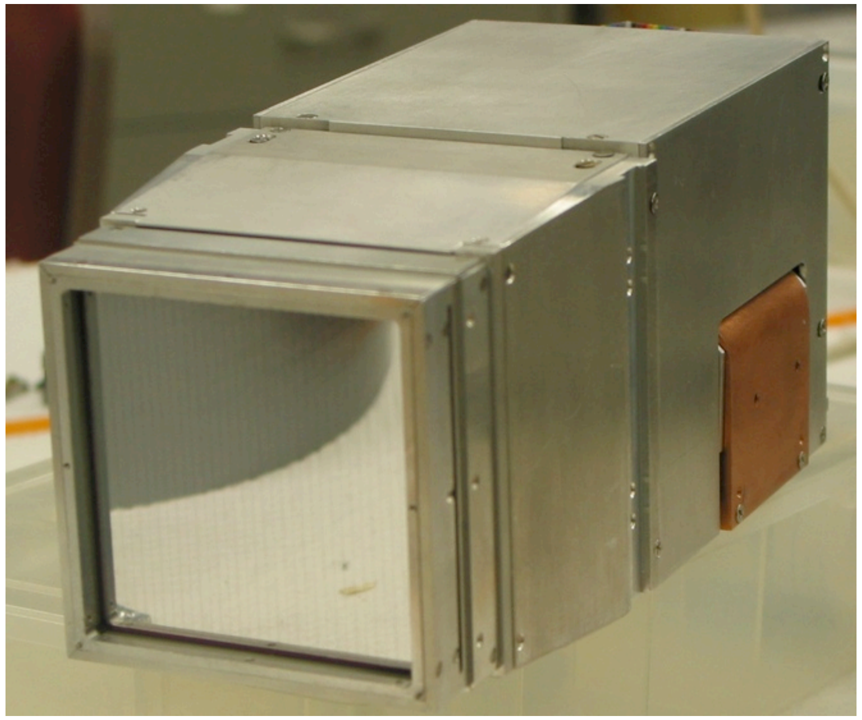

- Modular array of 20 Δ*E*-*E* telescopes
- 65-μm 32-strip SSSD
- 1.5-mm 32x32-strip DSSD
- Four 4-cm thick CsI(Tl) crystals with photodiode readout

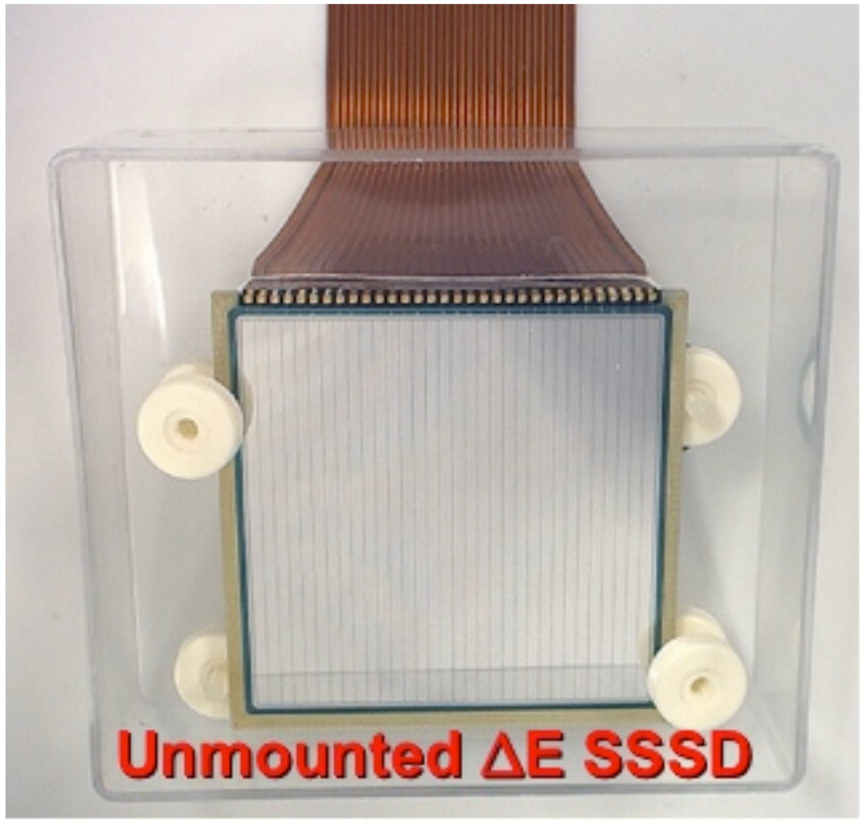

High Resolution Array (HiRA)

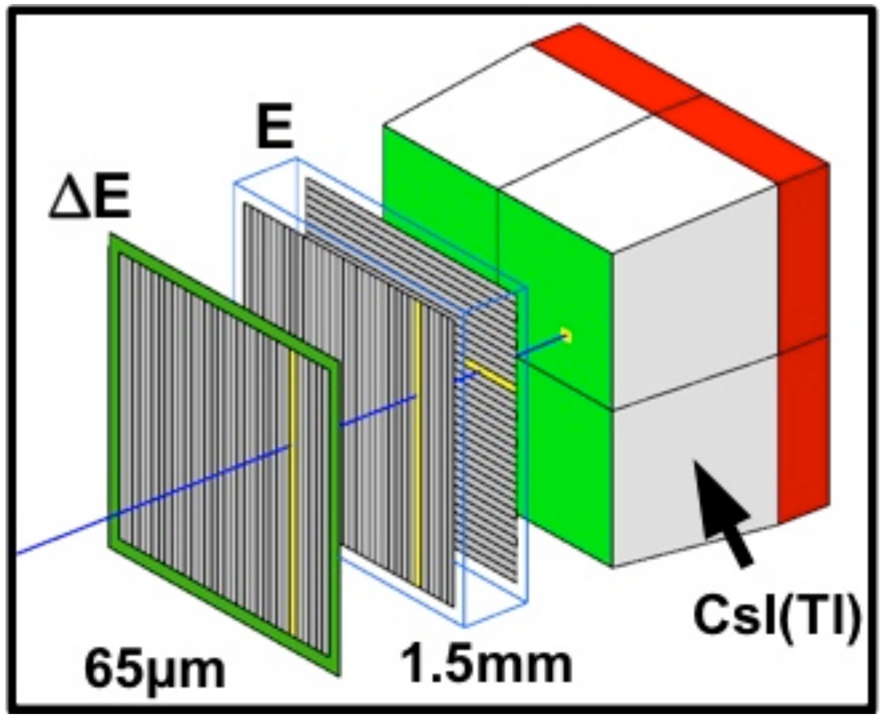

G.L. Engel *et al.* NIM A **573(3)** 2007

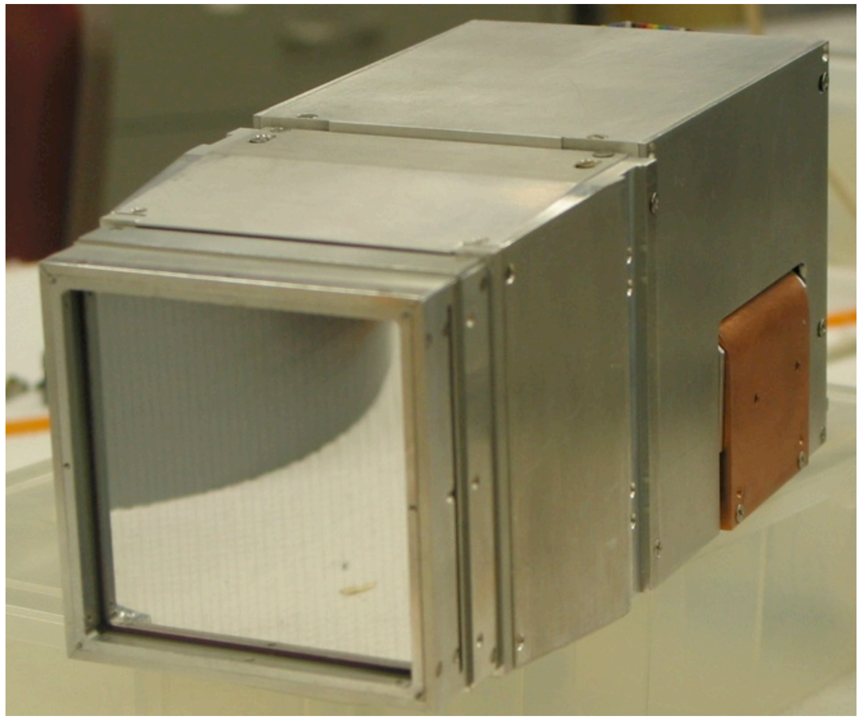

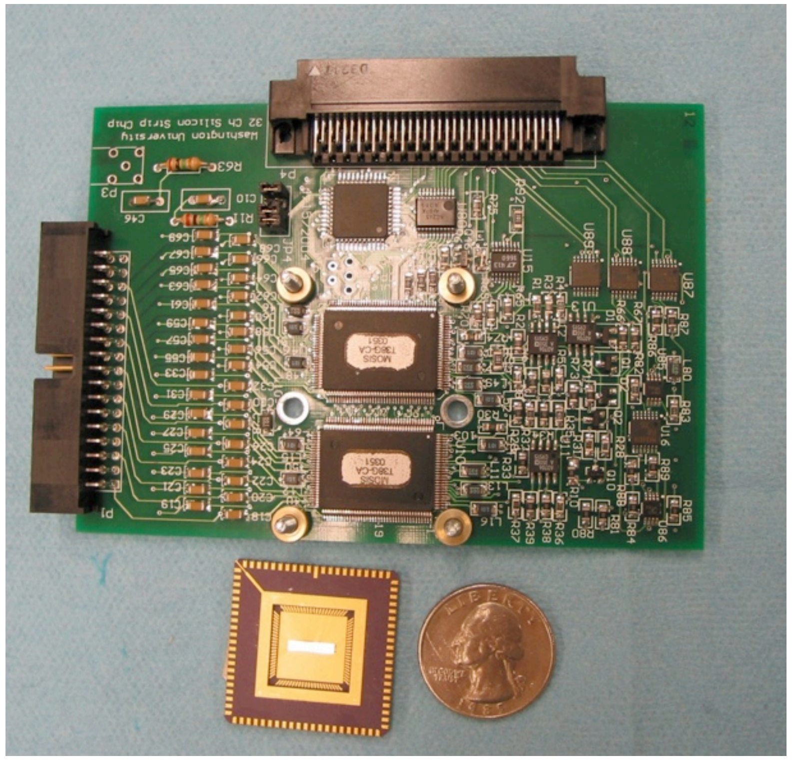

- Modular array of 20 Δ*E*-*E* telescopes
- 65-µm 32-strip SSSD
- 1.5-mm 32x32-strip DSSD
- Four 4-cm thick CsI(Tl) crystals with photodiode readout

High Resolution Array (HiRA)

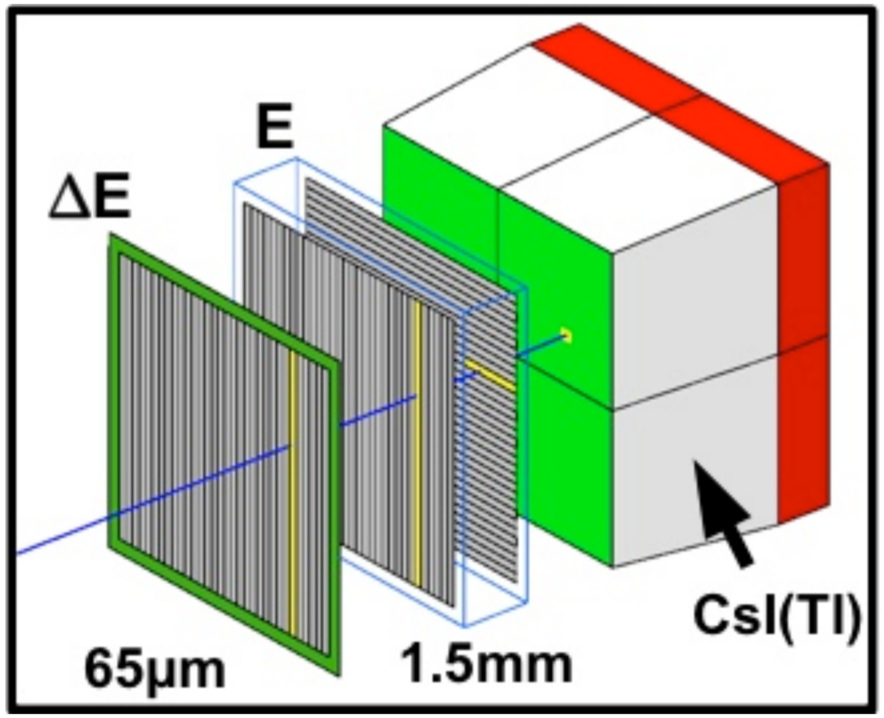

G.L. Engel *et al.* NIM A **573(3)** 2007

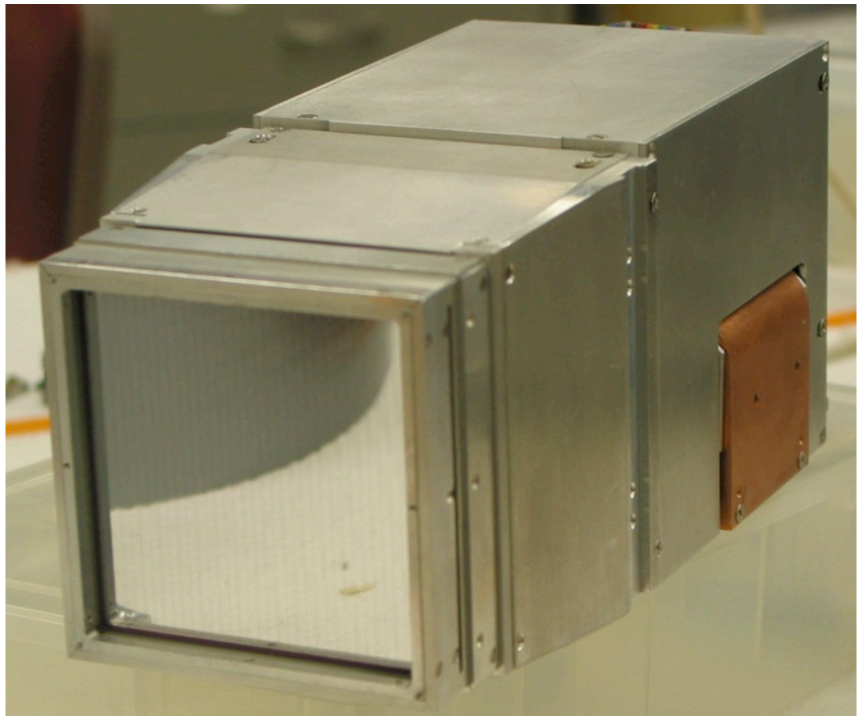

- Modular array of 20 ΔE-E telescopes
- 65-µm 32-strip SSSD
- 1.5-mm 32x32-strip DSSD
- Four 4-cm thick CsI(Tl) crystals with photodiode readout

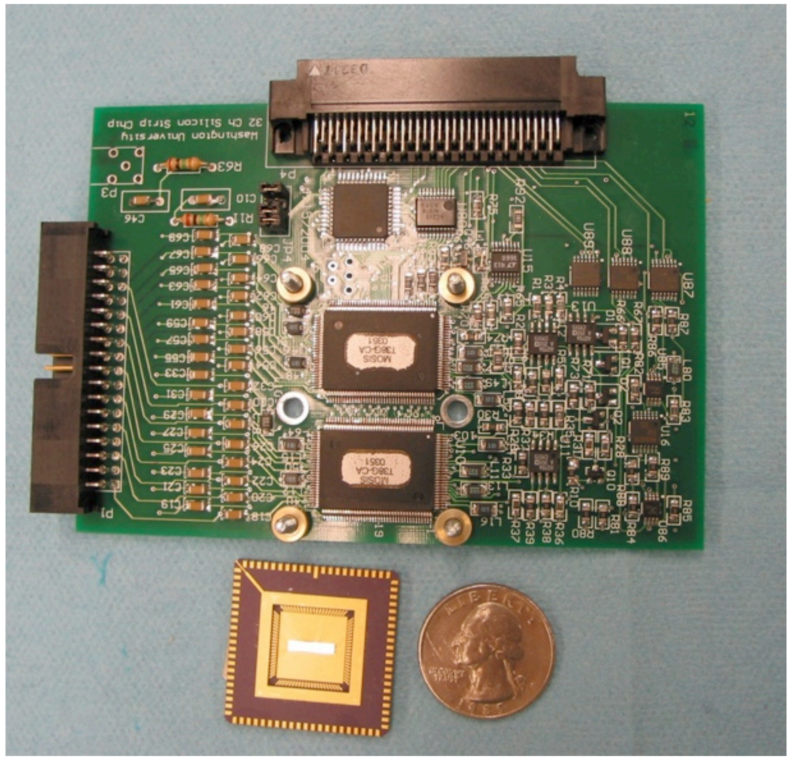

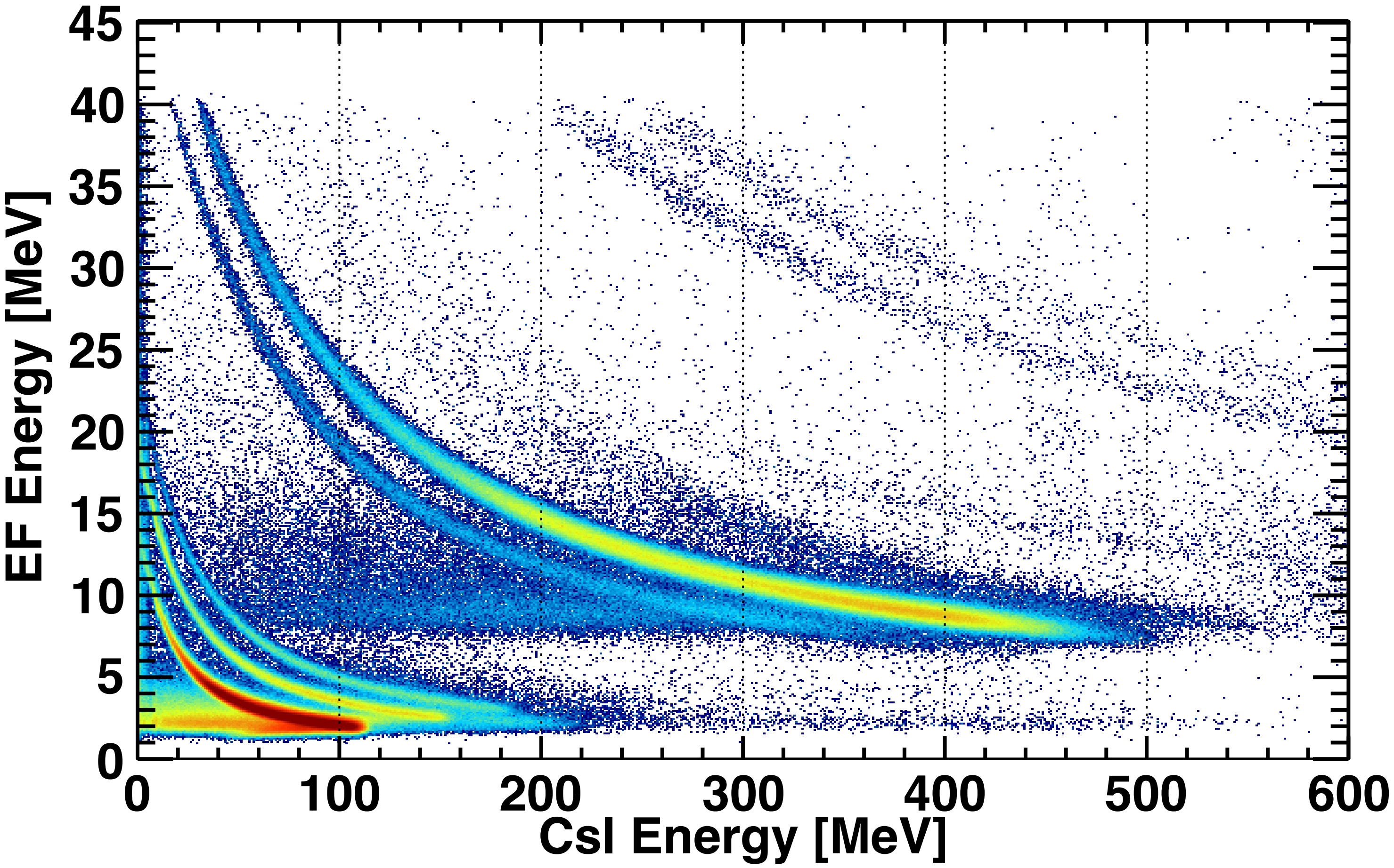

High Resolution Array (HiRA)

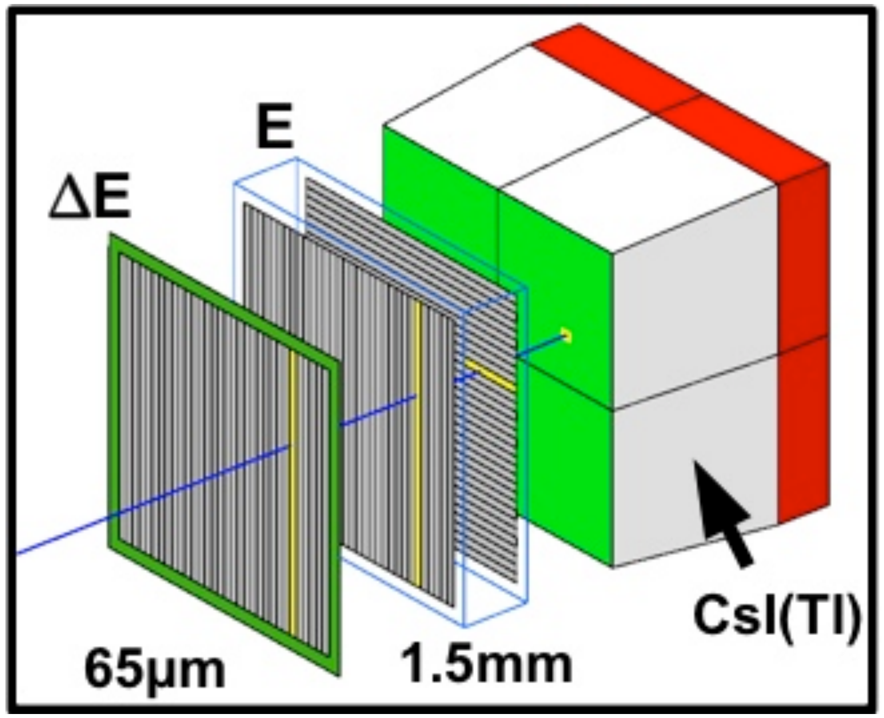

G.L. Engel *et al.* NIM A **573(3)** 2007

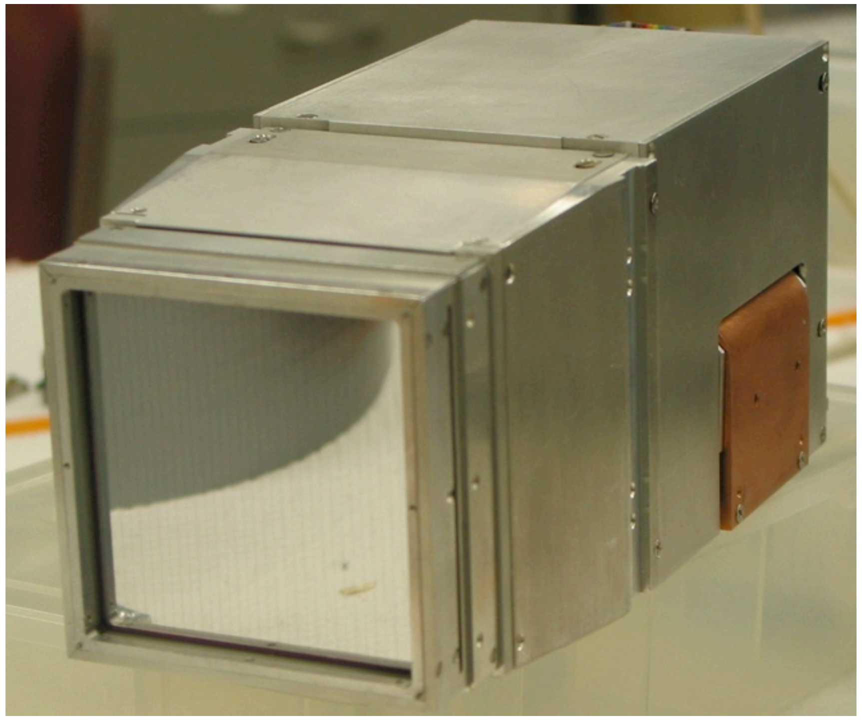

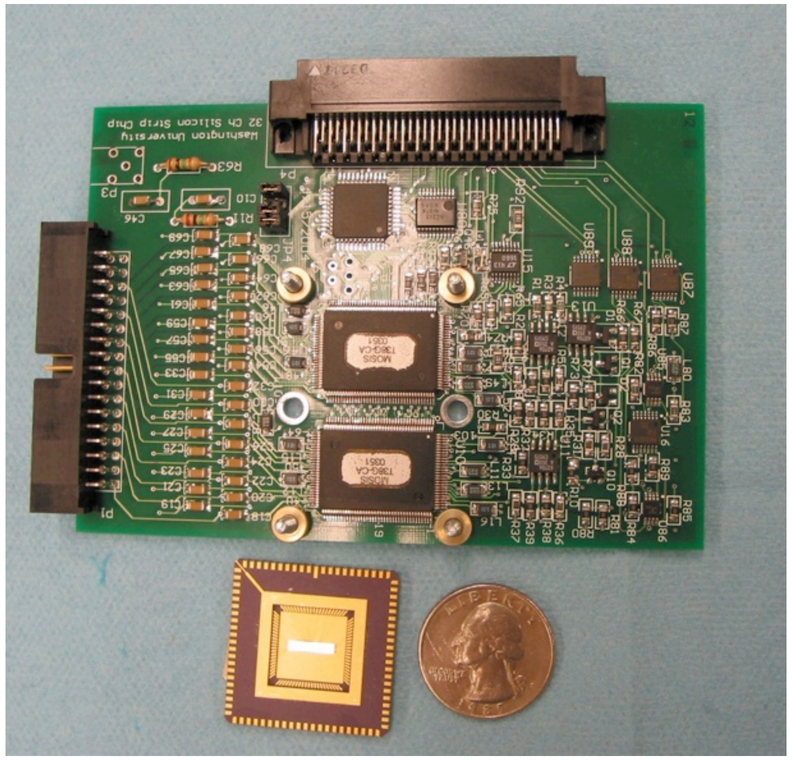

- Modular array of 20 Δ*E*-*E* telescopes
- 65-µm 32-strip SSSD
- 1.5-mm 32x32-strip DSSD
- Four 4-cm thick CsI(Tl) crystals with photodiode readout

High Resolution Array

Study of one-proton knockout on ^{9}C

$^{46}Ar(p,d)$ and $^{34}Ar(p,d)$ neutron transfer reactions

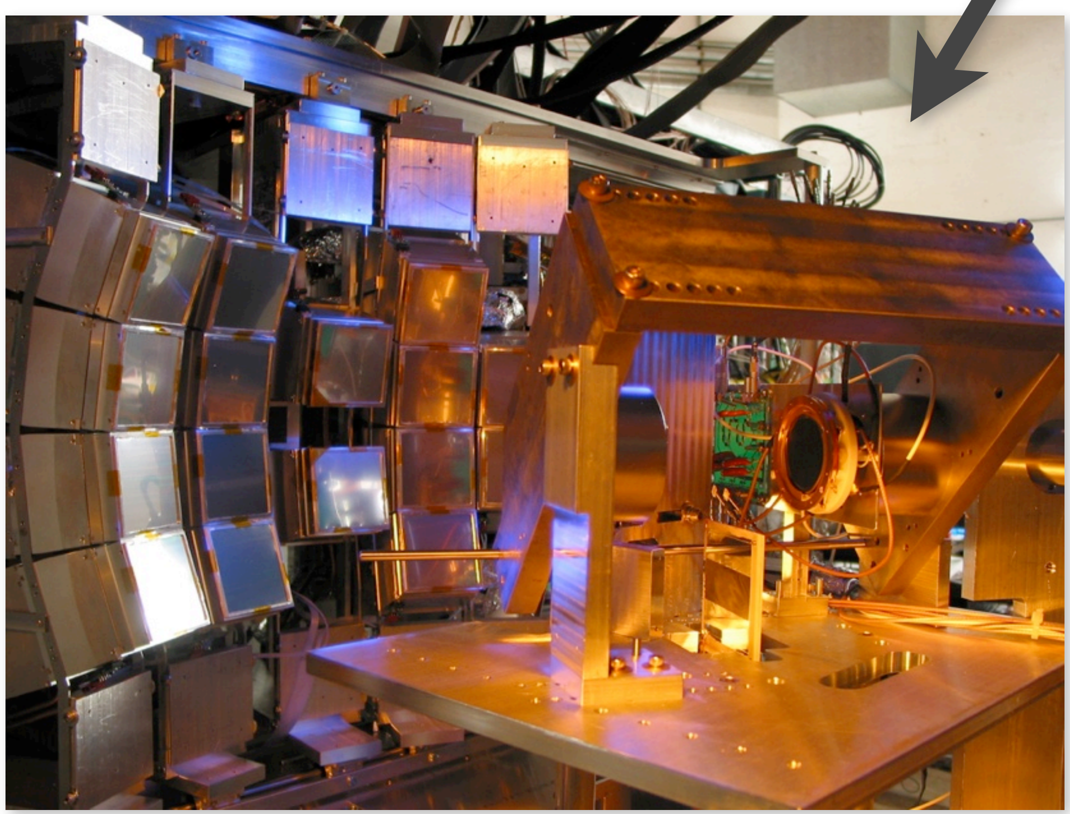

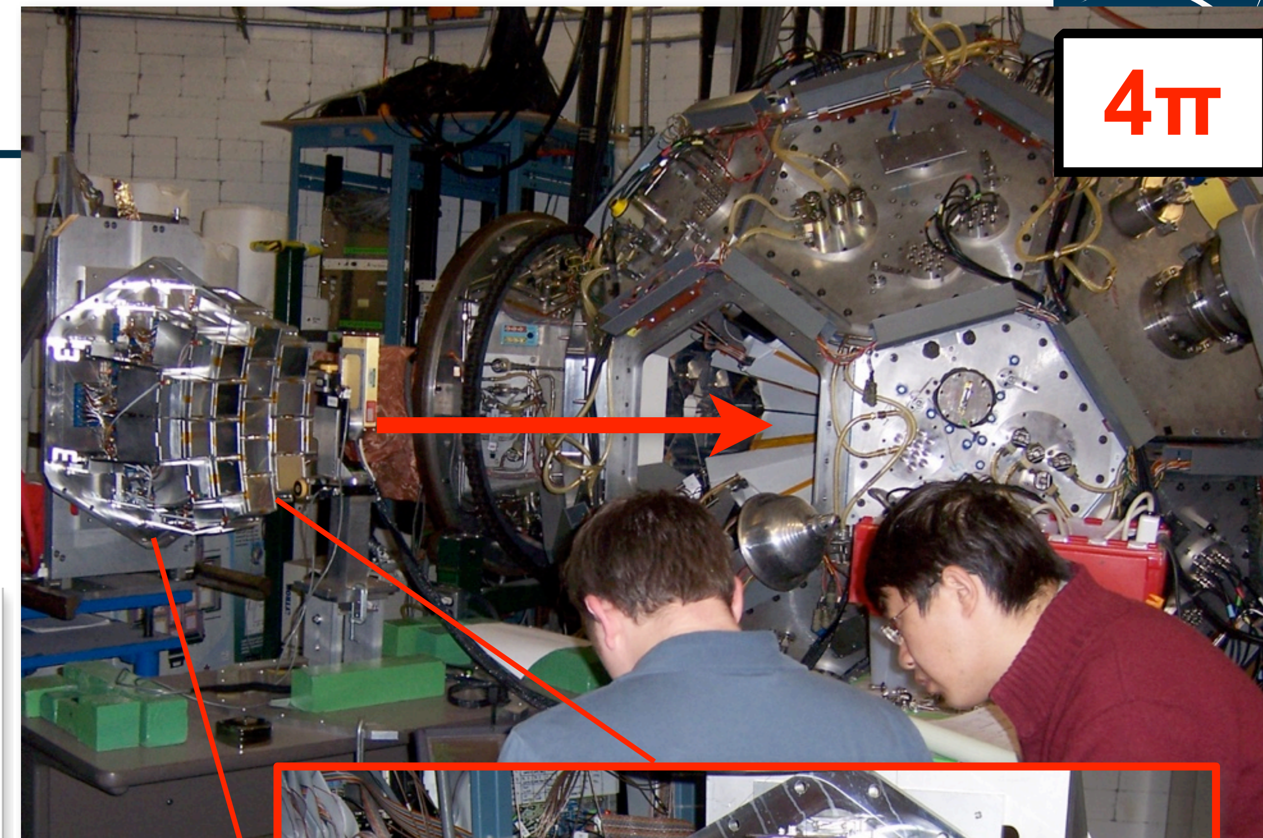

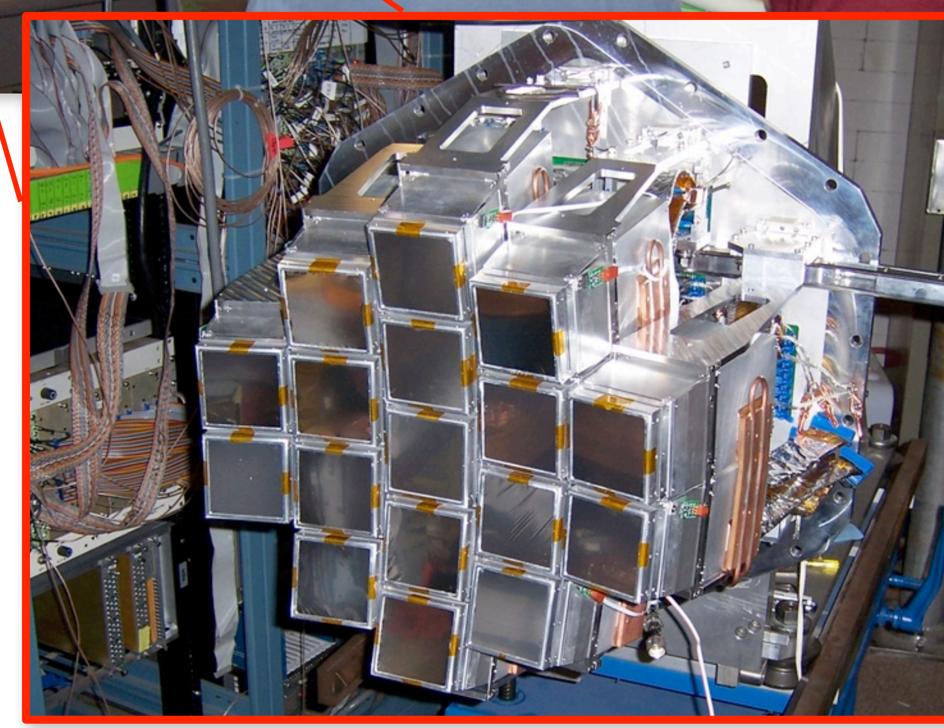

Nuclear EOS via two-particle correlation functions

HiRA exotic-beam transfer reactions

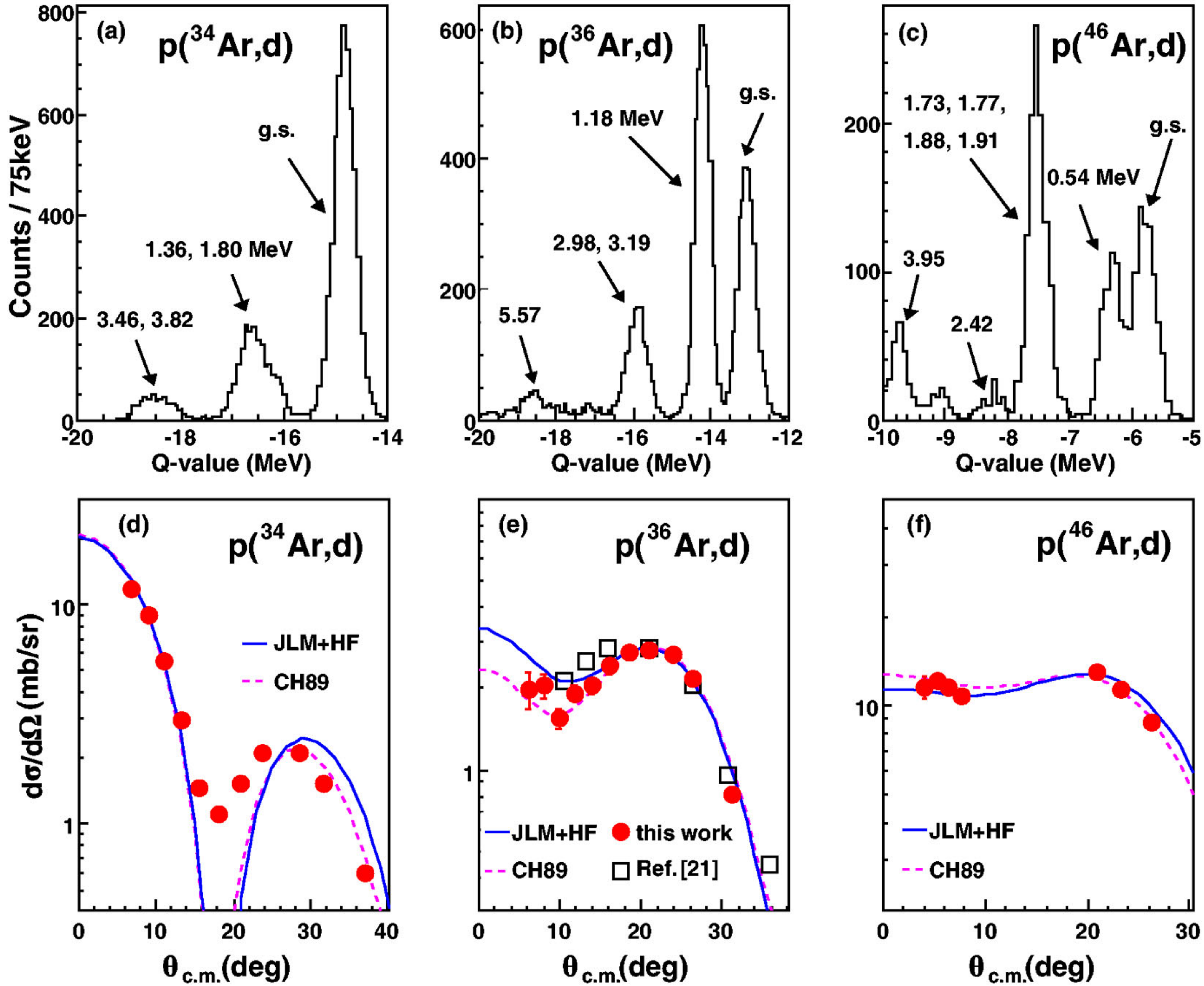

J. Lee *et al.*

HiRA exotic-beam transfer reactions

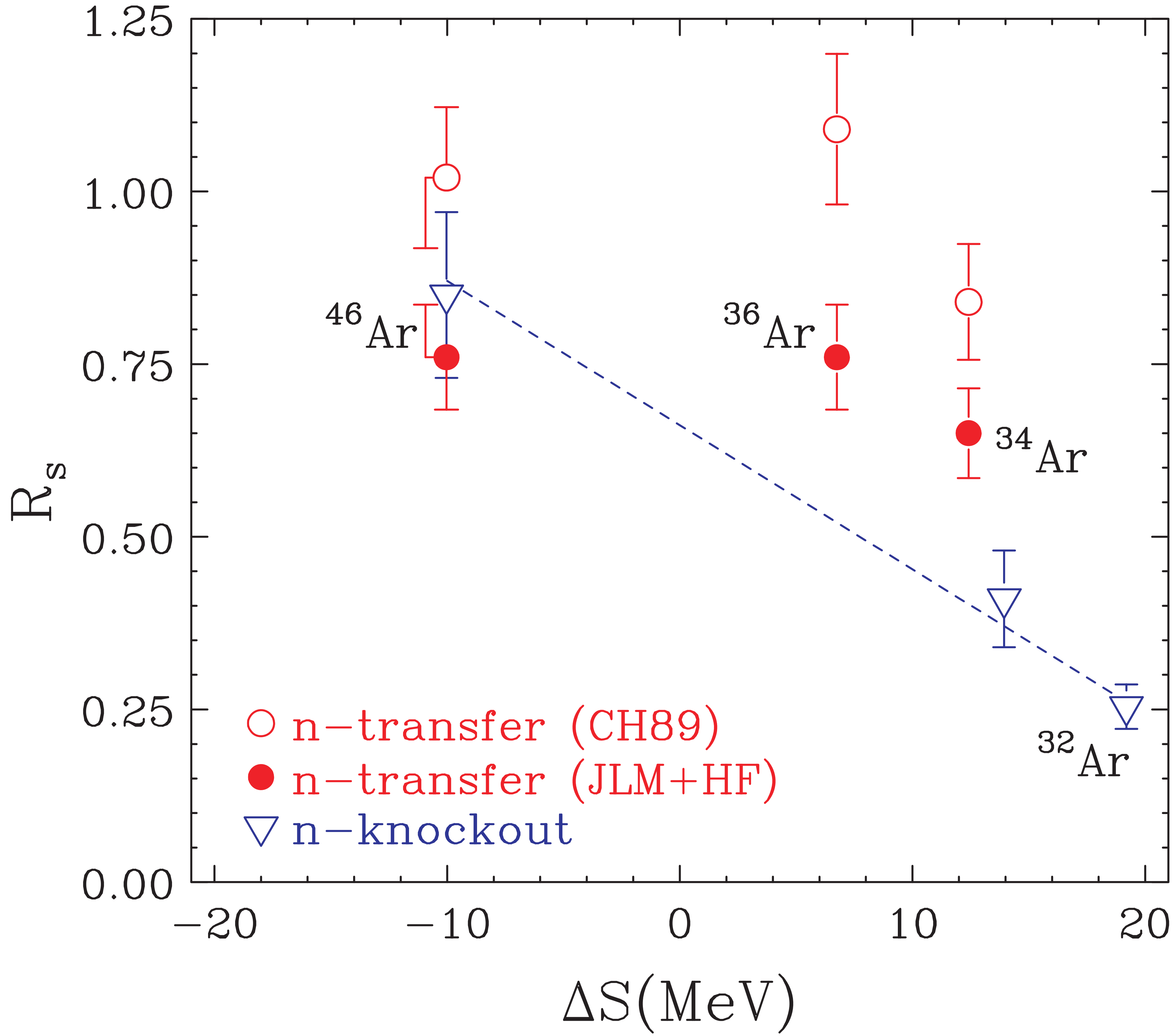

J. Lee *et al.*

The BGS (J. Gates)

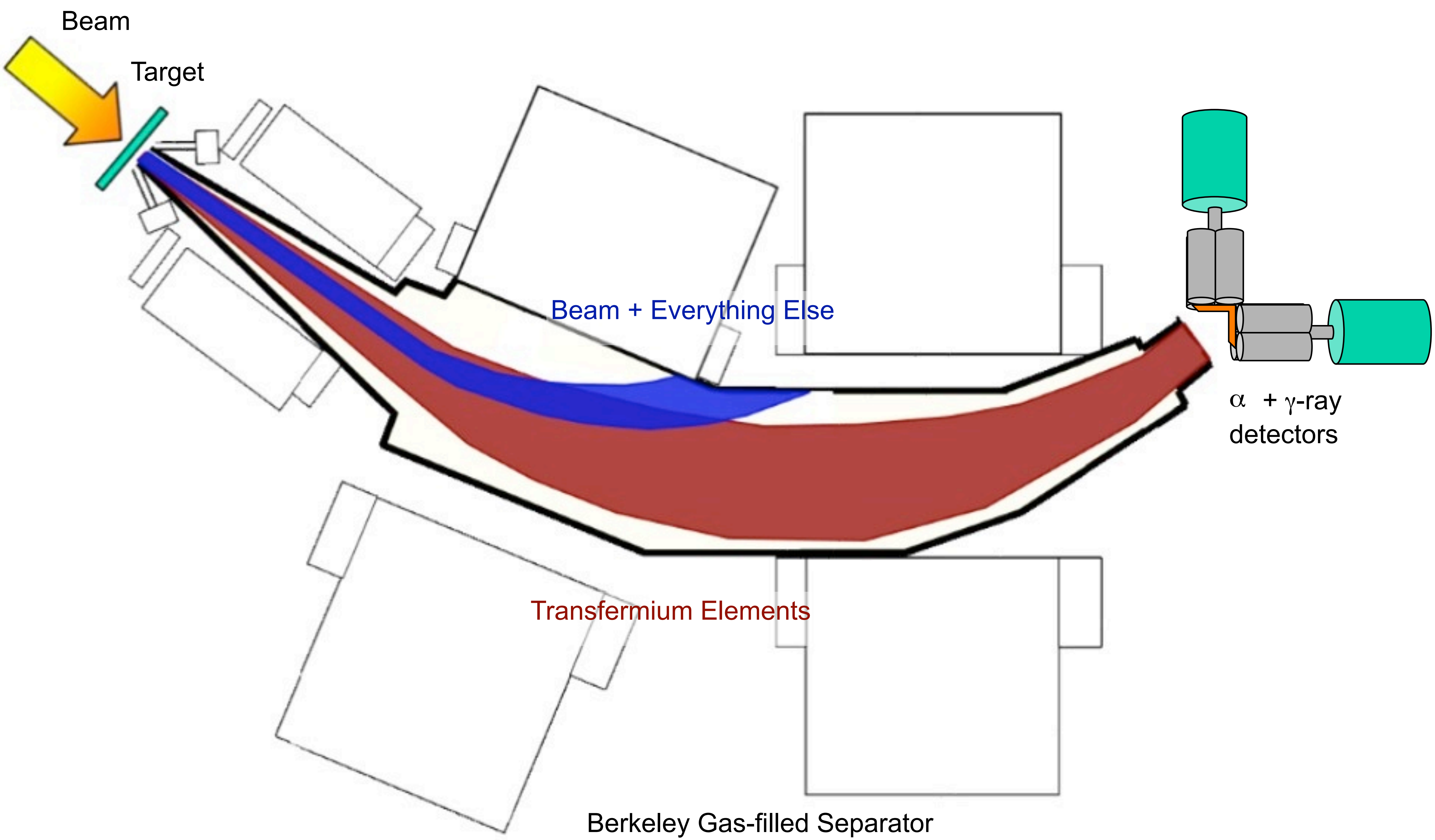

The BGS Si cube

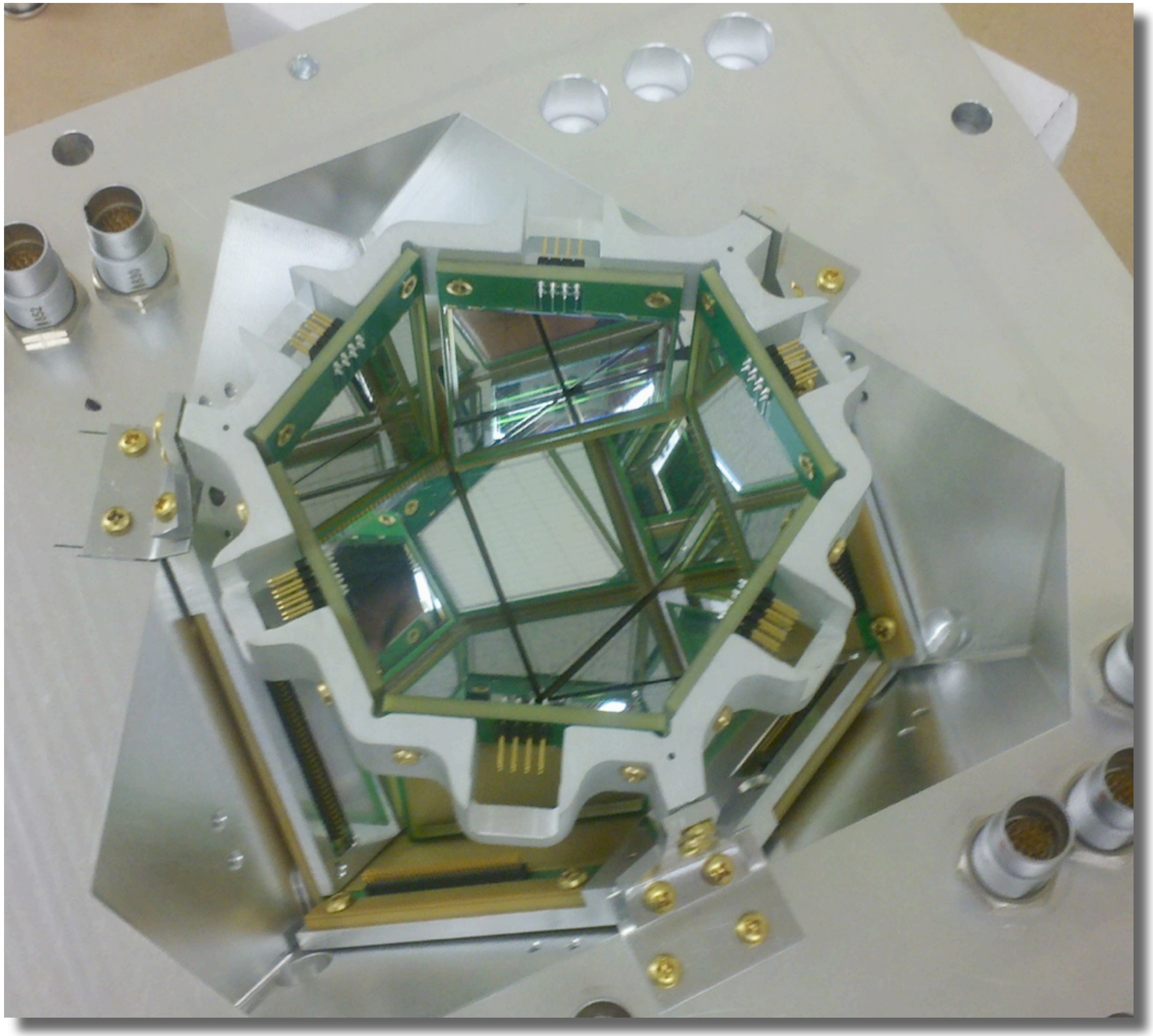

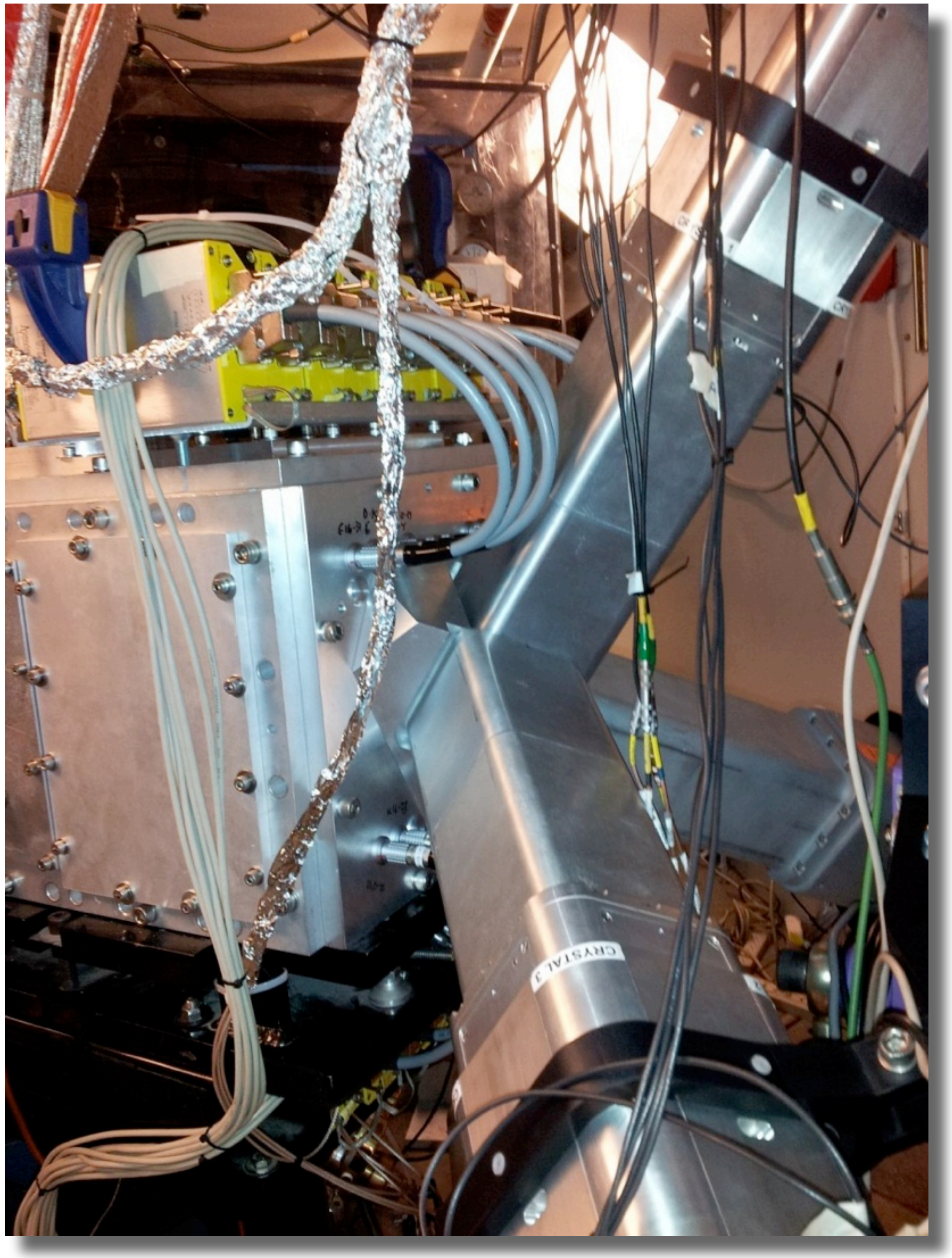

Fragmentation and isotope discovery

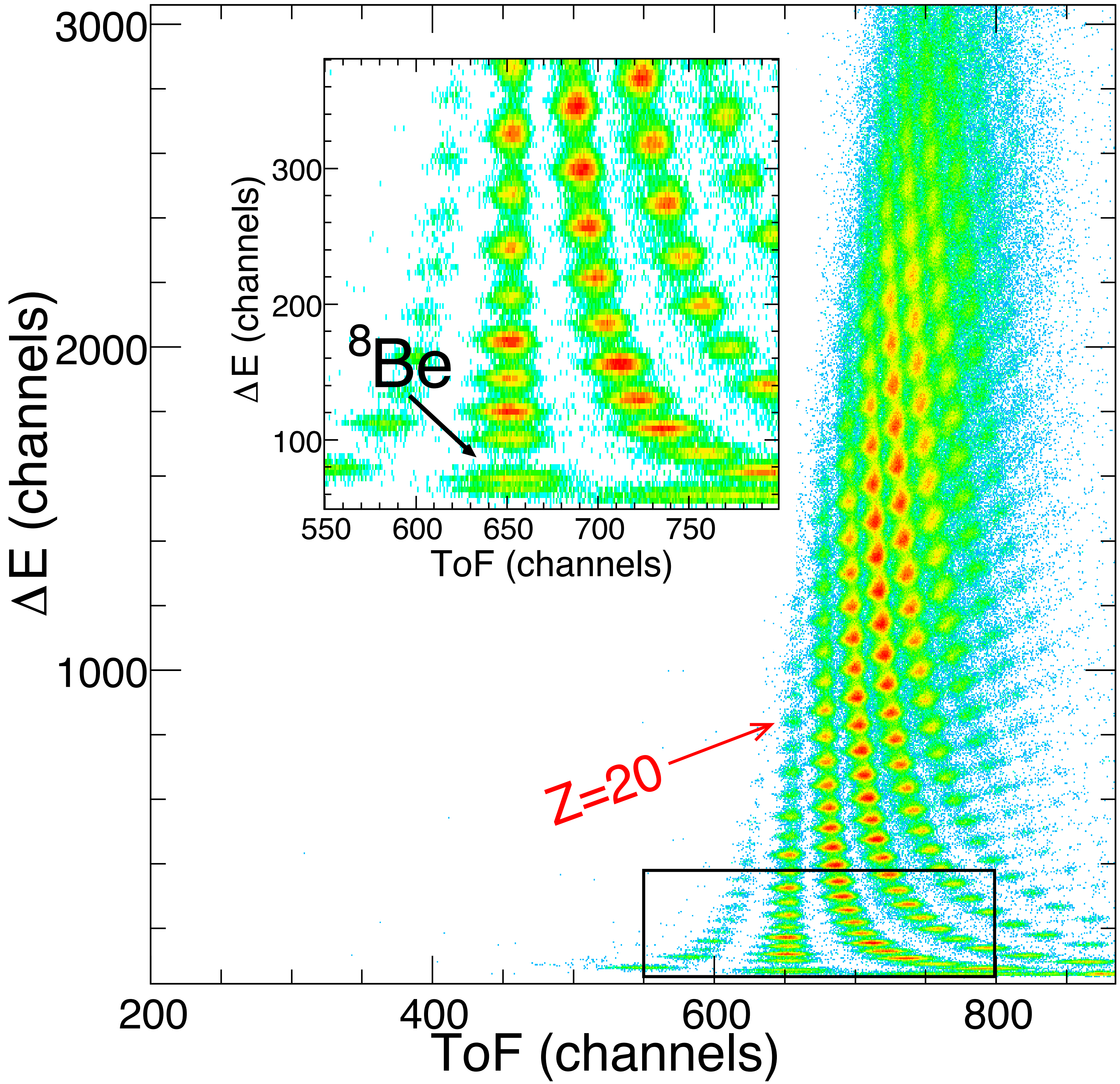

MoNA (Thanks to C.R. Hoffman)

Experimental setup

^{26}F beam @ 85 MeV/u ~20 pps

Neutrons detected around 0º

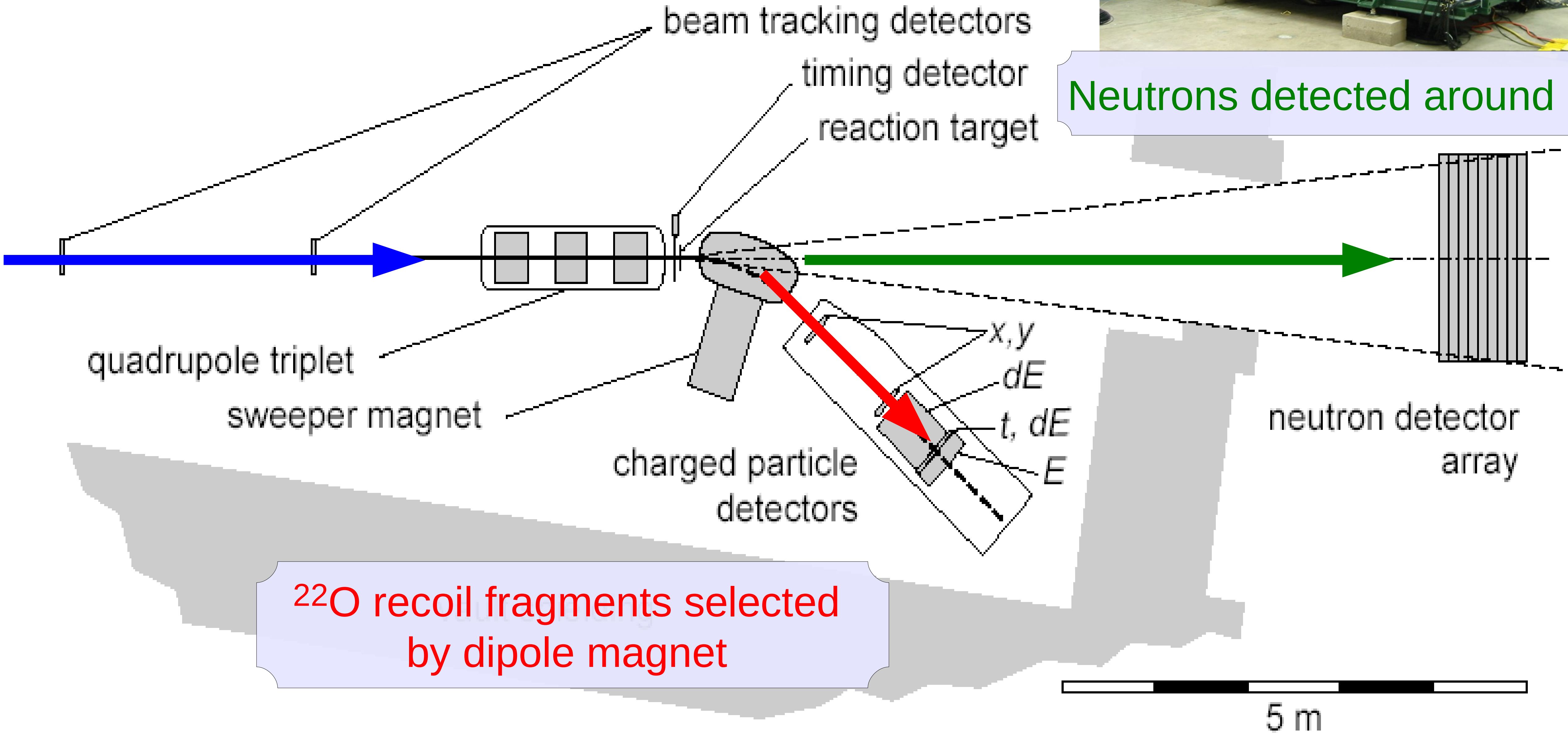

^{22}O recoil fragments selected by dipole magnet

MoNA

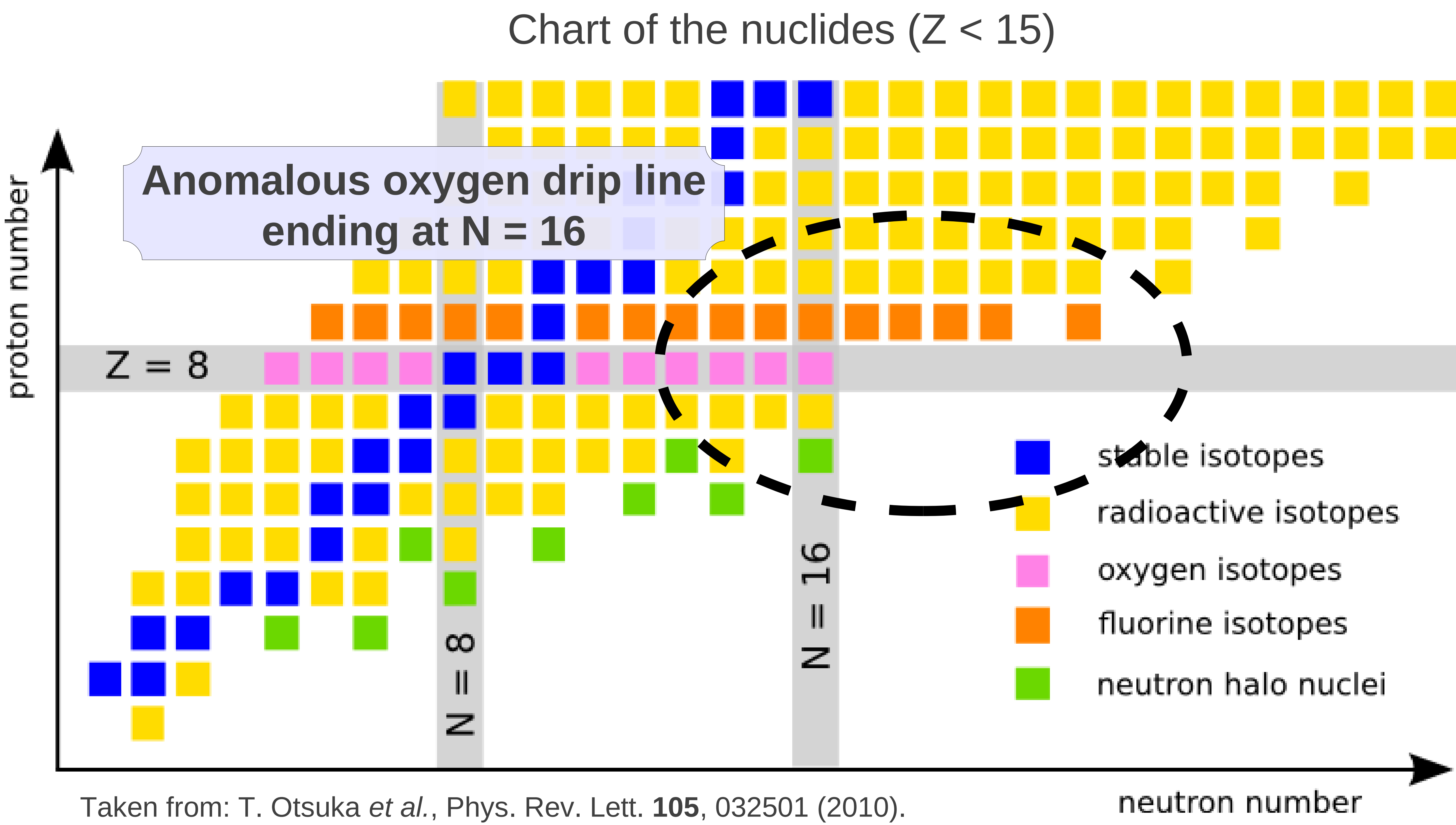

Taken from: T. Otsuka *et al.*, Phys. Rev. Lett. **105**, 032501 (2010).

MoNA

$$E_{\text{decay}} = \sqrt{m_f^2 + m_n^2 + 2[E_f E_n - p_f p_n \cos(\Theta_{\text{open}})]} - m_f - m_n$$

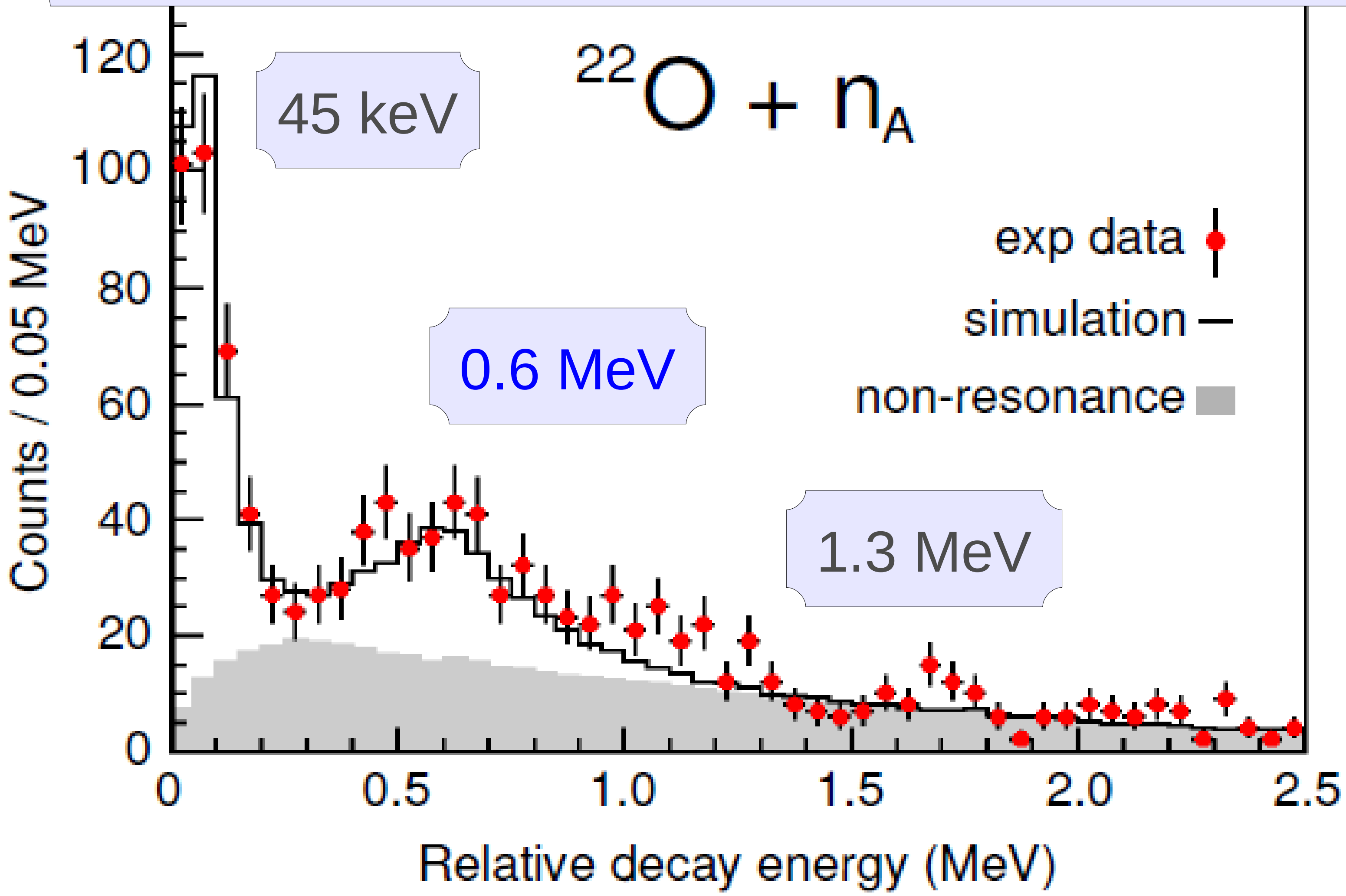

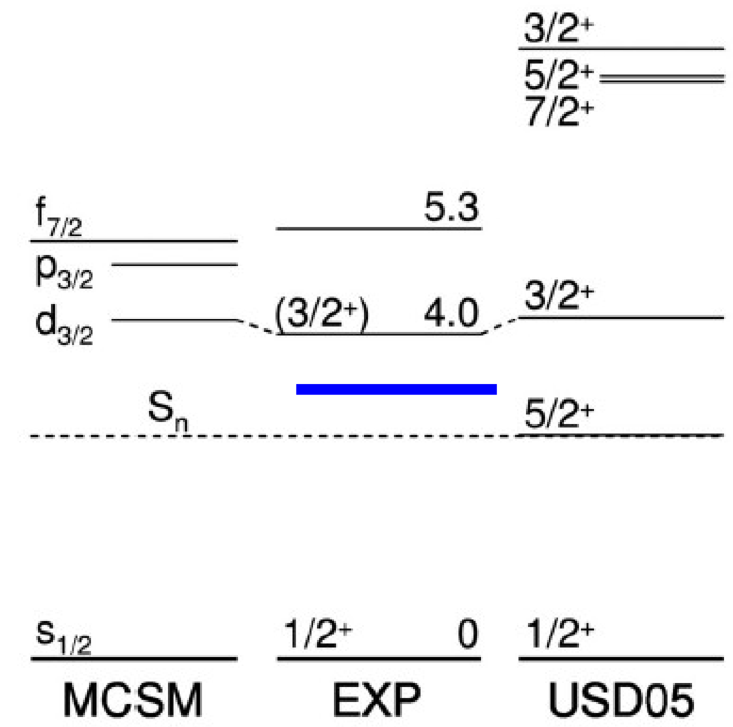

Taken from: Z. Elekes *et al.*, Phys. Rev. Lett. **98**, 102502 (2007).

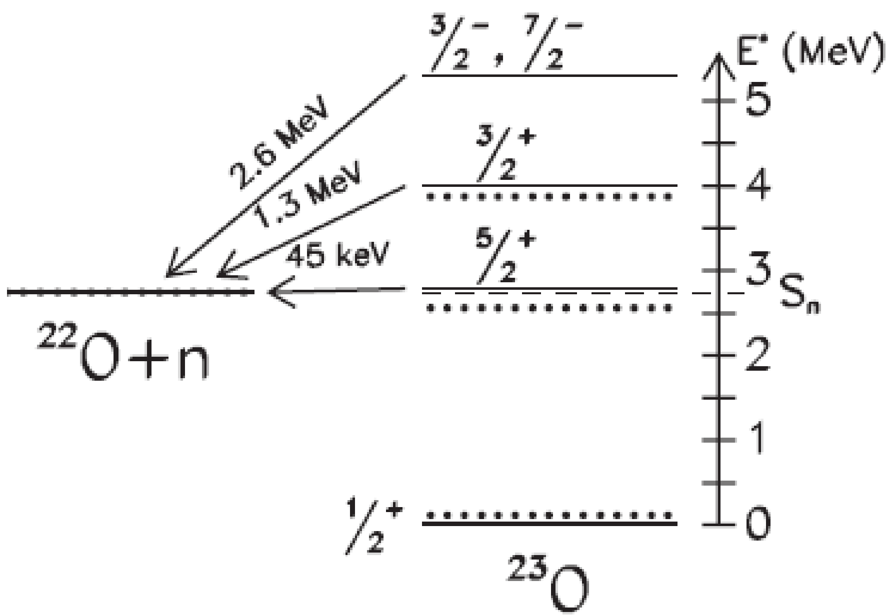

Taken from: A. Schiller *et al.*, Phys. Rev. Lett. **99**, 112501 (2007).

- Previously unobserved resonance at ~0.6 MeV
- Origin: No nearby states suggested by shell model
- Possible candidate for two-neutron coincidence

Summary

- Energy loss of charged particles.
- Semiconductor and silicon detectors.
- The ***p-n junction*** results in a contact potential and fixed space charges, creating a ***depletion region***. This region is the solid-state analog of an ionization chamber.
- Silicon and charged-particle detection techniques are used throughout physics.
- There is a lot of science being carried out with exotic beams that relies on the beneficial properties of silicon.
- There are a great deal of other detectors that I could not discuss!

References

1. Knoll, Glenn F. Radiation detection and measurement. Wiley. com, 2010.
2. Brownell, Gordon L., et al. "Positron tomography and nuclear magnetic resonance imaging." Science 215.4533 (1982): 619-626.
3. Leo, William R. Techniques for nuclear and particle physics experiments: a how-to approach. Springer, 1994.
4. Kittel, Charles, and Paul McEuen. Introduction to solid state physics. Vol. 7. New York: Wiley, 1996.
5. Carron, Neal Jay. An introduction to the passage of energetic particles through matter. CRC Press, 2006.
6. Tsoulfanidis, Nicholas. Measurement and detection of radiation. Taylor & Francis, 1995.

Additional Material

Electron-hole equilibrium concentrations

Assume:
$n_i = p_i = 10^{10}/cm^3$
(Close to Si at R.T.)

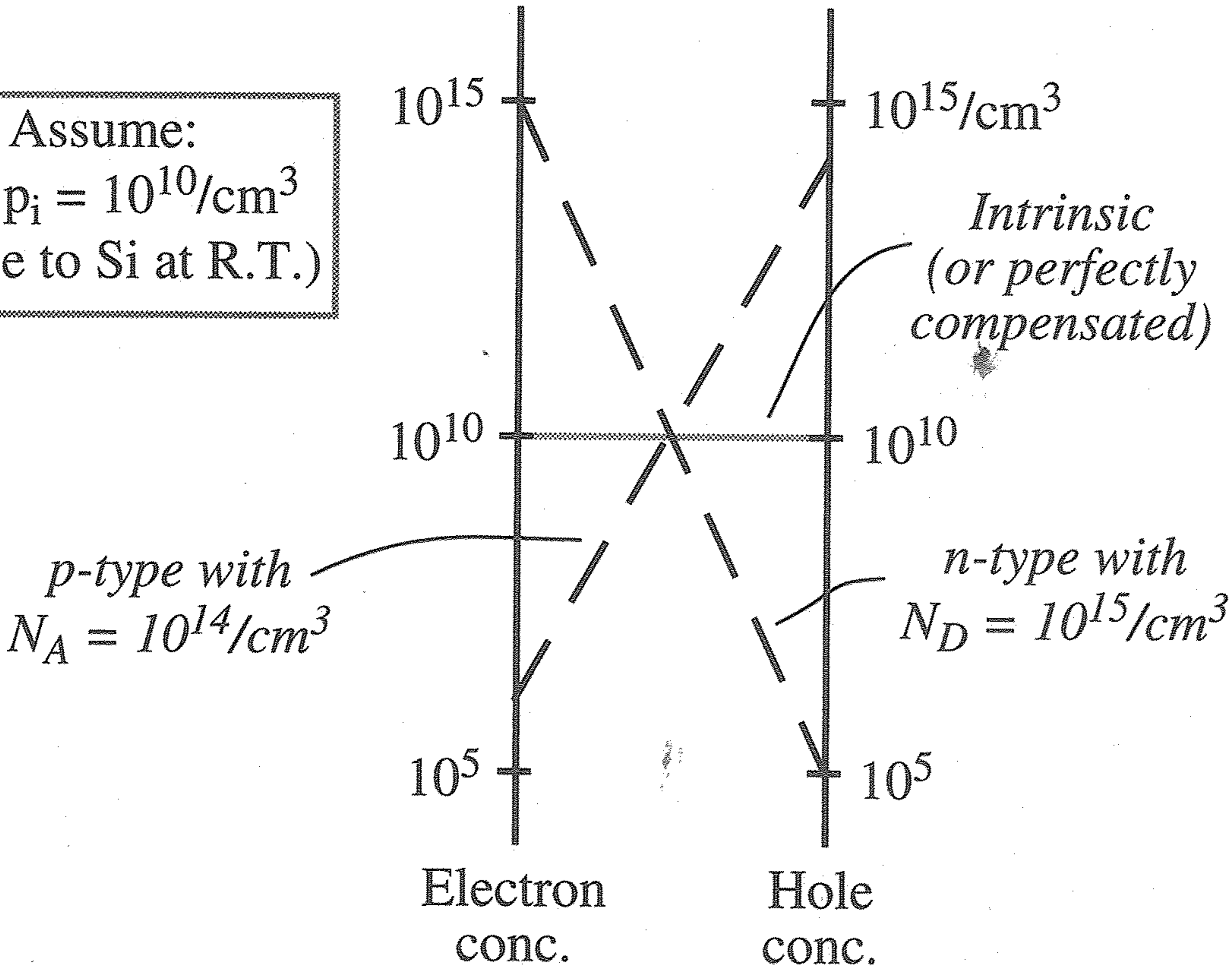

Micro-channel plate (MCP) tracking system

- Secondary electrons ejected from the beam interaction on target are detected by the MCP.
- *E*-field accelerates e⁻ while *B*-field confines trajectories.

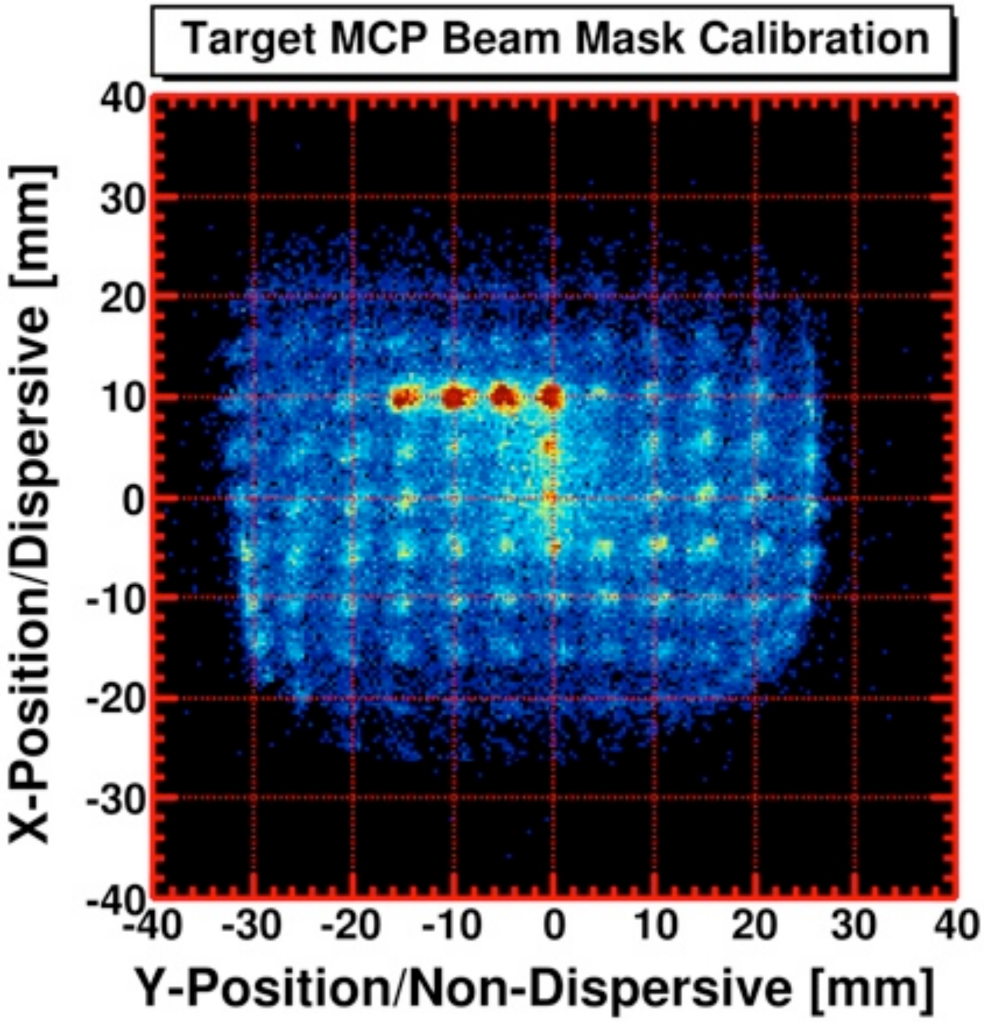

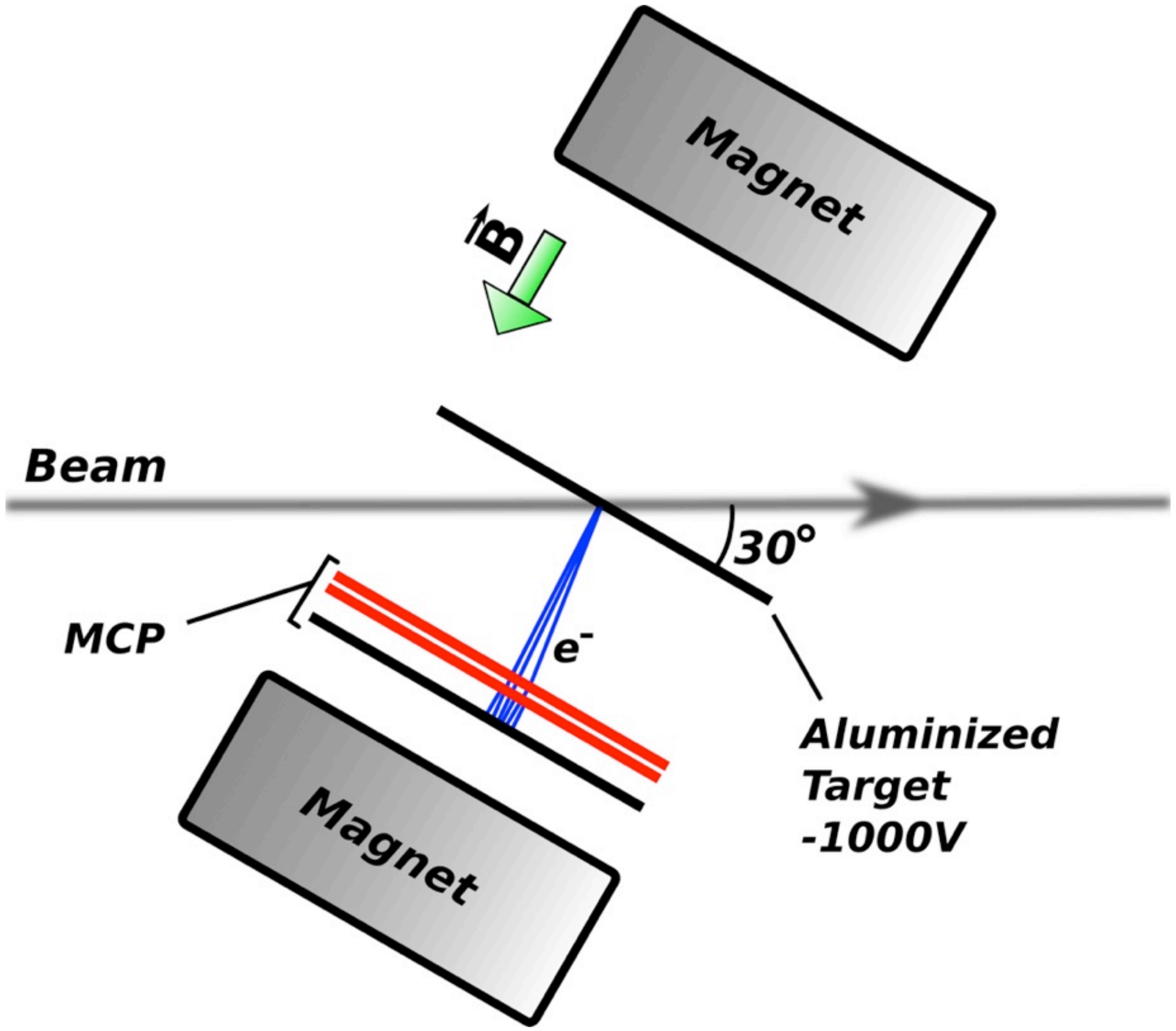

- Electron multiplication occurs in the channels of the MCP.
- Anode provides timing.
- Position information readout from four corner signals taken from a resistive anode.
- Capable of rates approaching 10^6 Hz.

Analogous proton decay

- ^{65}Se and ^{69}Kr are analogous systems:
  - Both $T_z = -3/2$ nuclei
  - Similar relative energies for states of interest.
- However, their decays are strikingly different!!!
- We can explain this difference if the spin of the analog state in ^{69}Br is higher than in ^{65}As.
- From mirror nuclei one expects $J^\pi = 3/2^-$ for the ^{65}As IAS while ^{69}Br must have $\ell \geq 3$, most likely $J^\pi = 5/2^-$.

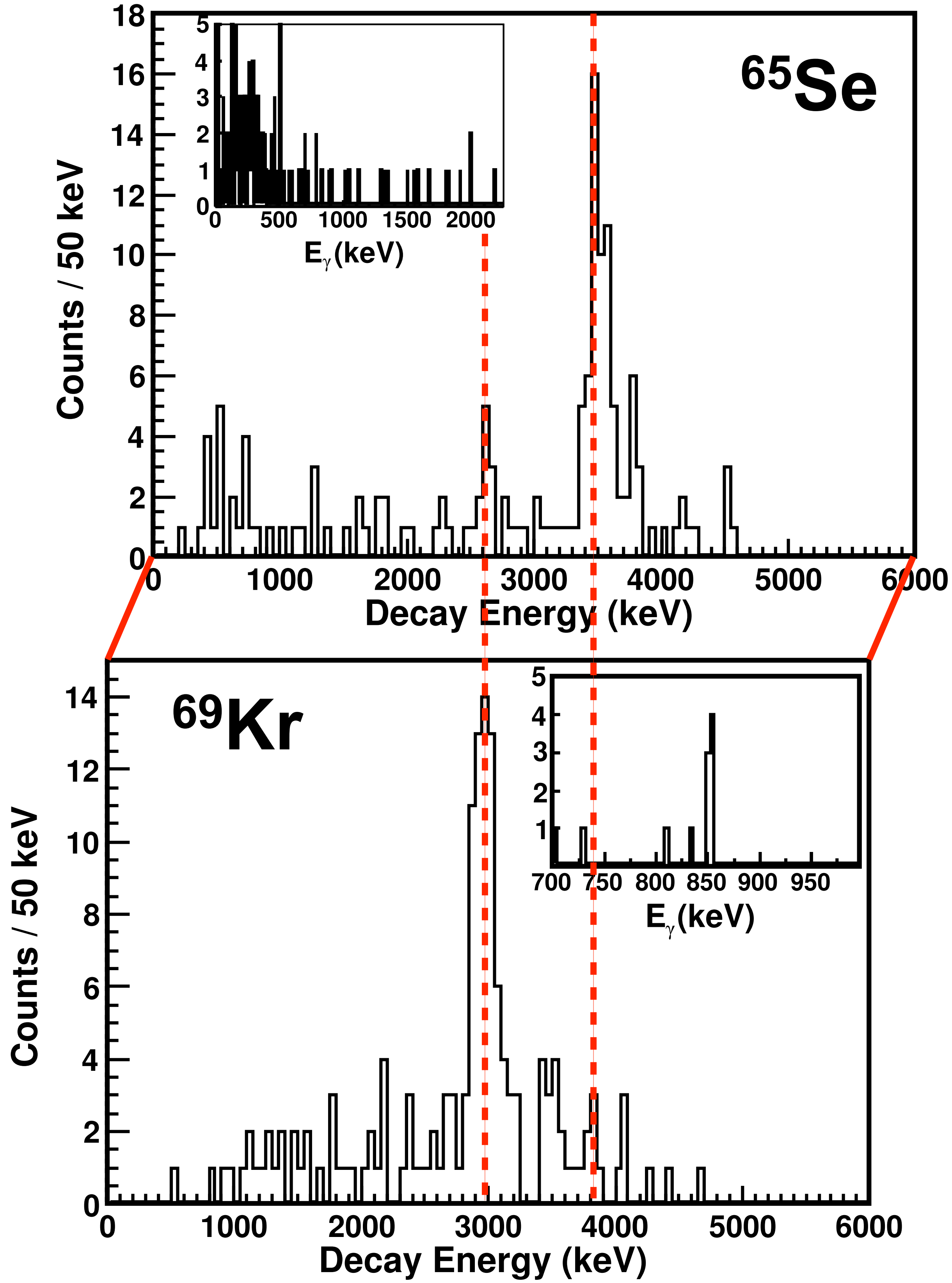

$T_z = 0$: ^{62}Ga, ^{66}As, and ^{70}Br

J. Savory *et al*. PRL **102**, 132501 (2009)

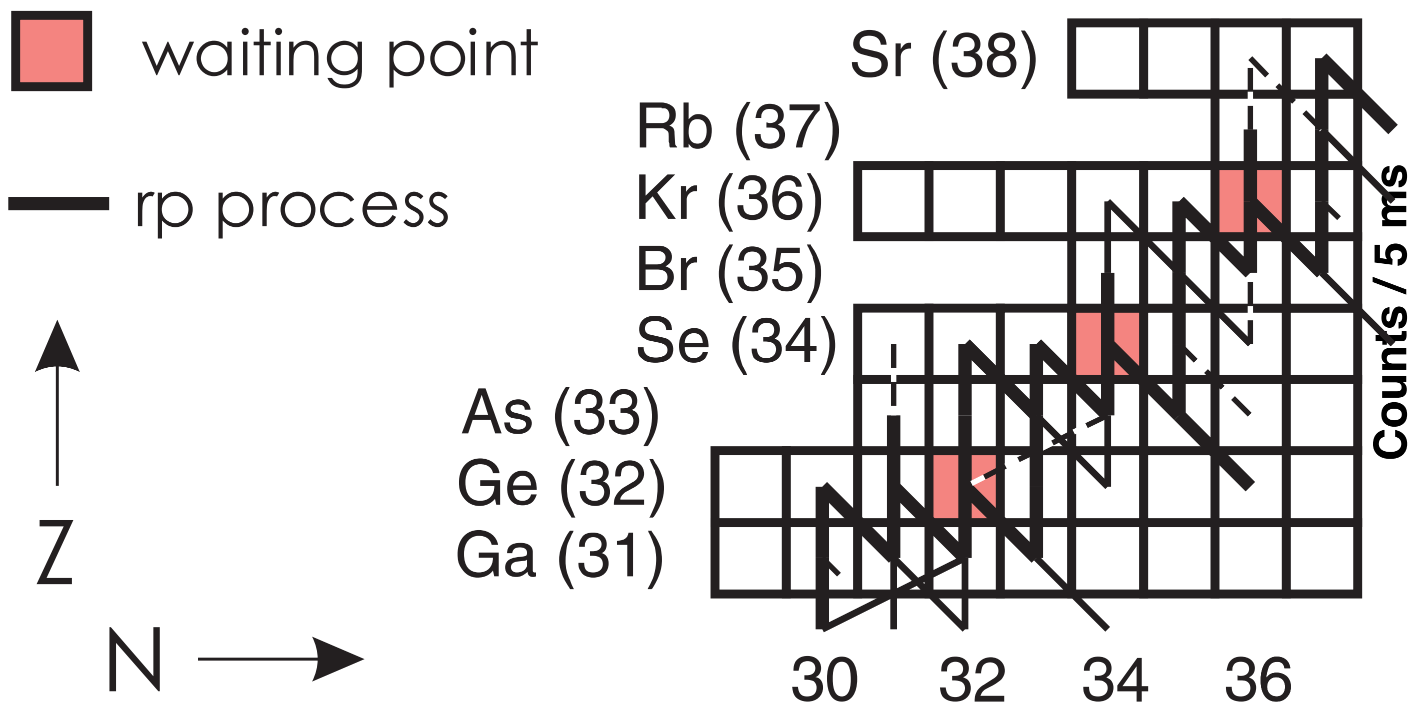

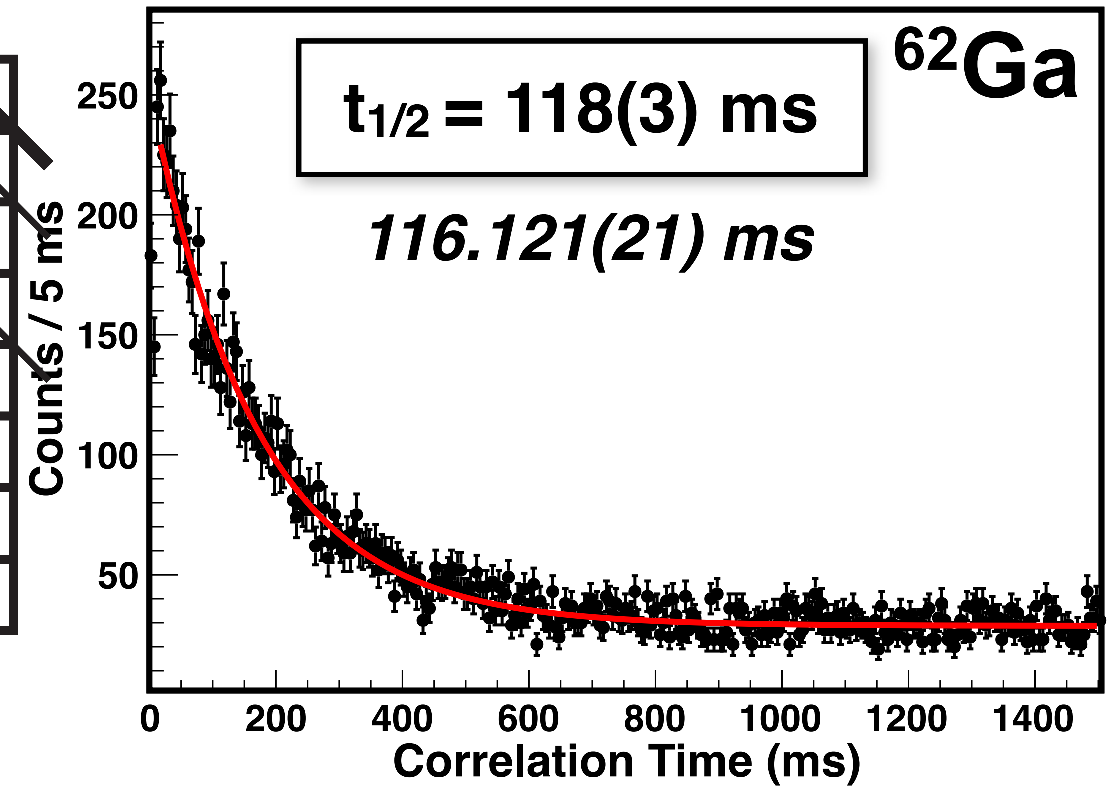

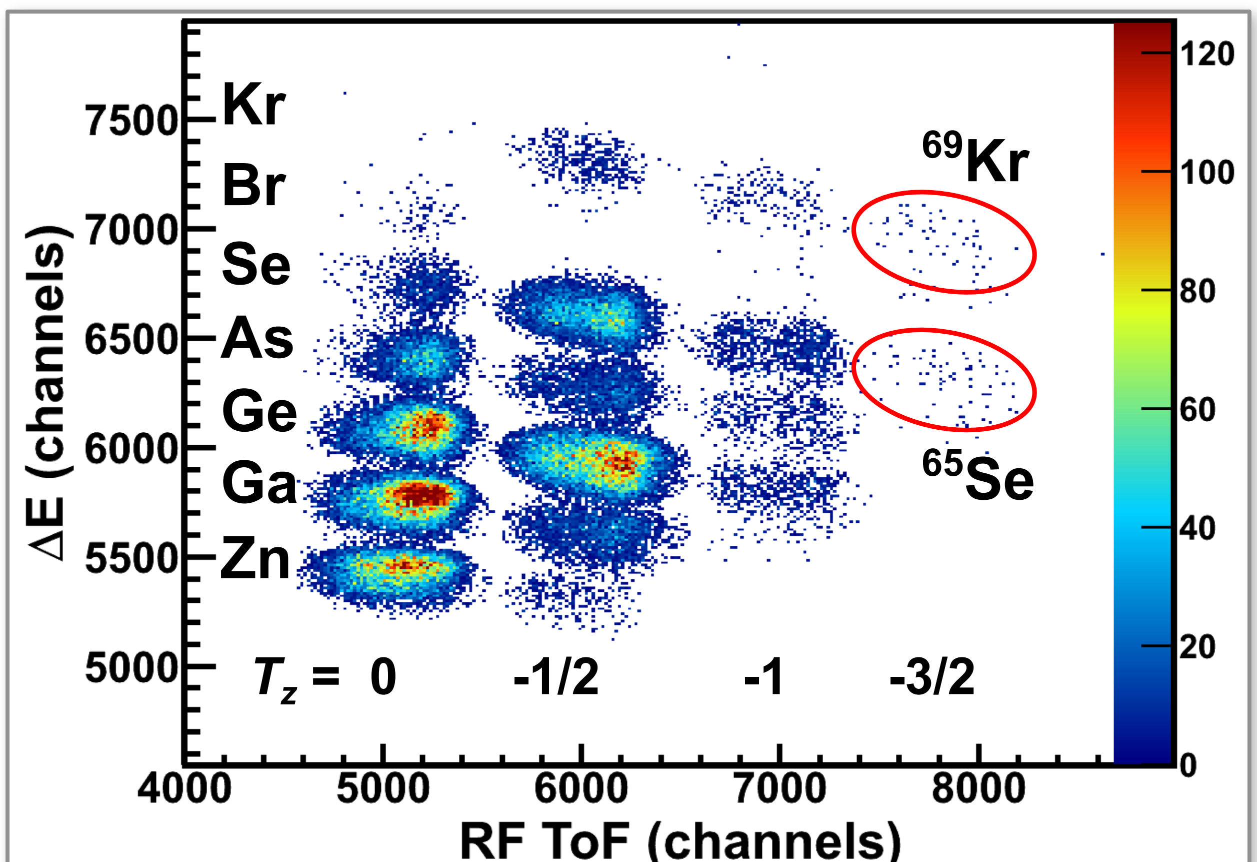

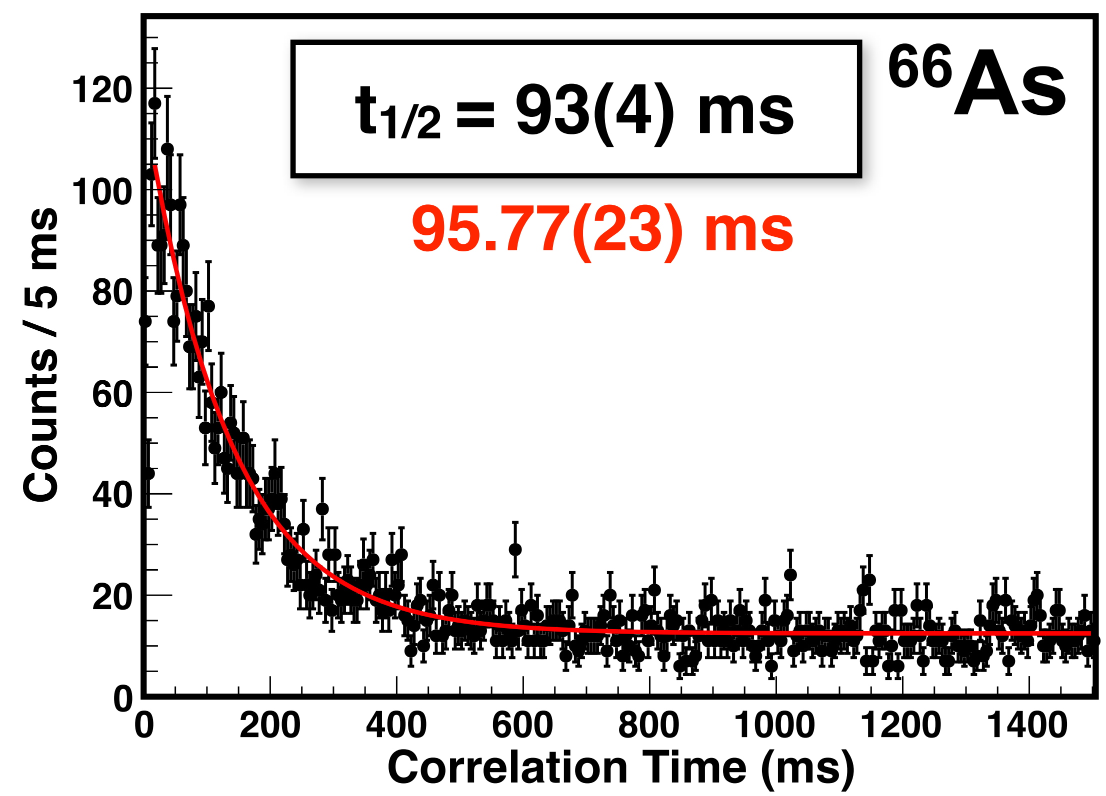

$T_z = 0$: ^{62}Ga, ^{66}As, and ^{70}Br

J. Savory *et al*. PRL **102**, 132501 (2009)